Optical Coherence Tomography Imaging of Tissue Engineered Skin Cultured Under Perfusion Conditions

Case Award with Kirkstall Ltd.

Caroline Robertson

Thesis submitted to the University of Sheffield for the

Degree of Master of Philosophy

Materials Science and Engineering

University of Sheffield

June 2013

Abstract

Tissue engineered (TE) human skin constructs are useful for the investigation of disease pathologies and for exploring the potencies and side effects of medicines and cosmetics. However, TE skin constructs are limited by their short lifespan of 14 days in the laboratory. Perfusion culture methods provide a flow of medium past TE constructs and have been suggested to increase their lifespan by improving the delivery of nutrients. Another challenge with TE skin constructs is our inability to assess their quality during long term culture without performing destructive histology.

The aim was to combine perfusion culture of TE skin constructs with the use of optical coherence tomography (OCT), a non-destructive imaging technique to follow the development of TE skin over time. Commercially available bioreactor chambers were modified in order to combine perfusion culture of TE skin at an air/liquid interface (ALI), which is necessary for skin maturation, with *in situ* OCT imaging during culture.

OCT imaging was able to non-invasively observe the developing structure of TE skin constructs during culture with minimal preparation. The combination of perfusion culture techniques and OCT imaging produced good quality TE skin and allowed observation of its development over the culture period. The design and development of perfusion culture systems were challenging, particularly with regard to maintaining a stable ALI and sterile conditions.

The current perfusion bioreactors while interesting in concept would require further development to improve ease of use. Further work on OCT analysis should focus on the establishment of robust quantitative measures of quality, for which epithelial thickness will be useful.

Acknowledgements

I would like to thank my primary supervisor Professor Sheila MacNeil for taking me as a student and for her support and guidance during this project. Dr Steve Matcher for being my second supervisor and helping with the OCT side of the project. Kirkstall Ltd. and their staff who have supported this project as a case award and provided the bioreactor chambers. The EPSRC for funding the research.

William Ward and Dr Shweta Mittar who have helped with the work using the first generation perfusion chambers. Dr Shweta Mittar has also helped with proof reading my work. Dr Zeng Lu who has spent many hours assisting me with taking OCT images. Dr Shannon-Xinshan Li who helped me to write the MATLAB scripts used to straighten the images and produce the averaged A-scan. Dr Anthony Bullock who has helped with discussions of my work and experimental planning. James Robertson who has provided moral support and assisted with proof reading.

I also have to thank everyone working in the S20 laboratory for their support and help on a day to day basis, and my friends who have supported me through the project.

Thank you

Contents

Abstract i
Acknowledgements iii
Contents v
List of Figures ix
List of Tables x
Abbreviations xi

1. INTRODUCTION 1

1.1 Aim and Objectives 1
1.2 Motivations 2
1.3 Literature Review 3

1.3.1 Skin 4
1.3.2 Clinical Requirement for Skin Replacements 4
1.3.3 Skin Substitutes 6
1.3.4 Journey to Developing the MacNeil Research Group's TE Skin Model 7
1.3.5 Bioreactors in Tissue Engineering and Skin Culture 11
1.3.6 Automated Bioreactors 12
1.3.7 Mechanical Stimulation 15
1.3.8 Culture of Skin Cells on Microcarriers 16
1.3.9 Perfusion through a Scaffold 19
1.3.10 Perfusion of Skin at an Air/Liquid Interface 24
1.3.11 Discussion of Bioreactor Culture of Skin Materials 26
1.3.12 Optical Coherence Tomography 34
1.3.13 OCT Theory 34
1.3.14 Image Production 36
1.3.15 Resolution 36
1.3.16 Tissue Optics 37
1.3.17 OCT Imaging in Dermatology 38
1.3.18 OCT Imaging in Tissue Engineering 41
1.3.19 Investigations of the Use of OCT imaging of the MacNeil Reconstructed Skin Model 43
1.3.20 Summary of the Literature 45

1.4 Design Requirements for a Perfusion System to Culture TE Skin at ALI 47
1.5 Project Outline 50

2. MATERIALS AND METHODS 51

2.1 General Materials and Methods 51

2.1.1 Culture Medium 51
2.1.2 Production of De-Epidermized Dermis 51
2.1.3 "3T3" Cell Culture and Irradiation 52
2.1.4 Keratinocyte Isolation and Culture 52
2.1.5 Fibroblast Isolation and Culture 53
2.1.6 Production of TE Skin Constructs 53
2.1.7 Histology 54
2.1.8 Perfusion Systems 54
2.1.9 OCT Systems 55
2.1.10 Preparation of TE skin for OCT imaging 56
2.1.11 OCT Imaging of TE Skin Samples 57

2.2 First Generation Perfusion System 57
2.3 Second Generation Perfusion System 60

2.3.1 System Setup 60
2.3.2 Increasing Output Flow Rate 60
2.3.3 Aluminium Stand versus Empty Control 62
2.3.4 Sponge Stand 62
2.3.5 Sponge Toxicity Assessment by Resazurin Reduction 62
2.3.6 Assessment of the Ability to Maintain Sterility 63

2.4 OCT imaging of TE Skin Constructs 63

2.4.1 Poor Quality TE Skin Constructs 63
2.4.2 Batch Feed versus Single Feed of TE Skin Constructs 64
2.4.3 Manual Measurement of Epithelial Thickness by Line Tracing 64
2.4.4 Production of Averaged A-Scan 66

2.5 Culturing TE Skin in First Generation Perfusion Chambers and Imaging Using OCT 66

2.5.1 Perfused ALI Sample Setup 66
2.5.2 Static ALI and Submerged Sample Culture 68
2.5.3 OCT Imaging of Samples Cultured in First Generation Systems 68

3. DEVELOPING THE PERFUSION CULTURE BIOREACTOR SYSTEM 69

3.1 Introduction 69
3.2 Results 71

3.2.1 First Generation Bioreactor System 71
3.2.2 Second Generation System 73

3.3 Discussion 85
3.4 Summary 92

4. OPTICAL COHERENCE TOMOGRAPHY IMAGING OF TISSUE ENGINEERED SKIN CONSTRUCTS 94

4.1 Introduction 94
4.2 Results 97

4.2.1 Interpreting OCT images 97
4.2.2 Time Course Development of TE Skin Constructs 99
4.2.3 Poor Quality TE Skin 103
4.2.4 Analysis of Epithelial Thickness Measurements from OCT and Histology 105
4.2.5 Production of Averaged A-Scans 107

4.3 Discussion 109
4.4 Summary 114

5. OCT IMAGING OF TE SKIN CONSTRUCTS CULTURED UNDER PERFUSION CONDITIONS 116

5.1 Introduction 116
5.2 Results 117

5.2.1 Setup of the Perfusion System 118
5.2.2 Implementation of OCT for Observation of Construct Development 120
5.2.3 Observation of Histology 121
5.2.4 Quantitative Comparison of Sample Structure Using Construct Scoring 123

5.3 Discussion 123
5.4 Summary 127

6. SUMMARY AND CONCLUSIONS 128

6.1 Summary 128
6.2 Future Work 130
6.3 Conclusions 130

7. REFERENCES 132
8. APPENDICES 139

Appendix 1 139

List of Figures

Figure 1.1: The structure of skin. 5
Figure 1.2: Schematic diagram of a Michelson Interferometer 35
Figure 1.3: Flow chart documenting considerations for perfusion culture of TE skin at an air/liquid interface. 48
Figure 2.1: Schematic diagram of the in-house swept source OCT system 55
Figure 2.2: Schematic diagram of the in-house polarisation sensitive swept source OCT system. 56
Figure 2.3: Schematic diagrams of the first generation "Pisa" air/liquid interface perfusion system. 59
Figure 2.4: Schematic diagram of the second generation perfusion bioreactor system. 61
Figure 2.5: Manual measurement of epithelial thickness by line tracing method. 65
Figure 2.6: Explaining the production of the averaged A-scan 67
Figure 3.1: Modification and set up of the first generation "Pisa" bioreactor system. 72
Figure 3.2: Photographs of the setup of second generation bioreactor system. 74
Figure 3.3: Methods to ensure output flow rate exceeds input flow rate. 77
Figure 3.4: Photographs illustrating the effect of the aluminium grid on the level of liquid inside the chamber. 80
Figure 3.5: Determining the suitability of using porous sponge as a stand to maintain air/liquid interface. 81
Figure 3.6: Graph showing viability of fibroblasts following indirect exposure to the sponge investigated as a stand to maintain an air/liquid interface. 82
Figure 3.7: Assessing the ability of the bioreactor system to maintain sterility. 84
Figure 4.1: OCT image interpretation. 98
Figure 4.2: OCT images and histology of good quality TE skin. 100
Figure 4.3: Graph to compare epithelial thickness measured from OCT images on day 7 and 14; investigating the difference between feeding regime. 102
Figure 4.4: Demonstrating the ability of OCT to detect poorly developing constructs. 104
Figure 4.5: Graphs comparing epithelial thickness measurements from histology and OCT images. 106
Figure 4.6: A-scan study on 7 day TE skin construct. 108
Figure 5.1: Time course OCT images and corresponding histology 119
Figure 5.2: Scoring of the TE skin constructs. 122

List of Tables

Table 1.1: Methods used to maintain temperature and pH buffering in bioreactor cultures.. 29
Table 1.2: Comparing studies using single pass or re-circulation of medium. 31
Table 1.3: The focal distances, magnifications and spot sizes of the Thorlabs lenses used in this work. 50
Table 3.1: Comparing features of the first and second generation bioreactor systems. 87

Abbreviations

ALI	Air/liquid interface
BrdU	5-bromo-2-deoxyuridine
CEA	Cultured epithelial autograft
DED	De-epithelialized dermis
DMEM	Dulbecco's modified eagle's medium
DMSO	Dimethyl sulfoxide
ECM	Extra-cellular matrix
EDTA	Ethylenediaminetetraacetic acid
FCS	Foetal calf serum
GAG	Glycosaminoglycan
H&E	Haematoxylin and eosin
HuDMEC	Human dermal microvascular endothelial cells
i3T3	Irradiated murine 3T3 fibroblasts
IMS	Industrial methylated spirit
MTS	(3-(4,5-Dimethylthiazol-2-yl)-5-(3-carboxymethoxyphenyl)-2-(4-sulfophenyl)-2H-tetrazolium)
MTT	(3-(4,5-Dimethylthiazol-2-yl)-2,5-diphenyltetrazolium bromide
OCT	Optical coherence tomography
PLGA	Poly(lactide co-glycolic acid)
SDS	Sodium dodecyl sulphate
TE	Tissue engineered
PBS	Phosphate buffered saline

1. INTRODUCTION

This project investigates methods of culturing tissue engineered (TE) skin under physiologically relevant conditions using perfusion culture techniques. In addition non-invasive imaging by optical coherence tomography (OCT) is implemented to assess development of TE skin during culture.

1.1Aim and Objectives

The overall aim of this project is to develop improvements in the methodology of culturing and imaging 3D tissue engineered human skin which is used for both *in vitro* and *in vivo* applications.

The specific objectives were to:

- Develop a bioreactor system to culture TE skin under perfusion conditions at an air/liquid interface (ALI).
- Investigate the use of OCT imaging of TE skin during culture.
- Design methods to analyse resulting images in terms of quality control.
- Culture TE skin within the perfusion bioreactor system.
- Implement OCT imaging to non-invasively investigate TE skin *in situ* during culture within perfusion bioreactors.

The MacNeil research group have extensive experience in the culture of 3D TE skin models based on co-culture of keratinocytes and fibroblasts on de-epithelialized dermis (DED). Recently the group have begun to investigate the use of OCT imaging to observe the development of these constructs. This project builds on the experiences of

the MacNeil group to advance these technologies and improve the engineered skin construct as well as establishing quality assessment.

1.2 Motivations

TE skin is defined as a scaffold or substrate seeded with the cells present in skin, usually fibroblasts and keratinocytes, to provide an imitation of the native skin. It is important that the engineered skin is able to reproduce the functions of native skin, ultimately, this is to provide a barrier to minimise water loss and prevent pathogen invasion. TE skin is a valuable resource with applications stretching from clinical repair of damaged skin to academic investigation of a range of research questions including mechanisms behind skin development and disease pathology[1].

Although many TE skin models have been developed (reviewed in [2] and [3]), this investigation focuses on the TE skin construct described by the MacNeil research group[4]. While this TE skin construct is a good approximation of native skin, providing a similar epidermal structure and a dermis containing fibroblasts it was found that the constructs displayed the optimal morphology after ten to fourteen days of culture at an ALI but beyond this time the quality decreased[5]. Therefore, it is desirable to increase the viable time in culture. This would give the clinicians a longer window in which to transplant the construct onto a patient.

Prolonged viability would also allow longer time course experiments to be performed *in vitro*. The benefits of increasing time in culture include the ability to use the skin model to study disease pathologies which require time to respond to the disease stimuli. In addition, following disease initiation, the effect of potential treatments can be investigated if constructs can maintain viability for several weeks.

For these reasons this study aims to investigate the use of perfusion culture to improve the lifespan of the TE skin constructs. It is hypothesised that perfusion culture would

improve the nutrient delivery to constructs. A continuous flow of medium would present a steeper diffusion gradient of nutrients leading to more efficient mass transfer[6]. The movement of the medium would allow nutrients to diffuse into the constructs more readily and at a faster rate. By the same mechanism the waste products from within the tissue would diffuse into the medium where they would be removed from the vicinity of the construct. Additionally, constructs would experience constant concentrations of medium constituents, as opposed to the acute fluctuations experienced by batch fed cultures[7]. It is hypothesised that this enhanced nutrition would be able to increase the viability of the constructs and maintain viability for a longer period of time.

Another limitation with TE skin is the inability to reliably check the structure of the developing tissue at multiple time points during culture. At present the quality of the construct is assessed by histology, which is a time consuming and destructive multistep process. A non-invasive technique is required to image the construct and assess its quality while in culture.

Optical coherence tomography (OCT) is a non-invasive imaging technique that can be used to assess the development of TE skin constructs over time. OCT has previously been used to observe the development of TE skin[8], however, the images obtained have not been vigorously analysed and characterised. Without this knowledge the use of OCT to determine the quality and stage of development of TE skin constructs would not be generally accepted. Therefore, this study aims to investigate the use of OCT for observation of the development of TE skin constructs.

1.3 Literature Review

This review of the literature aims to detail the development and subsequent progression of tissue engineered skin since its inception in the 1970's. It will then deal with the increasing trend of bioreactor culture techniques in tissue engineering, focussing on the

work that has been undertaken in the field of perfusion culture for engineered skin constructs. Finally, the topic of optical coherence tomography (OCT) imaging will be analysed, from the science behind how it works to its applications in TE skin and the stage at which this technology has reached in terms of reliably imaging tissue engineered constructs.

1.3.1 Skin

Skin is the organ that encapsulates our bodies; it is the barrier that protects us from pathogen invasion and water loss. Figure 1.1 illustrates the structure of the skin as observed from histology of native skin and a labelled schematic diagram. The lower region is the dermis; a highly collagenous extracellular matrix containing fibroblast cells. These fibroblasts maintain the extracellular matrix and act as a support cell for the cells in the epidermis. The dermis provides mechanical stability and a supply of nutrients from the circulation that diffuses into the avascular epidermis above[1,9].

The upper region is known as the epidermis, the major cell type found in the epidermis is the keratinocyte. The keratinocytes form a multilayered structure resting on the basement membrane[1,9]. As the keratinocytes divide they are pushed towards the surface of the skin and begin to differentiate to become corneocytes which merge together and fill with insoluble proteins and lipids[10]. The epidermis provides the impermeable barrier to water and pathogens.

1.3.2 Clinical Requirement for Skin Replacements

Damage to the skin increases the body's susceptibility to infection and dehydration. The severity of these pathologies is dependent on the extent of damage; hence it is imperative that the barrier is restored without delay[9].

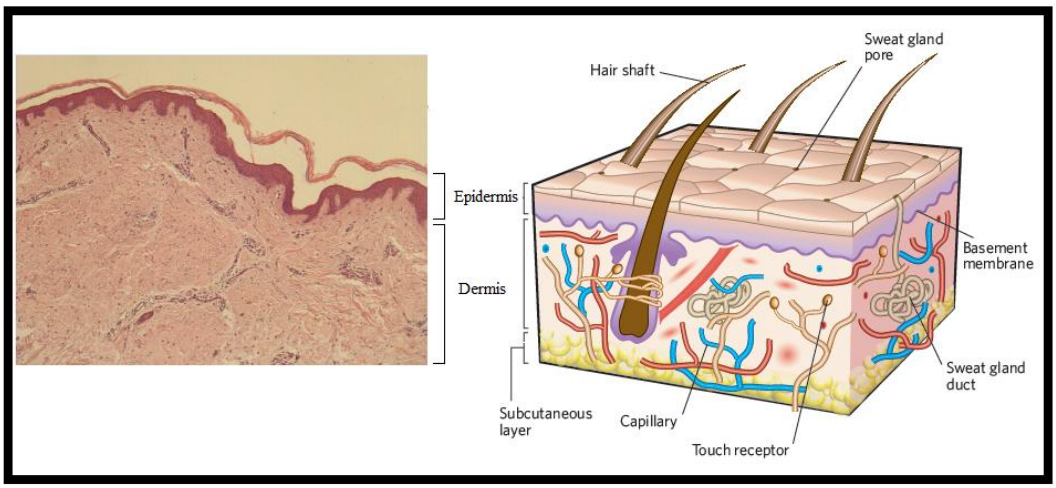

Figure 1.1: The structure of skin.

Left: Micrograph showing the structure of native split thickness skin as observed from haematoxylin and eosin stained histology. Note the presence of blood vessels in the dermis and the multilayered structure of the epidermis. Right: Schematic diagram labelling the structure of the skin reproduced with permission from Nature Publishing Group (http://www.nature.com/) from [1].

Chronic wounds and severe burns are two injuries to the skin that require clinical intervention for healing to occur. A chronic wound is a wound that does not respond to normal treatment. Venous ulcers, arterial ulcers and pressure ulcers in bed-bound patients can become chronic wounds[11]. A rise in chronic wounds has been reported in the Western world, which is mainly due to an increase in the aging population and incidence of type 2 diabetes[1]. Currently little can be done to treat chronic wounds, in most cases the wound is bandaged and kept clean. Patients are advised to address the underlying health problem causing the ulcer[12,13]. Although there are a range of dressings available, none of these actively treat the underlying cause; they allow the patients to live with the condition while relying on the ability of the body to repair the defect[13].

Burns are classified by increasing degree, or severity, depending on the depth of damage (for further explanation see [14]). The extent of damage and surface area of the skin injury will determine the treatment required[14]. It was not until the 1970's that an effective treatment for burns was developed; prior to this time even relatively minor burns carried a high risk of infection and sepsis. This new intervention was the split thickness autograft; split thickness skin (consisting epidermis and superficial dermis) is harvested from another area on the body and used to quickly cover the excised burn region[15]. The problem with this treatment is that it introduces a secondary wound, pain and donor site morbidity. For patients with damage to a high proportion of their total body surface area, there may not be enough unaffected skin to harvest in order to provide a barrier layer immediately. Multiple operations may be required to re-harvest grafts from the same locations as the donor sites repair.

Although the use of autologous split thickness skin grafts is not an ideal solution to repair wounds caused by more severe burns, they are still the gold standard for wound repair. The advantage of this type of graft is that it provides the wound with a supply of autologous cells that can repair the defect. Furthermore, they provide the native architecture of blood capillaries which allow the graft to "take" or inosculate with the host vasculature found in the vicinity of the wound.

1.3.3 Skin Substitutes

Development of skin substitutes containing autologous cells from small skin biopsies has the potential to heal severe burns and chronic wounds by providing a source of autologous grafts without removing a large quantity of skin. The various skin substitutes that are currently commercially available, as well as potential future products are thoroughly documented in the 2010 article by Shevchenko *et al.*[2].

These biological skin models also have the potential for academic study in circumstances such as the skin reaction to certain substances and the investigation of

processes such as wound healing, progression of disease pathology and efficacy of potential treatments[1]. Use of *in vitro* models enables a reduction in animal testing and may provide more accurate results as the tissue tested can be human and therefore more physiologically relevant than animal tissue. This is also in-line with the government initiative of "Replacement, Refinement and Reduction" of the use of animals in research[16].

1.3.4 Journey to Developing the MacNeil Research Group's TE Skin Model

Without the advances made by Rheinwald and Green in the 1970's the MacNeil reconstructed skin model would not have been possible, so this section of the review begins at this point. In 1975 Rheinwald and Green demonstrated the effective culture and expansion of primary human keratinocytes from a small biopsy of harvested skin tissue[17]. Previously it was possible to grow keratinocytes in monolayer, but these had a poor ability for subculture and so could not be expanded to increase the cell yield. Until this method of expanding keratinocytes was described the concept of creating TE skin replacements was not feasible as sufficient numbers of keratinocytes could not be obtained.

Breakthrough work with a murine teratoma keratinocyte cell line enabled an insight into the requirements necessary for primary keratinocyte culture. It was found that the presence of a low concentration (0.4 µg/ml) of hydrocortisone in the medium was required for reliable subculture; including stratification and outward migration of colonies and increased cell yield. It was also discovered that primary keratinocytes require the presence of fibroblasts to prevent premature differentiation; fibroblasts secrete growth factors and matrix proteins to stabilise keratinocytes[14]. In order to prevent fibroblasts over-populating the culture, it was possible to use non-dividing irradiated murine 3T3 fibroblast cells[17,18].

Subsequently this group described the requirement for epidermal growth factor to increase the colony forming ability of keratinocytes, which in turn increased the number of passages these cells could undergo without deterioration[19]. These developments enabled the production of cultured epithelial autografts (CEAs) as the first step in the production of tissue engineered skin replacements. CEAs consist of autologous keratinocytes that are cultured and expanded *in vitro* to form multilayered sheets of cells[20,21]. These can be transplanted onto patients to provide a source of autologous epithelial cells to help the skin repair and form a new barrier; however a dermal replacement is not provided. CEAs were developed and used clinically from the 1980's for the treatment of burn wounds.

Although CEAs are the most common skin replacement used clinically, none of the engineered skin tissues developed to date have enjoyed sufficient success to be in routine use at this point in time[22]. Aside from the time required to expand sufficient cells, one major problem with the CEA is their sensitivity to shearing forces which can cause blistering and damage. This problem can be circumvented by providing a secure dermal-epidermal attachment by using a one stage dermal-epidermal replacement graft[5].

Early work by the MacNeil research group demonstrated the production of a one stage reconstructed skin model[4]. This method used acellular human dermis, known as de-epithelialized dermis (DED) as a substrate on which skin cells were seeded to produce a product to transplant onto patients suffering from severe burns. The concept was to use autologous cells (keratinocytes[17] and fibroblasts[4]) obtained from a small biopsy and expanded to obtain a sufficient yield. These autologous cells were then seeded on donor DED from another patient to produce a product that would not suffer from rejection by the immune system.

Initial studies seeded the fibroblasts onto the reticular side of the DED and keratinocytes onto the papillary side of the DED. Following cell attachment the

constructs were cultured at an ALI to encourage differentiation of the keratinocytes to stimulate the barrier function required of a skin substitute[23]. It was later found that seeding both cell types onto the papillary side of the DED produced comparable TE skin, so that it was possible to seed both keratinocytes and fibroblasts together in a more efficient one step process[24]. Tissue engineered skin cultured using this method produced a structure very similar to native skin, as observed by haematoxylin and eosin (H&E) stained histology. However, the model lacked structures such as sweat glands and hair follicles found in native skin; the cell types necessary to produce these structures were not included in the model[4].

The DED, or acellular dermis, was produced by removing viable cells from donor skin using a sodium chloride salt splitting technique to remove the epidermis and destroy viable cells within the dermis[22]. It was shown that this DED retained its basement membrane proteins, which are an essential requirement for attachment and organisation of keratinocytes. This study also confirmed the requirement for fibroblasts in the model to ensure strong dermal-epidermal attachment which was necessary to prevent blistering and provide an advantage over CEAs[5].

Observation of the histology showed that these skin constructs had optimal structure and organisation between ten and fourteen days in culture at an ALI[5]. This limited the timeframe during which the construct could be transplanted onto a patient in the clinical situation. This in turn relied on the patient being in sufficient health within a small time window to undergo surgery. Furthermore, at the time this work was undertaken, non-invasive imaging techniques to assess the quality and development of constructs did not exist. The only way to confirm the construct was of sufficient quality for the patient to receive was by undertaking histology which is time consuming, labour intensive and uses up samples of the constructs[5].

The use of human dermis in the form of DED in the TE skin construct is not altogether safe and brings with it an inherent risk of disease transmission to recipients[22]. This was minimised by investigating methods of sterilisation of the donor tissue, aiming to reduce the disease risk without damaging the physical and biochemical properties of the structure. It was found that sterilisation by ethylene oxide with a glycerol pre-treatment produced the best results[22]. DED prepared in this way had suitable mechanical properties, it retained the correct dermal morphology and it also retained collagen IV which is a protein found in the basement membrane. After ten days of *in vitro* culture at ALI, TE skin produced from this sterilised dermis was able to produce good quality skin as assessed by histology[22].

When this type of construct, which was cultured *in vitro* for ten days, was transplanted onto a nude mouse model for a period of two weeks, the graft "took" to the wound bed and began the healing process. The corresponding histology of the graft showed good quality skin. This study confirmed the ability to sterilise the dermis without causing excessive damage to the structure or biochemistry, and showed that the engineered skin could be successfully transplanted *in vivo*[22].

Following this work, the skin construct was tested clinically for contracture release on six patients. The results were disappointing, with contraction, loss of epidermis and scarring being the main problems in 4 out of the 6 constructs[25]. Essentially it was found that these skin constructs did not "take" well on the poor wound beds that arose in clinical settings. It was suggested that the poor take was due to slow neovascularisation of the graft and the resulting poor nutrition[25].

Efforts were then made to encourage vascularisation of the skin constructs to accelerate take on clinical wound beds. This was attempted by co-seeding Human Dermal Microvascular Endothelial Cells (HuDMECs) with the fibroblasts onto the reticular surface of the DED prior to seeding keratinocytes on the papillary dermis. This study

found that only modest penetration of HUDMECs into the dermis was achieved, as shown by factor VIII staining of these cells within the reticular dermis[25].

It was later found that seeding endothelial cells (HuDMECs and HMEC-1 endothelial cell line) on the papillary surface of the DED greatly increased the extent of migration through the dermis[26] when compared to the previous model that seeded the cells on the reticular surface. Subsequent work delivered transglutaminase inhibitors in the culture medium, which were thought to stimulate an endothelial phenotype in the population of fibroblasts[27].

Although attempts at increasing the angiogenic potential of the TE skin constructs have been pursued, the results have been disappointing and no major improvements to the skin model have been established. Extensive further work is required in this area to fully understand how neovascularisation can be achieved in skin constructs.

1.3.5 Bioreactors in Tissue Engineering and Skin Culture

Having discussed the current state of reconstructed TE skin constructs, the focus will now move to the bioreactor culture of skin. Originally bioreactors were associated with the bioprocess industry[28] but more recently bioreactors have been implemented in tissue engineering. Bioreactors are taking an increasingly important role in tissue engineering in general, although, at this stage their use has not become standard practice. A bioreactor in tissue engineering may be described as an engineered system for the maintenance of cells and tissues in culture, which provides some benefit or functionality over standard static culture techniques. This could be achieved by changing the way that nutrients are provided to the sample, or by providing some kind of mechanical stimulation.

Aims of bioreactor culture include; automation and control of culture parameters, mechanical stimulation and enhanced nutrient delivery. This can be achieved either by

provision of a continuous supply of fresh medium or mixing the medium to provide an equal distribution of nutrients. The conditions created can increase the similarity of culture to the *in vivo* environment, thereby increasing the functionality and relevance of the engineered tissue to both clinical and academic applications. The flow or perfusion culture of engineered tissues such as bone[29,30] and heart valves[31] have become of widespread interest over the recent years. These tissues require specific mechanical stimulation to produce the correct function. This mechanical stimulation is provided by perfusion culture conditions. In comparison there are few studies of TE skin implementing perfusion conditions.

The general state of bioreactor culture in tissue engineering is discussed further in reviews by Martin *et al.*[32] and Wendt *et al.*[28]. This review will now discuss and evaluate the literature available specifically concerning the use of bioreactors in the culture of materials aiming to repair damaged skin and other 3D skin materials. The review is organised in terms of category of bioreactor, then chronologically.

1.3.6 Automated Bioreactors

In tissue engineering automation is the use of machines to perform the culture of cells or tissue automatically. Successful automation would be advantageous as it would mean that human intervention during culture would not be required. It would be possible to seed, feed and passage the cells without manual manipulation of hundreds of culture dishes. It would also allow the close control of chemical parameters such as pH and concentration of important molecules. This enables standardisation of culture conditions and improves repeatability. The ability to minimise human intervention is advantageous to reduce labour costs and potential for contamination, which is very important if the tissue generated is to be used clinically. Furthermore, use of automated bioreactors in tissue culture has the potential to enable the scale-up necessary to produce clinically relevant quantities of tissue.

Automated Culture of Keratinocytes

Manual techniques for the culture of keratinocytes for CEAs may require as many as one hundred 75 cm^2 flasks to obtain sufficient cells to treat a burn wound[33]. In this case the time required to perform standard culture tasks is great and the opportunity for contamination is considerable. Early skin bioreactor work by the Prenosil research group[33–36] developed a system to automate and scale-up the process of cultured epithelial autograft (CEA) production.

Keratinocytes were cultured in a bioreactor known as the "Kerator" to form sheets of cells for use as CEAs and sub-confluent epidermal autografts. The Kerator was capable of seeding the keratinocytes and changing the medium automatically. An actuator was used to rock the culture vessel to mix and distribute the medium or cell suspension on addition, and tilt to aid media removal from the system. However, under standard conditions this was a static culture technique and did not aim to improve nutrient delivery to samples by perfusion.

Stacked culture chambers allowed the culture of up to 5280 cm^2 of keratinocytes, which is a considerable surface area at one time. A mass flow controller was used to ensure constant CO_2 levels in air; gassing occurred in series through each of the chambers in turn. Temperature was controlled by placing the system on a hot plate within a polystyrene box and mixing the air using a fan. It was shown that the automation process did not have adverse effects on the cell viability and efforts to scale-up the production of keratinocytes were successful using this automated bioreactor system[33,34].

In the later studies a phase contrast microscope and CCD camera were used to monitor the progress of the cells in the lowest chamber during culture. The camera could move along one horizontal plane to allow observation at multiple positions in the culture vessel. LabVIEW software with IMAQ Vision add-on was used to calculate cell

density. It was found that the most accurate value for cell density was obtained when multiple images were observed[34–36].

Subsequent work used the Kerator to expand keratinocytes for use in producing engineered skin substitutes with both epidermal and dermal portions based on collagen glycosaminoglycan (GAG) sponges[37]. Use of the Kerator was attractive due to the ability to automate the process and reduce manual labour while scaling-up keratinocyte expansion. This group developed a semi-automated technique to passage the cells within the Kerator. The work highlights the need to translate well established protocols for standard culture into practical solutions for the particular bioreactor system in operation.

Standard passaging protocols were not suitable for use in the Kerator bioreactor; following application of trypsin, the culture vessel could not be tapped to dislodge the remaining keratinocytes. This problem was overcome by application of ethylenediaminetetraacetic acid (EDTA) prior to the addition of trypsin. It was found that this protocol did not adversely affect the harvested keratinocytes in terms of morphology, viability and barrier formation on engineered skin substitutes. Efforts to scale-up production of large quantities of keratinocytes were successful using this automated bioreactor system[37].

The most recently published work using the Kerator was published in 2009 by Kalyanaraman & Boyce. The bioreactor was used in an attempt to reduce the expense of culturing a large number of cells[38]. This work followed on from the previously described study and made use of expanded keratinocytes to produce engineered skin substitutes for transplantation *in vivo*. 5-bromo-2-deoxyuridine (BrdU) staining showed that keratinocytes within the engineered skin substitutes cultured for 2 weeks had similar proliferative capacity when obtained from the Kerator or standard flasks.

When these constructs were transplanted onto a full thickness wound model on athymic mice for a period of 6 weeks there was no difference in wound healing between grafts containing keratinocytes from either culture condition[38]. Grafts had good take on the wound beds and immunostaining for human leukocyte antigens (HLA-ABC) showed that human cells were present in 78% of animals for both culture conditions. Therefore, these human cells were able to persist in the skin constructs after transplantation *in vivo*. Therefore, it has been shown that the Kerator bioreactor was able to successfully expand keratinocytes for use as CEAs and in engineered skin substitutes transplanted in an *in vivo* wound model.

1.3.7 Mechanical Stimulation

Bioreactors have been used fairly commonly to provide mechanical stimulation to tissue engineered constructs. Provision of a more accurate mechanical environment with regard to the physiological conditions has been shown to aid cells to become more functional[29].

Cyclic Strain on Fibroblasts Seeded on Chitosan Scaffolds

In the study by Lim *et al.* human dermal fibroblasts were cultured on chitosan scaffolds within a bioreactor designed to provide cyclic strain to the construct[39]. The bioreactor was placed inside a humidified incubator at 37^{o}C and 5% CO_2 and cultured for 1 or 3 weeks. The bioreactor produced a stretch of 7% of the original scaffold length at a rate of 1 Hertz.

Samples exposed to strain stimulation displayed a more homogeneous distribution of fibroblasts and an increased thickness of construct when compared to equivalent static samples[39]. It was found that production of the extracellular matrix (ECM) proteins vimentin, fibronectin and collagen I was increased when samples were exposed to the

mechanical stimulation. This work showed that stretching of 3D constructs containing fibroblasts was beneficial for increased ECM production.

Mechanical Stimulation to Increase the Area of Split Thickness Skin Grafts

Another description of a bioreactor for skin culture under mechanical stimulation was described by Ladd *et al*.[40]. This study aimed to increase the area of native tissue obtained from split thickness skin harvested from the patient. The bioreactor was designed to stretch and expand the native skin *in vitro*, before transplantation back onto the patient. Current clinical methods to expand split thickness skin grafts are extension using a balloon expander prior to harvest, and meshing the split thickness graft. Extension is uncomfortable for the patient and meshing leaves a patterned scar which is aesthetically unpleasing. The inadequacies of these methods are driving research in this area to improve the quality of life and clinical outcome for the patients.

Harvested skin was placed in a rig and submerged in medium for a period of 5 days in an incubator[40]. Incremental uniaxial tension expanded the skin in steps by an additional 20% of its length each day for five days. It was reported from observation of the histology that the bioreactor successfully increased the size of the tissue, while maintaining viable and proliferative cells. It was also suggested that following response to the stretching stimulus the fibroblasts within the skin would be primed for wound healing and may proliferate more readily.

1.3.8 Culture of Skin Cells on Microcarriers

Microcarriers are small beads that allow the attachment and growth of anchorage dependent cells. Cultures are maintained in an agitated condition to ensure suspension of the particles. This type of culture provides a huge surface area for cell proliferation and expansion.

Spinner Flask Culture of Micro Scale Dermal Units

Palmiero *et al.* used spinner flask culture and microcarriers to form 3D dermal tissue[41]. Bovine fibroblasts were seeded in a spinner flask bioreactor onto porous gelatine microcarriers where they proliferated and began to produce ECM. Once cultures were established they were known as "micrometric tissue precursors" to reflect their nature as living "bricks" of tissue which were built up to create larger structures. At this point the microcarriers were transferred to an assembly culture system where they were moulded to the required shape. The close proximity of the micrometric tissue precursors enabled cell to cell and cell to matrix bonds to form between units to act as a glue to stick the whole structure together and form a compact structure of dermal tissue.

On individual microcarriers H&E staining showed that the fibroblasts entered the pores as well as adhering to the surface. Fibroblasts also produced ECM which coated the microcarriers[41]. It was found that the number of cells per bead and the diameter of the beads increased with time. Collagen I, the major constituent of the dermis was found in and around the microbeads. It was also found that expression of collagen I increased in the microcarrier culture condition when compared to static monolayer culture. It was suggested that the 3D stirred culture provided an environment more similar to the *in vivo* condition and thus enabled more normal function of the cells.

When the microcarriers were cultured in the assembly chamber the dermal units began to fuse; H&E staining showed that the structure produced mimicked the native dermis with a characteristically low ratio of cells to matrix[41]. Masson-trichrome staining demonstrated the presence of collagen fibres and immunohistochemical investigation confirmed the presence of collagen I. The structure formed had reasonable mechanical stability and handling was possible without damaging the structure, however the mechanical similarity to native dermis was not investigated. It was possible to create a macroscopic tissue construct from repeating micro scale units using spinner flask

culture methods. The micro units produced had enhanced function in comparison to those produced by static monolayer culture.

Formation of 3D Epidermis in a Rotary Bioreactor

In work by Lei *et al.* a rotary bioreactor system was used to simulate microgravity and provide a 3D dynamic culture system for epidermal stem cells cultured on microcarriers[42]. Perceived advantages of this system were that it ensured suspension of microcarrier-cell constructs, it improved cell to cell interaction and it allowed aggregation and development of 3D tissue. Previously the system had been noted to promote proliferation and delay differentiation of a range of cell types, thus improving the ability to scale-up production.

Initially epidermal cells were seeded onto microbeads within the rotating vessel at 12 rpm; this speed imparts a free fall condition on the cell constructs and increased the efficiency of cell attachment to the microcarriers[42]. After 24 hours the mixture was divided in half to provide a static and dynamic condition. The static sample was put into well plates and the dynamic sample remained in the rotating culture vessel which was increased to 22 rpm for the remaining 14 days of culture.

In the rotation condition the epidermal cells accumulated and formed a 3D multilayered structure on the surface of the carrier[42]. MTS assay showed that these cells proliferated at day 5 and 10. The percentage of Ki67 positive cells were greater at day 10, indicating proliferation. Furthermore, expression of involucrin, a marker of terminal differentiation was down-regulated in the rotating samples. However, the samples cultured under static conditions were only able to support a monolayer of cells on the surface. The number of cells did not increase with time, indicating that there was very little proliferation. Correspondingly Ki67 expression was decreased; however

involucrin expression was up-regulated in comparison to the rotating case, indicating that more of the cells underwent terminal differentiation.

Under rotation conditions a 3D epidermal structure was formed on each microcarrier, this structure was highly proliferative and differentiation was delayed[42]. This indicates that stem like cells can be maintained on microcarriers, and delayed differentiation could increase the lifespan and expansion of these cells. In combination with the previously described concept of using microcarriers as building blocks, these constructs could be used to build a larger structure.

1.3.9 Perfusion through a Scaffold

Perfusion bioreactors are a common category of bioreactor; they provide a continuous flow of medium through or past the TE construct. The term "perfusion" relates to the delivery of blood *in vivo;* the flowing medium in the culture system is analogous to the blood circulation. Therefore, culture of cells or tissues under perfusion conditions may more closely mimic the conditions found *in vivo* with even distribution of nutrients, a constant supply of fresh medium and a mechanical stimulation which could be chosen to be similar to the physiological condition.

Single Pass Perfusion of Fibroblasts within a Polyglycolic Acid/ Polylactic Acid Mesh

The study by Halberstadt *et al.* was the earliest study found in the literature detailing the bioreactor culture of a 3D skin product in 1994[43]. Human neonatal dermal fibroblasts from foreskin were cultured on a porous polyglycolic acid/ polylactic acid mesh intended for use as dermal replacements. The bioreactor described provided a closed environment with a single pass flow of medium perfusing through 16 parallel culture vessels.

The flow rate was determined by investigating the rate of glucose depletion in the medium, which indicates the metabolic activity of the sample[43]. A constant difference

in glucose concentration was established across the culture vessels, which also ensured sufficient contact of secreted proteins (e.g. growth factors) with the samples. Metabolic activity of the samples increased with time in culture; therefore flow rate was increased incrementally from an initial rate of 5.0 ml/hour to 8.5 ml/hour to compensate for this increase in metabolism.

It was found that perfusion could speed up the production of the dermal constructs; perfused samples took 16 days to produce structures of comparable quality to 22 day static cultures[43]. MTT assay showed that 16 day perfused samples had comparable viability (and therefore cell number) to 22 day static samples. Furthermore, observation of immunofluorescence histology showed that expression of collagen I, decorin and fibronectin was very similar between static and perfused samples at these time points. Perfusion culture allowed accelerated production of dermal constructs of similar quality in terms of viability and secretion of ECM proteins in comparison to static methods. Savings in time would correspond to reduced costs to make the process more economically viable.

Re-circulating Perfusion Culture of Oral Keratinocytes on Collagen Chondroitin Sponges

Following a long pause in the publication of perfusion culture studies, the study by Navarro *et al.* in 2001 produced engineered oral mucosa under perfusion conditions[44]. Although this tissue is not skin, this study has been included since oral mucosa is a similar epithelial tissue with some similar requirements. One major difference between skin epithelium and oral mucosal epithelium is that the oral mucosa does not require an ALI to promote differentiation and barrier formation; it is found in a wet environment *in vivo*. In this study oral keratinocytes were cultured submerged in 3D bovine collagen chondroitin sponges. Re-circulating perfusion through the scaffold at a flow rate of 1.3 ml/minute was applied 24 hours after seeding.

Perfusion caused an initial faster rate of proliferation of the oral keratinocytes which produced a multilayered morphology after just three days of culture, in comparison to static controls which had a single layer at this time point[44]. At subsequent time points; 7 and 14 days, this effect became less pronounced as the static constructs began to catch up. It was suggested that the enhanced proliferation was due to increased nutrient exchange associated with perfusion. Perhaps if the flow rate was increased to meet the additional metabolic demand as the cells proliferated, the proliferation could have been maintained.

Perfusion also caused significantly more shrinkage of the collagen chondroitin sponge, manifested as a greater decrease in diameter compared to the static counterparts[44]. It was suggested that the shrinkage was due to degradation of the scaffold by the flow of medium, and that *in vivo* this would be even faster due to the destructive enzyme environment. With careful optimisation of culture parameters this study suggests a place for perfusion culture of epithelial tissues in tissue engineering.

Automated Single Pass Perfusion Culture of Keratinocytes in a Collagen-GAG Matrix

The study by Kremer *et al.* combined the concept of automating culture with the benefits of perfusion which gives rise to a more efficient growth of cells[45]. The system aimed to use perfusion culture to scale-up, reduce labour, reduce cost and optimise the environment for keratinocytes cultured in INTEGRA (collagen-glycosaminoglycan (GAG)) matrix. This study produced a composite skin model with the collagen-GAG matrix acting as a dermal replacement and the keratinocytes forming an epithelium. Six constructs were placed in a submerged culture vessel and exposed to a continuous single pass flow of unused medium at a rate of 1 ml/hour. The medium was buffered with HEPES and the temperature was maintained using a hot plate.

Following five days of perfusion culture the constructs were transplanted *in vivo* by suturing onto an athymic mouse wound model[45]. Keratinocyte seeded constructs cultured under perfusion conditions were able to accelerate wound healing in comparison to acellular equivalents. However, comparison between static and perfused cultures was not considered in this investigation, so advantages of perfusion over static culture cannot be ascertained. It was concluded that this perfusion system was able to produce composite skin constructs more quickly and therefore more cost efficiently than conventional CEAs because of the short 5 day culture before transplantation. The next step suggested was culture at an ALI. This study did not justify the parameters used in the perfusion culture; it is unknown whether any optimisation steps were taken. It would be interesting to discover whether optimisation could further improve construct production.

Re-circulating Hydrostatic Pressure Perfusion of Fibroblasts Seeded on a Collagen Sponge Construct

Mizuno *et al.* investigated two bioreactor systems for the culture of dermal fibroblasts on collagen sponges; a "hydrostatic pressure/ perfusion" system and a re-circulating perfusion culture system[46]. The hydrostatic pressure perfusion system applied an oscillating compression of 0-0.5 MPa at 0.5 Hertz to the fluid and therefore the sample. The perfusion system provided a continuous flow of 0.05 ml/minute. It was shown that both bioreactor systems could improve the viability and proliferation of fibroblasts within collagen sponges. It was also shown that bioreactor culture could increase cellular migration distance through the sponge. They found that the hydrostatic pressure perfusion system enabled cells to migrate further than the standard perfusion system. Whereas static culture was unable to provide the environmental conditions and nutrition required to produce 3D tissues inside the scaffold.

Re-circulating Perfusion System for Artificial Dermis

The work by Seol *et al.* described a perfusion system for the culture of artificial dermis consisting of human dermal fibroblasts seeded on a poly(lactide co-glycolic acid) (PLGA) scaffold[47]. The whole system was placed inside an incubator to maintain temperature and gas concentration, and a stirrer in the medium reservoir ensured distribution of nutrients. The perfusion system had a closed loop configuration and provided a continuous re-circulating flow of 20 ml/minute. Perfusion was able to significantly increase proliferation of fibroblasts after 7 days as assessed by an increase in DNA content and also increased GAG production after 3 and 7 days. After 14 days of perfusion culture, samples had a significantly higher elastic modulus in comparison to static samples. It was suggested that this was due to the uniform distribution of fibroblasts and ECM. Perfusion culture was able to benefit the production of artificial dermis in terms of mechanical properties and normal function. However, the viability of cells was not commented on.

Re-circulating Perfusion Culture of Fibroblasts on Hyaluronic Acid Scaffolds

In a study by Figallo *et al.* dermal fibroblasts were cultured on porous 3D hyaluronic acid scaffolds[48]. Perfusion techniques were employed to improve the distribution of nutrients throughout the scaffold; flow rates of 0.3 and 1.0 cm^3/minute were investigated on cultures for 2 and 4 days. MTT assay following 2 and 4 days culture was used to assess cell viability. It was found that the lower flow rate of 0.3 cm^3/minute was too low to maintain fibroblast growth; the viability decreased between day two and day four, at which point only the centre of the seeded area remained viable. This is likely to be due to the parabolic flow profile, with the centre receiving the fastest flow rate and preferential diffusion gradient for nutrient delivery and removal of waste.

At the higher flow rate of 1.0 ml/min, even colouration by the MTT product confirmed viability of cells across the diameter of the scaffold[48]. Increasing viability between two

and four days confirmed that the fibroblasts were proliferating. However, measurement of detached cells at day four also suggested that this flow rate was damaging and caused cells to become detached. Far fewer cells were detached at the lower flow rate of 0.3 ml/min which suggests that there is a middle ground still to be found to optimise this culture condition. Although static controls were not implemented, it is clear that the flow of medium aided the survival of cells in the centre of the construct. The edges of the construct would experience the slowest flow rate; so when the average flow was too slow the cells at the edges did not survive.

1.3.10 Perfusion of Skin at an Air/Liquid Interface

This section deals with the perfusion culture of skin at an ALI. The ALI is an important signal for the terminal differentiation of keratinocytes[23]. If barrier function is required of the construct it must be exposed to an ALI to ensure this function is stimulated.

Single Pass Perfusion Culture of Keratinocytes and Fibroblasts Seeded on Scaffolds at an Air/Liquid Interface

The study by Sun *et al.* in 2005 describes the first use of a bioreactor system to culture engineered skin models at an ALI under a continuous, single pass flow of medium[7]. The rationale for using perfusion culture techniques was that build-up of harmful waste products between batch feeds could adversely affect keratinocyte growth and maturation. Therefore, the system used a single pass of medium, ensuring waste products would be discarded and not re-circulated around the system. Although the medium was supplied in a single pass manner, the flow rate applied was very low; 8.3 µl/minute which would have ensured that sufficient benefit from secreted cell factors and signals was achieved before the medium was removed.

The system was sealed allowing sterilisation, seeding and perfusion to occur within the closed environment necessary for aseptic culture of tissue constructs[7]. Keratinocytes and fibroblasts were seeded on a range of scaffolds; acellular human dermis (DED),

electrospun fibrous mat materials and non-woven cellulose scaffold (Azowipes). Initially seeding occurred under submerged conditions, and then the level of the medium was lowered to provide an ALI.

It was reported that the co-culture of fibroblasts and keratinocytes seeded on either electrospun scaffolds or acellular human dermis had a significantly higher viability by MTT assay when fed by continuous single pass perfusion for two weeks, than those that were batch fed under static conditions[7]. Therefore, perfusion culture at an ALI provides a benefit to cell viability due to enhanced nutrition.

Re-circulation Perfusion Culture of Keratinocytes and Fibroblasts Seeded on Collagen Glycosaminoglycan Sponges at an Air/Liquid Interface

Kalyanaraman *et al.* also developed a method to expose tissue engineered skin containing both keratinocytes and fibroblasts seeded on collagen-GAG sponges to ALI flow conditions[49]. The perfusion system provided a continuous re-circulating flow beneath the constructs to maintain an ALI. The system was placed in an incubator to maintain a stable temperature and concentration of gas. Keratinocytes and fibroblasts were seeded on collagen-GAG sponges and cultured either under static or perfusion conditions.

Constructs were cultured for up to 21 days under static conditions and under three different flow rates; 5 ml/minute, 15 ml/minute and 50 ml/minute to establish the most suitable flow rate[49]. Analysis of constructs was by MTT assay for viability, BrdU staining for proliferating keratinocytes and H&E stained histology to observe the morphology. The flow rate of 5 ml/minute was found to be most suitable; the higher flow rates caused the construct to produce a less organised morphology. Furthermore, constructs cultured under flow at 5 ml/minute for two and three weeks had a significantly higher viability according to the MTT assay than the static control. This

indicates that perfusion culture may enhance nutrient delivery and maintain the viability of skin constructs over an extended culture period.

Having established an appropriate flow rate for the culture of engineered skin constructs, the work moved on to *in vivo* validation of the culture technique[49]. The constructs (perfused at 5 ml/minute and static controls) were cultured for two weeks and transplanted onto an athymic mouse wound model. Under *in vivo* conditions both construct types were able to promote wound healing, decreasing the wound area with time. H&E stained histology showed engraftment of both the static and perfused grafts. These results suggest that perfusion conditions did not improve the construct sufficiently for clinical observation. This investigation has demonstrated some valuable methods to quantify and characterise the quality of constructs and provides some encouraging results and a useful starting point for the establishment of perfused skin culture at an ALI.

1.3.11 Discussion of Bioreactor Culture of Skin Materials

The literature available detailing the bioreactor culture of engineered skin materials has been introduced in this chapter. Analysis of the literature brings to light some of the issues associated with this technology which are detailed under appropriate subheadings in the following section. Understanding these issues is important to establish the requirements of future systems, how these can be achieved and to predict potential problems.

Observation of samples

The Prenosil research group, who were the second research group to develop a bioreactor related to skin culture, were also the only group to mention the desire to observe the cells over time[33,35]. Culture within a bioreactor can (depending on design) make it difficult or impossible to position the vessel under a microscope to view the

progress of the cells or engineered tissue. In this study a CCD camera with specially developed optics was used to monitor the culture over time. The camera was mounted in such a way as it could image the cells along one plane, but it was not able to move around the culture vessel to observe the whole culture which limits the field of view. Additionally, this system was only able to image one stack of the multilayered culture vessel and has to assume an even distribution of the cells.

This system was based on the principles of a light microscope to view the sample, which is excellent for observing the thin layers of cells in this study. However, this system would not be able to image opaque samples, such as the skin models based on DED which would require a different technology to enable 3D imaging through the thick, opaque material. The concept of continual imaging of samples during the culture is useful; however, the difficulty or expense of achieving this may have prevented its implementation in the other studies in the literature. Future bioreactor design should consider this problem and allow non invasive, *in situ* imaging during culture.

Maintenance of Temperature and pH

Every culture system must provide a stable environment for the cells. In addition to nutrient supply, the temperature and pH are very important variables which must be controlled. Static culture systems are stored inside an incubator which maintains the temperature at 37^{o}C and CO_2 normally at 5%; these parameters mimic the situation within the body. The concentration of CO_2 gas affects the pH of the medium; therefore the percentage of CO_2 required depends on the medium used.

Bioreactor systems are characteristically more complicated than static counterparts; often comprising separate medium reservoirs, culture vessels, connecting tubing and drivers such as pumps. This can make it difficult to position the system within an

incubator; a further consideration is the compatibility of electrical components with the warm, humid air of the incubator.

There are three options identified to ensure maintenance of temperature and pH. The first solution is to place the bioreactor system inside an incubator. It may only be essential for some of the components to be inside the incubator, such as the culture vessel and medium reservoir; other components such as electrical equipment could be positioned outside the incubator.

The second option is to heat the system by placing it on a hot plate or in a water bath and to gas the culture vessels directly. This may prove difficult due to limitations in equipment, especially when there are multiple culture vessels. Thirdly, the system can be maintained at the correct temperature by a hotplate or water bath and the buffering system of the medium can be changed. For example HEPES buffering does not require a 5% CO_2 atmosphere, so provided the culture vessel is maintained at the correct temperature, it does not need to be positioned within a gassed incubator. Table 1.1 records the methods used in the studies analysed in this chapter. In practice the method chosen is likely to be dictated by the bioreactor system implemented and the available equipment.

1. Incubator	2. Hot plate or water bath and direct gassing	3. Hot plate/ water bath and alternative (HEPES) pH buffering system
Halberstadt *et al*. (1994)	Prenosil & Villeneuve (1998)	Kremer *et al*. (2001)
Navarro *et al*. (2001)	Kino-Oka & Prenosil (1998)	
Mizuno *et al*. (2004)	Prensosil & Kino-Oka (1999)	
Seol *et al*. (2005)	Kino-Oka & Prenosil (2000)	
Sun *et al*. (2005)	Kalyanaraman & Boyce (2007)	
Lim *et al*. (2007)	Figallo *et al*. (2007)	
Kalyanaraman *et al.* (2008)	Kalyanaraman & Boyce (2009)	
Ladd *et al.* (2009)		
Palmiero *et al.* (2010)		
Lei *et al.* (2011)		

Table 1.1: Methods used to maintain temperature and pH buffering in bioreactor cultures.

Re-circulation verses single pass of medium

In perfusion systems it is possible to either allow medium to pass through the system just once in a single pass manner before it is disposed, or to re-circulate and recycle the medium. Single pass of medium ensures that a fresh supply of nutrients is supplied to the sample and that the waste products secreted by the cells are removed immediately, preventing adverse effects on the sample. Re-circulation may be advantageous by allowing contact with secreted growth factors and the sample, as they are not removed from the system. Re-circulation of medium may also provide a mechanical stimulation, as the flow of medium imparts a shear stress on the sample, which could be tuned to mimic the natural situation of blood flow in the body.

When the medium is provided in a single pass manner it would not be feasible to use a high flow rate because the medium would have to be replaced very frequently; this is

costly in labour and financially. Additionally, the beneficial growth factors secreted would be lost from the system very rapidly. By re-circulating the medium it is possible to use a high flow rate because the medium is recycled and does not need to be replaced. Therefore, when using a high flow rate the mechanical stimulation would be much higher, as shear stress depends on fluid flow speed as shown by equation 1.1.

Equation 1.1: $\tau = \mu \frac{du}{dy}$

τ = shear stress

μ = dynamic viscosity

u = velocity

y = distance from boundary plate

Each of the studies presented chooses one method of medium provision as shown in table 1.2; most studies used a re-circulation of medium. However, none of these investigations compared results obtained from the two techniques so it is not possible to ascertain which is preferable. The lack of investigation may be due to the difficulty associated with setting up a single experiment; it would be a great deal of work to compare these two methods. Furthermore, it would be difficult to choose a flow rate at which to compare re-circulating and single pass flow; re-circulating flow allows high flow rates for mechanical stimulation, and single pass flow allows low flow rates for maximum contact with growth factors before they are disposed. Furthermore, it is not feasible to compare these techniques at a range of flow rates because at high flow rates the single pass method would require a huge volume of medium which is economically unfeasible.

Single pass	Re-circulating
Halberstadt *et al*. (1994)	Navarro *et al*. (2001)
Kremer *et al*. (2001)	Mizuno *et al*. (2004)
Sun *et al*. (2005)	Seol *et al*. (2005)
	Figallo *et al*. (2007)
	Kalyanaraman *et al*. (2008)

Table 1.2: Comparing studies using single pass or re-circulation of medium.

Comparison between static and perfused samples

In order to assess the effectiveness of perfusion culture techniques it is important to compare results from perfusion culture with those from standard static culture. Additionally a fair comparison is only possible when just one variable is changed; perfusion culture or static culture. In a number of the studies investigated the standard culture conditions for static and perfused samples were not consistent which makes comparison of results less meaningful. It is possible that practicalities in setting up these experiments made it difficult to ensure consistency between conditions.

The study by Figallo *et al.* used static culture techniques to ensure biocompatibility of their scaffold, but then moved on to perform perfusion experiments without using static controls [48]. In the study by Navarro *et al*. static and perfused cultures were compared, however these experienced different feeding regimes[44]. Both static and perfused samples received the same volume of medium per sample over the culture period. Multiple perfused samples shared culture medium which was replaced every seven days, whereas individual static samples received 4 ml of medium which was half changed twice a week. It would have been more consistent to also allow static samples to share medium and perfused samples to receive the full volume of culture medium

initially. Then the effect of static batch feed and continuous perfusion could be compared.

The study by Kalyanaraman *et al*. (2008) also showed discrepancies between treatment of static and perfused samples[49]. The volume of medium provided was not consistent; perfused samples received 1200 ml of re-circulating medium weekly. Whereas, the static controls received daily medium changes of 240 ml; this is a total of 1680 ml in a week. Static samples received a greater volume of fresh medium which may have influenced the results obtained; therefore this was not a fair comparison. There was no explanation of why these volumes were chosen or why they were different. It was suggested that optimal nutrient supply would give rise to the maximal viability, but it is difficult to conclude whether differences observed between corresponding static and perfused constructs were because of the method of feeding or the volume of medium provided.

On the other hand, Sun *et al*. explained that the flow rate for their perfusion system was chosen based on delivering the same volume of medium over the same time as received by standard static cultures under a batch feeding regime[7]. Therefore, the only difference between static and perfused samples was that static samples received a batch feeding regime and perfused samples received medium in one feed which was slowly pumped past the constructs.

Flow rate

Each perfusion study investigated quotes a flow rate that was used in the experiment, however, none of the authors explain at which point in the system this flow rate applies. One may assume this is the flow rate as the fluid leaves the pump, although, it could also be assumed that this is the flow rate of fluid entering the culture vessel or flowing through the vessel. Changes in geometry within the system change the flow rate.

Ambiguity in defining the flow rate makes it difficult to compare the flow rates used in each study.

Another point to note about flow rate is how it is chosen. In most studies it appeared arbitrary. In the study by Sun *et al.* flow rate was chosen such that the perfused constructs would receive the same volume of medium as static constructs over the culture period by a single pass of medium[7]. While Halberstadt *et al.* chose the flow rate to ensure a constant gradient of nutrient depletion across the system[43]. It would also be interesting to attempt to mimic a physiological flow rate through or past the tissue by choosing a flow rate that would be similar to the *in vivo* blood flow rate in the tissue. It is plausible that quasi-physiological flow rates would be beneficial to promote angiogenic potential in constructs. However, at this stage this has not been attempted for skin tissue engineering.

Quantification of quality of constructs

It is important to be able to assess the quality of constructs to objectively determine the effectiveness of a particular culture condition or treatment. Observation of histology is a useful indicator of the quality of the tissue; correct organisation implies good functional properties, although this is not a quantitative method of determining quality. The study by Ladd *et al*. used histology to give information about viability and proliferation of the skin cells by looking at their morphology[40]. However, more quantitative or specific tests such as the MTT assay for viability and BrdU staining for proliferation used by Kalyanaraman *et al*. would be more reliable[49]. Other studies have also assessed ECM production [39,41] and mechanical properties [40,47] to obtain more information about samples.

1.3.12 Optical Coherence Tomography

The topic of optical coherence tomography (OCT) imaging will be analysed. Starting with an introduction to the theory behind the technology and moving on to its applications in dermatology and tissue engineering. A final focus will be the previous work undertaken imaging the MacNeil group's reconstructed TE skin model.

OCT is an imaging technique that is often described as an optical analogue to ultrasound imaging[50]. OCT produces greyscale cross sectional images of the structures within a sample based on changes in refractive index. OCT imaging is well suited to biological applications due to its properties of non-invasive, non-contact[51] image acquisition and safety; the StratusOCT 3 (Carl Zeiss Meditec, USA) OCT system received FDA approval in 1993[52]. Furthermore, exogenous contrast agents are not necessary as image contrast is formed by the internal structure of the sample[53]. The use of OCT for *in vivo* use was first described in the field of ophthalmology in 1993[54–56], and since then has become well established in this field[57]. OCT also has *in vivo* applications in detection of epithelial cancers[58], dermatology[53,59] and intra-vascular[60,61] imaging.

1.3.13 OCT Theory

OCT interrogates the sample using a near infra-red beam of light; when the incident beam reaches a boundary between structures it experiences a difference in refractive index. This causes a proportion of the light to be back-scattered and detected as the sample signal. The Fresnel equations describe the proportions of the incident beam that are reflected and transmitted at a refractive index boundary[62]. In contrast to ultrasound imaging, the sample signal cannot be directly detected as the speed of light is too fast ($3x10^8$ m/s). Therefore, a Michelson interferometer is implemented[63]; this device uses a beam splitter to equally split the incident signal into a sample and reference arm, figure 1.2 shows a diagram of the setup. The sample arm beam reaches the sample and is

back-scattered; simultaneously the reference arm beam reaches a mirror and is reflected[64,65].

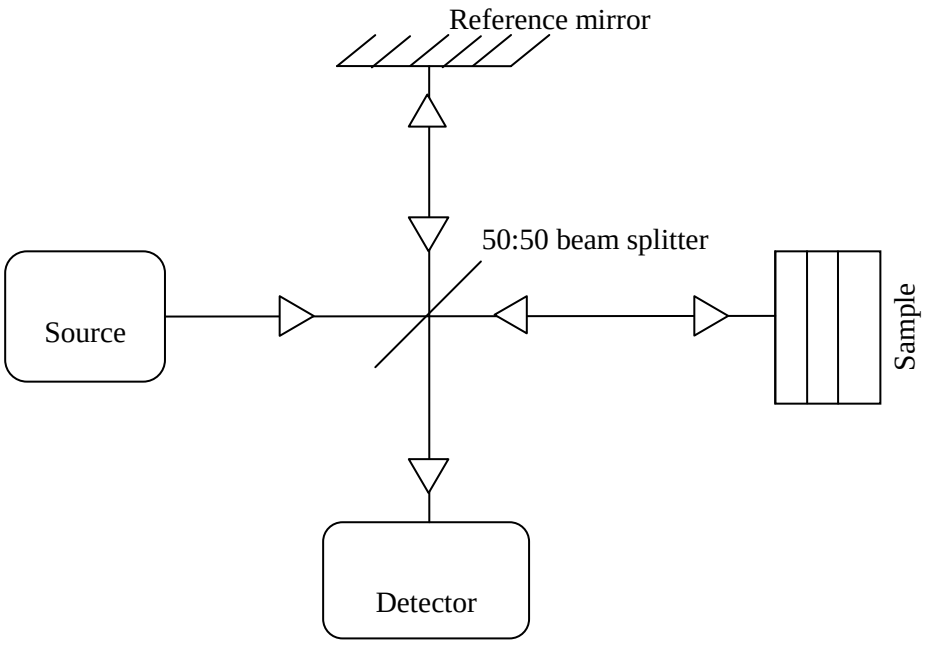

Figure 1.2: Schematic diagram of a Michelson Interferometer

This diagram depicts a Michelson interferometer. The light leaves the source and reaches a half silvered mirror which splits the beam equally into a reference arm and a sample arm. The light travels along these respective paths until it reaches the mirror (reference arm) and a refractive index mismatch (sample arm) where it is reflected and retraces the original path. When it reaches the half silvered mirror, the light from the two paths recombine by superposition and is detected by the detector.

The reflected sample and reference beams superimpose; interference occurs when the two beams are matched to within one coherence length, indicating that the beams have travelled the same distance. This constructive interference creates the OCT signal. This signal encodes information of the depth at which the interaction and subsequent back-scattering occurred and the size of the difference between the refractive indices of the internal structures. OCT assumes that each photon of light is only scattered once,

therefore multiply scattered photons contribute to noise in the system[66]. This issue is minimised by the rejection of signals outside the coherence gate[67].

1.3.14 Image Production

An A-scan is a single interrogation into the depth of the sample at one lateral position; it is a sequence of intensity values through the depth of the sample[64]. In order to create a two dimensional image of the internal structure the beam is scanned along the lateral direction of the sample to obtain multiple adjacent A-scans. These adjacent A-scans are combined and plotted as a greyscale map of intensities known as a B-scan. This gives information about the size and depth of refractive index boundaries and consequently the location of these structures. Advances in technology have increased the image acquisition rate to enable volumetric imaging[68]. In this case the beam is scanned in a raster pattern to collect sequential B-scans which can be used to build up 3D volumetric datasets known as C-scans.

1.3.15 Resolution

The resolution of OCT images is approximately 15 μm in the lateral direction[64] and falls between that of ultrasound which has a lower resolution, and confocal microscopy which has a higher resolution. The use of light in OCT image acquisition, which has a smaller wavelength than the sound waves used in ultrasound accounts for the increased resolution when compared to ultrasound imaging. However there is a trade-off between increased resolution and depth penetration which is compromised[52,69]. One unusual feature of OCT is that the axial and lateral resolutions are decoupled and are affected by different parameters. The axial resolution depends on the coherence length of the light source and can be increased by using low coherence light sources. The axial resolution is given by equation 1.2. The lateral resolution is determined by the optics of the system; the focused spot size of the beam. Equation 1.3 defines the lateral resolution.

Equation 1.2: $\Delta z = \frac{2ln2}{\pi n} \frac{\lambda_o^2}{\Delta\lambda_{FWHM}}$

Where:

λ_o = central wavelength

λ_{FWHM} = full width at half maximum of spectral profile

n = refractive index of the sample

Equation 1.3: $\Delta x = \frac{4\lambda}{\pi} \frac{f}{d}$

Where:

Δx = lateral resolution

λ = source centre wavelength

f = focal length of the lens

d = spot size on the objective lens

1.3.16 Tissue Optics

In *in vivo* skin chromophores such as melanin and haemoglobin are major causes of absorption[70], while differences in structure and consequently refractive index cause scattering[59,70]. Scattering is a particularly important interaction in the dermis. The wavelengths in the near infra-red region of the electromagnetic spectrum are used in OCT imaging of biological tissues; these wavelengths produce the most favourable outcome in terms of absorption, scattering and depth penetration[71].

1.3.17 OCT Imaging in Dermatology

OCT has a long standing history of use for *in vivo* imaging having first been applied in ophthalmology in 1993[54], two years after the first publication introducing this technology. Imaging of the eye was a natural place to begin as the transparency of the eye tissues allowed excellent penetration of the incident beam[51]. The first published record of OCT for observation of the skin was in 1997[72]. Imaging of turbid tissues such as the skin has proven more challenging than imaging of the eye as signals are quickly attenuated upon entry into the tissue due to their highly scattering nature. Therefore, application in dermatology has not been so widespread.

Alternative non-invasive methods of imaging the skin are high frequency ultrasound[73] and confocal microscopy[72]. However, the gold standard for observation of skin morphology is histology which is highly invasive and non-repeatable, creating a wound where the sample is taken[51]. High frequency ultrasound has the advantage of greater depth penetration than OCT imaging, but decreased resolution. Confocal microscopy has a lower depth penetration than OCT imaging but a higher resolution and can distinguish individual cells[72]. The penetration of OCT beams is sufficient to observe the epidermis and papillary dermis which is ideal to investigate epithelial health[72].

The structure of normal healthy *in vivo* skin is described in the literature[69,72]. The stratum corneum is only visible in areas where it is at its thickest; these are palmoplantar regions such as palms of hands and soles of feet. In these regions the stratum corneum appears as a thick dark layer, the signal is low as this structure is poorly back-scattering. The living part of the epidermis has a brighter signal than the stratum corneum and these structures are easily distinguished. Finally the dermis begins when the signal drops off under the living epidermis; collagen fibrils in the dermis create a more highly scattering, brighter signal and cause the signal to increase again. In other areas of the body, such as the forearm, the stratum corneum is not visible as it is

not resolved by OCT. However, in this case the contrast between the epidermis and the dermis is increased and appears more clearly defined. There is a bright entrance signal above the dark, poorly back-scattering epidermis which is followed by a brighter signal caused by the dermis.

In addition to distinguishing the epidermal and dermal regions of the skin, structures including blood vessels[59], sweat ducts[72], hair follicles[59] and eccrine ducts[74] could be distinguished qualitatively in normal skin. However, individual layers, cells or subcellular structures are too small to be resolved by OCT imaging[72]. OCT has also been used to investigate disease pathologies; this imaging technique has the advantage that it is non-invasive and real time compared to histology. OCT has the potential for use to detect the location of the pathology, the severity and effectiveness of treatments. Conditions such as psoriasis and contact dermatitis[59], lentigo maligna melanoma and the scabies mite have been observed[72]. A comprehensive list of pathologies has been considered[53].

OCT can be used to determine the effects of topical application of lotions and drugs. Lademann *et al*. (2005) showed that the hydration of the skin could be investigated following application of moisturizing treatments; dry skin exhibited bright spots in the stratum corneum on OCT images which disappeared as the treatment began to take effect[75]. The time dependent changes associated with irritation by sodium dodecyl sulphate (SDS) have also been investigated[73].

This qualitative information is very valuable to give an indication of what is happening inside the skin. However, quantitative information is also important to remove subjectivity from the analysis. Examination of the averaged A-scan, at the region of interest can give objective information about the situation. The literature has used this averaged A-scan to determine the epithelial thickness. Studies by Welzel *et al.* identified the peak to peak distance as the distance from the surface to the dermal-

epidermal junction[59,73]. However, work by the Gambichler group later determined that this measurement was an overestimation and that the distance from the entrance peak to the valley before the second peak was a more reliable measurement of epidermal thickness[51,74,76,77].

In order to establish the accuracy of epithelial thickness measurements from the averaged A-scan, comparisons were made between measurements from OCT images and histology. However, it was noted that standard formalin fixed and paraffin embedded histology methods caused distortion of samples and so this was not a valid comparison[77]. It was found that performing cryostat histology caused less distortion and a more accurate comparison[76].

Subsequently the manual measurement of epithelial thickness by line tracing of the epithelium was investigated and considered to be more accurate than use of A-scan measurements in comparison to cryostat histology measurements[76]. Additionally epithelial thickness has been measured manually at five predetermined locations across the OCT image according to variations in brightness and averaged between these locations[74]. This method was considered to be feasible to undertake and found that epithelial thickness decreased as the age of the volunteer increased. However, comparison between these measurements and histology were not possible as volunteers were healthy and biopsy was not justified.

OCT has been used in a range of clinical circumstances in dermatology from understanding the normal state of the skin, to disease characteristics and treatment effects. The technique has been used to provide qualitative images which could be interpreted by a trained observer. However, moves towards more objective quantitative methods of analysis, such as measurement of the epithelial thickness have also been explored. Challenges arose in the validation of epithelial thickness measurements from OCT images in comparison with similar measurements from histology. It was

preferable to use cryostat histology as this technique minimised distortion artefacts, maintaining original geometry. Epithelial thickness can give information on disease state, and could be compared to values measured at multiple time points to assess changes following application of treatments.

1.3.18 OCT Imaging in Tissue Engineering

The properties that make OCT imaging well suited to *in vivo* imaging also advocate its use in tissue engineering to assess development of engineered constructs during culture. OCT is a non-contact technique, so unlike ultrasound it can interrogate the sample without contact between the detector and the sample. This is important in tissue engineering to maintain sterility of constructs. Thus, the ability to observe development of constructs in a non-invasive way allows assessment of the development with time. Furthermore, when constructs are required for clinical use OCT imaging could become an invaluable tool in quality control when histology is not feasible due to constraints with time and the requirement to destructively remove a biopsy of the construct for histology. In addition efficiencies can be made in time course experiments if samples are not destroyed at each time point, reducing costs and use of materials.

The imaging of tissue engineered constructs was investigated by Mason *et al.* (2004). This group described the utility of OCT imaging for quality control of tissue engineered constructs in terms of the ability to assess microstructure and defects *in situ* within a bioreactor[52]. Mesenchymal stem cells were incorporated into a sodium alginate gel to form tubular coronary artery like structures. Initial images showed the ability of *in situ* OCT imaging to distinguish cells in the hydrogel which were indicated by bright spots due to their higher refractive index.

The study by Yeh *et al.* (2004) investigated OCT imaging of burn healing in an *in vitro* skin model based on collagen matrix[78]. The constructs were cultured at an air/liquid interface and wounded using a Nd:YAP laser. Burning the skin construct caused

structural changes to the collagen which was manifested as a decrease in OCT signal. Over 7 days the construct began to repair and the OCT signal increased in the burned region. This study highlighted the importance of imaging the same location at multiple time points, but did not describe how this was achieved.

Yang *et al.* (2006) later described another investigation of OCT in tissue engineering[79]. Bone cells were seeded into a porous poly(l-lactic acid) scaffold and imaged using both a time domain OCT system and a full field OCT system. The time domain images were able to display the porous nature of the scaffold; the scaffold material was highly scattering, and the air in the pores was poorly scattering so walls appeared bright and pores appeared dark. When bone cells were seeded into these scaffolds it was observed that the pores became filled with cells. After 5 weeks culture the penetration depth of the images was decreased and the pores were filled in, indicating development of the constructs.

The full field OCT system produced en face, rather than cross sectional images of the constructs at a higher resolution than the time domain system[79]. After 1 week of culture, cross sectional full field OCT images could discern clusters of cells and the walls of the scaffold, although contrast was very poor as the refractive indices of these structures were similar. Adherence of magnetic beads with a high refractive index onto the exterior of the cells created contrast to distinguish cells from the scaffold walls.

The study by Spöler *et al.* (2006) built on the concept of using OCT to visualise the structure of the sample by using this imaging technique to monitor development of engineered constructs over time[80]. Engineered skin constructs were produced by seeding keratinocytes and fibroblasts into collagen gels which were cultured at an air/liquid interface. The authors identified the ability of OCT to allow time course investigations of the same sample, rather than examining different samples at each time point. In order to find the same location repeatedly full thickness holes were cut into the

samples as reference points to allow repeated imaging of the same location. Histology and immunohistochemistry were completed on this image location in order to validate the work.

In this study the epidermis was characterised by low signal intensity, while the dermis was highly scattering and appeared bright[80]. A-scans were used to obtain information on the location of structural differences; ten adjacent A-scans were averaged. By day 7 of the experiment the epidermis remained proliferative and had not developed a stratum corneum. A deep valley below the entry signal of the A-scan indicated the location of the dermal/epidermal junction. On day 12 of the investigation a stratum corneum had developed and was characterised by a less scattering region on the OCT image in comparison to the living, proliferative epidermis. In the A-scan the stratum corneum was signified by an additional steep valley directly below the entry signal.

1.3.19 Investigations of the Use of OCT imaging of the MacNeil Reconstructed Skin Model

Collaborations between the MacNeil and Matcher research groups have provided some initial studies assessing the ability of a swept source OCT system to non-invasively image the reconstructed skin model based on DED. The OCT system implemented was a swept source Fourier domain system. The source was a swept laser with a central wavelength of 1300 nm. The mean spot size produced by the system optics was 25 µm which also describes the lateral resolution. The axial resolution was 10 µm in air[8,81].

OCT was implemented as a method to overcome the disadvantages of conventional imaging techniques. Standard light microscopy was not possible since the samples were opaque and had a three dimensional structure. Confocal microscopy was not suitable due to limitations of depth penetration and requirement for exogenous contrast agents. While histology is the gold standard method of morphological assessment, it is destructive and time consuming to perform[82].

Using OCT it was possible to image samples *in situ* within their normal culture environment; in culture plates at an air/liquid interface without any preparation. The ability to observe the sample *in situ* during culture allows the investigator to see the real structure without the distortions produced during processing for histology. Distortion and shrinkage of samples in the process of performing histology have previously been reported[83–85]. OCT imaging also holds potential for delicate samples and those that cannot be exposed to the solvents used in histological processing.

Initially skin constructs containing keratinocytes and fibroblasts based on both collagen gels and DED were investigated using a swept source OCT system[8]. It was found that those samples based on DED exhibited more image contrast than those based on collagen gel. Therefore, skin constructs based on DED were investigated further. The OCT imaging system was able to distinguish between the epidermis and the dermis; however, the resolution of the system limited the ability to observe the undulations of the rete ridges in the skin construct. Although, it was noted that prior to the addition of the cells, the undulating surface of the DED was visible. Following the application of fibroblasts and keratinocytes, the surface became smooth and over time a highly scattering epidermis developed and increased in thickness. The images shown appeared to indicate a bright stratum corneum at the surface, above a dark living epidermis and below that the brighter dermis, which corresponds to *in vivo* observations of normal skin (not palmoplantar skin)[69]. The observations from OCT images were verified by comparison with formalin fixed and paraffin embedded histology[8].

In addition this swept source OCT system was also used to image melanoma invasion and wound healing on the reconstructed skin model based on DED[81]. Observation of the OCT images demonstrated that the presence of melanoma cells caused the surface of the sample to become irregular and not smooth. Samples were also wounded by using a scalpel to cut through the thickness of the construct to follow the progression of wound

healing with time. The effect of the addition of a fibrin clot into the wound was assessed in terms of the rate of healing. OCT imaging was able to distinguish the extent of the wound and the presence of the fibrin clot when included. It was found that presence of the fibrin clot appeared to accelerate wound healing[81]. These studies highlighted the need to be able to repeatedly image in the same location at multiple time points to observe the progression of the same region. The investigators endeavoured to image in the same locations in the centre and at the edge of the constructs at each time point, although specific methods to achieve this were not described.

1.3.20 Summary of the Literature

In summary, the TE skin model established by the MacNeil research group mimics the morphology of native skin to provide a good imitation. It lacks structures such as hair follicles and sweat ducts and does not create the pigmentation produced by melanocytes as the cell types required are not included in the culture. The structure is expected to be fully developed between ten and fourteen days of culture at an ALI, however, beyond this time the organisation deteriorates. It would be advantageous to increase the restricted lifespan of the constructs to address this limitation.

Clinical use of TE skin has undergone preliminary tests to ascertain its suitability; aside from the time constraints over when it can be transplanted, it was found that "take" on difficult wound beds was not successful. This problem may be solved by promoting angiogenesis in the construct prior to transplantation onto a patient so that it may achieve vascularisation more quickly. Furthermore, the ability to non-invasively assess the progress of the construct during culture has not become routine; destructive histology is still the gold standard to ensure quality. The incremental advances in the technology and knowledge of culturing TE skin have been described. The implementation of perfusion culture techniques in the culture of TE skin may provide a further progression in the technology.

There are only a very limited number of publications available documenting the culture of skin materials in bioreactors. The system that has received the greatest success is the Kerator automated bioreactor used for the scale-up production of keratinocytes. A few studies were published from 1998-2000, and then two more were released by a different research group in 2007 and 2009. With this exception, the general trend in the field of bioreactor culture of skin is for each publication to come from a different research group, with work in these groups not being continued in the future.

Publications in bioreactor culture of 3D skin materials were released between 1994 and 2010, in recent years this field seems to have stagnated. The most recent study into the perfusion culture of engineered skin at an ALI was in 2008. This suggests that the solutions for the perfusion culture of TE skin at an ALI that have been developed to date have not been feasible as the work has not been continued. Many of the studies presented lacked consistent controls or have not exploited as much analysis as could have been implemented, so data obtained is minimal. Additionally, the investigations are fairly small and did not appear to progress beyond preliminary studies. These issues suggest that the development of a bioreactor system for the culture of skin is challenging.

Many research groups have identified a requirement for a bioreactor in which to culture engineered skin materials. The challenge to develop such a system has not been resolved to date, although there are a few studies that have made tentative steps in this direction. Future work would produce a system with close control over environmental aspects such as temperature, metabolites and CO_2, provide an ALI, enhanced nutrition and also allow imaging of the tissue without disturbing the culture.

OCT is an imaging technique that has shown potential in tissue engineering due to its non-invasive implementation. The OCT imaging of the MacNeil group's reconstructed skin model has been demonstrated; time course experiments have been investigated

along with the ability to use OCT to distinguish wounding of the skin model. The images obtained have been used qualitatively, but movement to quantitative measurements of the epithelial thickness or analysis of A-scan shape as implemented in dermatology have not been made.

1.4 Design Requirements for a Perfusion System to Culture TE Skin at ALI

This section describes the essential and desirable design features of a perfusion bioreactor system to culture TE skin at an air/liquid interface. Most simply this is to provide the same basic attributes as static culture, with some additional features specific to perfusion. Figure 1.3 shows the design considerations for perfusion culture of TE skin at an ALI.

It is of paramount importance that the system maintains a sterile environment in which to culture the tissue. Contamination of the sample would render the work useless as reliable results could not be collected. Additionally, the system must be able to maintain sterility over long culture periods to enable the testing of the hypothesis that perfusion would increase the lifespan of constructs. Sterility must be maintained for at least four weeks.

The system must allow provision of the correct environmental conditions. In static culture this is achieved by placing plates inside CO_2 incubators which maintain an atmosphere at 5% CO_2, 95% humid air and a stable temperature of 37^{o}C. Provided that these conditions are satisfied, the perfusion system would not need to be placed inside an incubator; these conditions could be supplied by different means. Furthermore, the system must allow the gas to enter the system without allowing contamination.

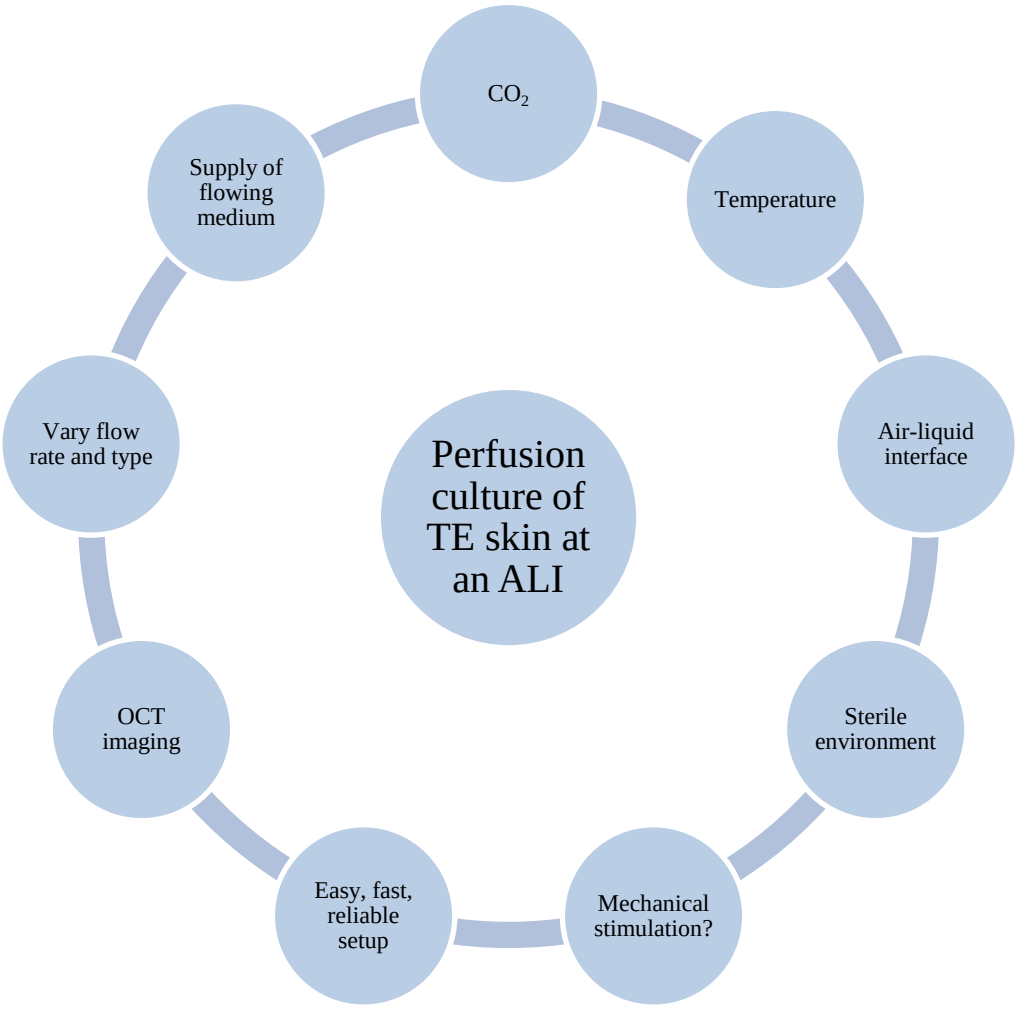

Figure 1.3: Flow chart documenting considerations for perfusion culture of TE skin at an air/liquid interface.

The perfusion system must allow a method to provide a supply of culture medium to the sample in a simple way and without route for contamination. It must be possible to allow the medium to flow through the system and past the construct while maintaining an ALI. It must be possible to vary the flow rate and to investigate both re-circulation and single pass of medium through the system.

The system must provide a stable ALI in a reliable manner. The sample must be supported such that the dermal region has good contact with the medium and can receive adequate nutrition. The epidermal region must be in contact with the air to

promote differentiation of keratinocytes. As previously noted the air must be sterile. The level must be stable even when the system or components of the system are moved to different heights or if the temperature changes.

The culture vessels should allow for easy storage during culture. They must stay upright and should use space efficiently. It must be possible to carry out multiple repeats at the same time. The system should be easy and fast to set up to prevent mistakes and reduce labour costs. The size of the reservoir bottle should be flexible. Another feature that may be desirable in a perfusion culture system is the ability to provide mechanical stimulation to the sample; this is likely to be in the form of shear stress provided by the flow of medium past the construct.

It is desirable to monitor the development of the tissue during culture. This must be *in situ* within the culture vessel and in a non-invasive manner to enable the culture to continue afterwards. The imaging technique specified in this project is OCT. To enable OCT imaging *in situ* while maintaining the sterility of the system, the vessel must be closed but still permit the OCT beam to reach the sample. Therefore, there must at least be a region in the culture vessel above the sample that allows the OCT beam to enter. The thickness of this region and the refractive index of the material must be minimised to reduce negative effects on image quality. The lid of a well plate has been successfully imaged through previously[8], it is approximately 1 mm thick transparent polystyrene. Therefore, similar materials would be appropriate to create an imaging window in the culture vessel.

The major issue with achieving OCT imaging of samples within culture vessels is the working distance of the lens which dictates the permissible height of the culture vessel. The lens must be positioned a specific focal distance from the sample to produce an in focus image. The focal distance depends on the lens specifications. Table 1.3 shows some of the specifications of lenses that this research group has access to. The LSM02

lens is the most desirable lens to use as it has the finest resolution; however this is at the price of working distance. When the LSM02 lens is used, the surface of the sample must be positioned 7.5 mm from the lens which limits the height of the culture vessel above the sample. The LSM03 lens can accommodate a taller culture vessel as it has a larger working distance.

Lenses (Thorlabs, New Jersey, USA)	LSM02	LSM03
Magnification	10X	5X
Lens working distance	7.5 mm	25.1 mm
Mean spot size	13 µm	25 µm

Table 1.3: The focal distances, magnifications and spot sizes of the Thorlabs lenses used in this work.

These design requirements set out must be considered in the design of perfusion systems to culture TE skin at an ALI.

1.5 Project Outline

In order to develop improvements in the culture of TE skin, the design and optimisation of a perfusion culture system is discussed. The use of OCT as an imaging technique for the study of TE skin is considered in response to developing imaging techniques for the observation of 3D skin constructs during culture. Finally these concepts are brought together to assess the utility of implementing perfusion culture for TE skin, and how OCT can be used to observe the TE skin *in situ* without using invasive or destructive techniques.

2. MATERIALS AND METHODS

2.1 General Materials and Methods

2.1.1 Culture Medium

Fibroblasts were cultured in fibroblast medium which consisted of Dulbecco's Modified Eagles Medium (DMEM) (Labtech International, East Sussex, UK) supplemented with 10% v/v foetal calf serum (FCS) (Labtech International, East Sussex, UK), and 2×10^{-3} mol/l l-glutamine, 100 IU/ml penicillin, 1000 µg/ml streptomycin and 250 µg/ml amphotericin B (all Sigma-Aldrich, Dorset, UK).

Keratinocytes were cultured in Green's medium which consisted of a 3:1 ratio of GlutaMAX DMEM (Invitrogen, Paisley, UK) and Ham's F-12 (Labtech International, East Sussex, UK) supplemented with 10% v/v FCS and 100 IU/ml penicillin, 1000 µg/ml streptomycin and 0.625 µg/ml amphotericin B, 5 µg/ml transferrin, $2x10^{-7}$ mol/l triidothyronine, 5 mg/ml insulin, 0.4 µg/ml hydrocortisone, 10^{-10} mol/l cholera toxin, 10 ng/ml epidermal growth factor and $1.8x10^{-4}$ mol/l adenine (all Sigma Aldrich, Dorset, UK).

2.1.2 Production of De-Epidermized Dermis

Skin was obtained from patients undergoing breast reductions and abdominoplasties. In accordance with NHS Research Governance procedures, fully informed consent was sought to enable use of waste tissue for research purposes under a protocol approved by the Ethics Committee of the Sheffield University Hospitals NHS Foundation Trust.

Split thickness human skin was incubated overnight in sterile 1M sodium chloride solution at 37^{o}C. This caused the epidermis to split from the dermis and to destroy viable cells within the dermis, while preserving the basement membrane and extracellular matrix. The following day the epithelium was peeled from the dermis and

disposed. The dermis was washed vigorously in phosphate buffered saline (PBS) three times and then incubated in medium for at least 48 hours to confirm sterility[4].

2.1.3 "3T3" Cell Culture and Irradiation

Murine 3T3 fibroblast cells were expanded in the laboratory, initially in T-75 flasks and then in cell stacks using fibroblast medium with new born calf serum (Labtech International, East Sussex, UK) substituted for the foetal calf serum. Cells were passaged with trypsin/EDTA (Sigma-Aldrich, Dorset, UK) which was deactivated with medium when the cells had detached. The cell suspension was then irradiated with a dose of 60 Grays to prevent proliferation. Irradiated cells were known as i3T3 cells and were frozen for storage in 90% FCS and 10% dimethyl sulfoxide (DMSO) (Sigma Aldrich, Dorset, UK) and stored in liquid nitrogen until required.

2.1.4 Keratinocyte Isolation and Culture

Keratinocytes were isolated as described by Rheinwald and Green (1975)[17]. Split thickness skin was cut into small squares, roughly 0.5 cm^2, and incubated at 4^oC overnight in 0.1% Difco Trypsin (Difco Labs, Michigan, USA). The epidermis was removed and the papillary surface of the dermis was gently scraped with a scalpel. The resulting cell suspension was centrifuged at 200g for 5 minutes and the pellet was resuspended in Green's medium and seeded in T-75 flasks with irradiated 3T3 murine fibroblasts (i3T3).

Medium was replaced three times a week. Cells were passaged when 70-80% confluent and re-plated with fresh i3T3 cells and used until passage 3. Stocks of keratinocytes were produced by freezing cells in 90% FCS and 10% DMSO and stored in liquid nitrogen.

2.1.5 Fibroblast Isolation and Culture

Fibroblasts were isolated (as described by [4]). Subsequent to keratinocyte isolation, the discarded dermis was minced very finely using a scalpel and incubated at 37^{o}C overnight in 0.5% collagenase A (Sigma Aldrich, Dorset, UK) solution in DMEM. When the skin was almost completely digested the solution was centrifuged at 400g for 10 minutes. The pellet was resuspended in fibroblast medium and initially seeded in a T-25 flask (subsequent passages were expanded and cultured in T-75 flasks).

Medium was replaced approximately twice a week. Cells were passaged when 80-90% confluent and used between passage 4 and 9. High passages were used to increase the purity of the cell population; without specific medium supplements other cell types die out. Stocks of fibroblasts were produced by freezing cells in 90% FCS and 10% DMSO and stored in liquid nitrogen.

2.1.6 Production of TE Skin Constructs

Skin constructs were produced (as described by [24]), co-seeding 300,000 keratinocytes with 100,000 fibroblasts in Green's medium within a 1 cm diameter stainless steel ring onto the papillary surface of DED. After 24 hours the medium within the ring was replaced. On the second day of submerged culture the constructs were raised from the bottom of the culture plate to an air/liquid interface (ALI) by positioning on 2-3 mm tall perforated stainless steel grids to allow media to reach the underside of the dermis. Medium was changed 2-3 times a week; each construct would require approximately 5 ml medium to reach the underside of the grid. However, exact volume of medium depended on the height of the grid. Constructs were usually cultured for a period of 14 days.

2.1.7 Histology

At the end of each experiment the skin constructs were washed with PBS and fixed in 3.7% formaldehyde solution in PBS at 4^{o}C for at least 24 hours. Samples were processed for histology (Leica TP 1020 tissue processor), then embedded in paraffin wax (Leica EG 1160 tissue embedding centre) and sectioned into 4-6 μm sections using a microtome (Leica RM 2145). Sections were placed in a water-bath to unfold and collected on microscope slides. Slides were placed to dry on a hot plate until the wax had adhered to the slide.

Standard haematoxylin and eosin (H&E) staining was performed. Briefly slides were de-waxed using xylene and rehydrated in decreasing concentrations of alcohol. They were stained with haematoxylin and washed with tap water. Then they were stained with eosin and dehydrated with increasing concentrations of alcohol and cleared using xylene. Finally slides were mounted with a coverslip and observed under a light microscope to examine the general morphology of the constructs.

2.1.8 Perfusion Systems

The Watson Marlow 205U peristaltic pump was used in all setups to propel medium through the system. Silicone tubes and luer connectors were used to connect components. Water dyed with blue food colouring was used to simulate liquid flowing through the system during bench top optimisation experiments. The colour allowed simple observation of the position of the liquid. Filters were used to clean the air entering the system; 0.2 μm pore filters (Sarstedt, Leicester, UK) enabled gas exchange with sterile air.

2.1.9 OCT Systems

In-House Swept Source OCT System

The in-house swept source OCT system implemented has previously been described[8,81] and a schematic diagram is shown in figure 2.1. Briefly the source, data acquisition and PC were part of the Michelson Diagnostics EX1301 system and connected to an in-house fibre optic Michelson interferometer. The source was a swept source laser with central wavelength of 1300 nm, a full width half maximum value of 110 nm and sweep rate of 10 kHz. The axial resolution in air was 10 µm. The lens used was the LSM03 (Thorlabs, New Jersey, USA) which had a working distance of 25.1 mm and a lateral resolution of 25 µm.

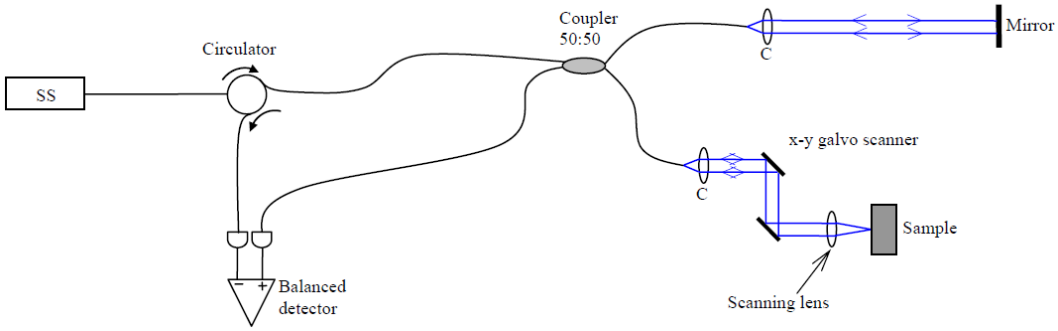

Figure 2.1: Schematic diagram of the in-house swept source OCT system

Diagram reproduced with permission from SPIE from [81].

Smith, L E; Lu, Z; Bonesi, M; Smallwood, R; Matcher, S J; MacNeil, S "Using swept source optical coherence tomography to monitor wound healing in tissue engineered skin" Progress in Biomedical Optics and Imaging ***7566****, pp75660I–75660I (2010)*

In-House Polarisation Sensitive Swept Source OCT System

An in-house polarisation sensitive OCT system was also used as shown in the schematic diagram in figure 2.2. Polarisation sensitive OCT is used to determine structural information from the birefringence properties of the sample. In this study standard structural information that was obtained by combining horizontally and

vertically polarised images. This system used the same components as the in-house swept source OCT system[86].

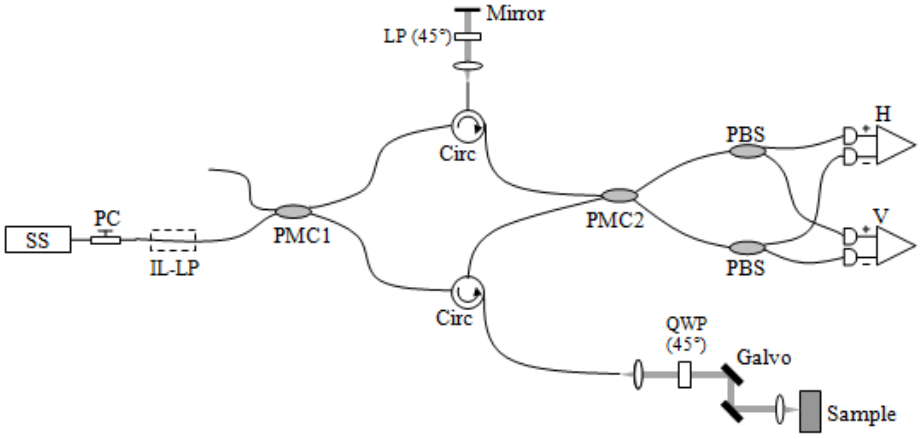

Figure 2.2: Schematic diagram of the in-house polarisation sensitive swept source OCT system.

SS: swept source, PC: polarization controller, IL-LP: in-line linear polarizer, PMC: polarization-maintaining coupler, QWP: quarter waveplate, PBS: polarization beamsplitter, H and V: balanced photo-detectors for horizontally and vertically polarized optical signals, respectively. Image kindly provided by Zenghai Lu.

EX1301 Commercial OCT System

In addition the EX1201 *in vitro* multi-beam OCT microscope system (Michelson Diagnostics, Kent, UK) was implemented in the OCT characterisation experiments. The lens was LSM02 (Thorlabs, New Jersey, USA) with working distance of 7.5 mm and lateral resolution of 7.5 µm. The axial resolution was 10 µm in tissue.

2.1.10 Preparation of TE skin for OCT imaging

Samples were sealed in standard culture vessels to prevent spillages of medium. For transportation to the imaging systems samples were placed inside a polystyrene box with a warm bottle of water to maintain temperature and reduce condensation on the lid of the vessel which deteriorated image quality. In this way samples were transported to

the OCT facility. Condensation was removed from the lid by gently warming with a hair dryer.

In-House Swept Source OCT System and In-House Polarisation Sensitive Swept Source OCT System

The in-house swept source OCT system and the in-house polarisation sensitive system used lenses with a long working distance. Imaging of samples was possible in 6 well culture plates which were sealed with autoclave tape to prevent spillage of culture medium.

EX1301 Commercial OCT System

Samples imaged by the EX1301 commercial system were cultured on the shortest stainless steel grids within a Petri dish which had a lower lid than the 6 well plates to accommodate the use of a lens with a shorter working distance. Dishes were sealed with autoclave tape

2.1.11 OCT Imaging of TE Skin Samples

Samples were placed on the OCT stage which was manipulated in horizontal and vertical directions. The horizontal movements could locate the area of the sample to be imaged. The vertical movements focussed the image on the screen to find the optimal distance from the lens. Images were taken at multiple locations across the sample to obtain a representative analysis of the sample composition. Following OCT imaging samples were returned to culture.

2.2 First Generation Perfusion System

The system in its entirety was provided by Kirkstall Ltd, Sheffield, UK. An air filter (0.2 μm pore size) was positioned on the reservoir to permit gas exchange with the medium, while maintaining sterility. Tygon silicone tubing (SLS, Yorkshire, UK) was

used to connect system components together. Marprene pump manifold tubing (Watson Marlow, Cornwall, UK) was used to connect the system to the pump.

The setup of the first generation system is shown in figure 2.3. Three chambers were connected in series to a 20 ml reservoir bottle and the pump. The pump drew medium from the reservoir, through the chambers and returned it to the reservoir allowing re-circulation of medium. The whole system was placed inside a CO_2 incubator. The chambers were modified by addition of an input and output tube in the lower half of the chamber. A stand was inserted to support the sample at the ALI. A glass coverslip was used to create a window in the roof of the chamber to allow OCT imaging.

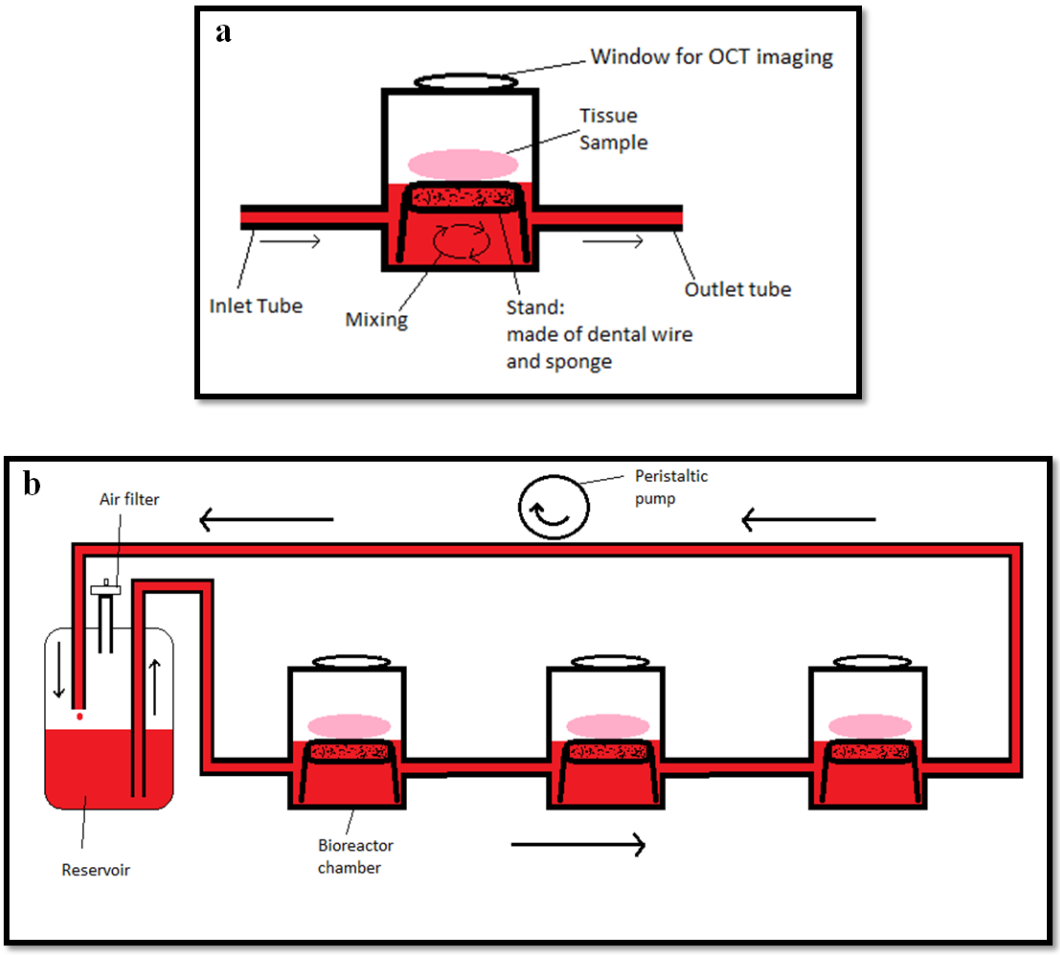

Figure 2.3: Schematic diagrams of the first generation "Pisa" air/liquid interface perfusion system.

a) Diagram of the bioreactor chamber with features labelled. The tubes shown were added to the chamber by cutting holes to allow insertion and gluing in place. A window was added in the lid with a glass coverslip to provide a window for OCT imaging. A stand was inserted inside the chamber to lift the tissue sample to an air liquid interface. b) Diagram of the perfusion system showing three chambers connected in a series configuration. The reservoir was connected to three chambers in series; the chambers were connected from output to input and then the final output tube passed through the peristaltic pump which pulled the medium through the chambers. Medium was returned to the reservoir and was re-circulated through the system in a continuous manner. An air filter was positioned on the reservoir so that gas exchange could occur.

2.3 Second Generation Perfusion System

2.3.1 System Setup

The modified chambers including aluminium stands were provided by Kirkstall Ltd. A 100 ml glass bottle was used as the reservoir. A 0.2 μm air filter was positioned on the reservoir and the chamber to enable gas exchange. Versilic silicone tubing (SLS, Yorkshire, UK) was used to connect system components together and as pump manifold tubing. An alternative stand for ALI was produced from sponge (Boots No 7 facial exfoliating sponge, Boots, Nottingham, UK) which was cut to size to fill the chamber up to the height of the ALI.

2.3.2 Increasing Output Flow Rate

The output flow rate was increased by using adjusters on the clips that held the tube onto the pump to change the compression of the tube. A short section of the 1.5 mm internal diameter silicone tubing was attached to the pump and the input end was positioned inside a reservoir of water. The pump was switched on at 10 rpm and once the system had stabilised after 5 minutes the output was positioned inside an empty container. The volume of water that passed through the pump in 5 minutes was determined by mass.

Positive positions on the adjuster increased the compression of the tube and decreased the flow rate through the tube. Negative positions on the adjuster decreased the pressure on the tube and increased the flow rate through the tube. Therefore, the maximum difference in flow rate was created by using a positive compressed position on the chamber input tube and a negative lightly compressed position on the chamber output tube.

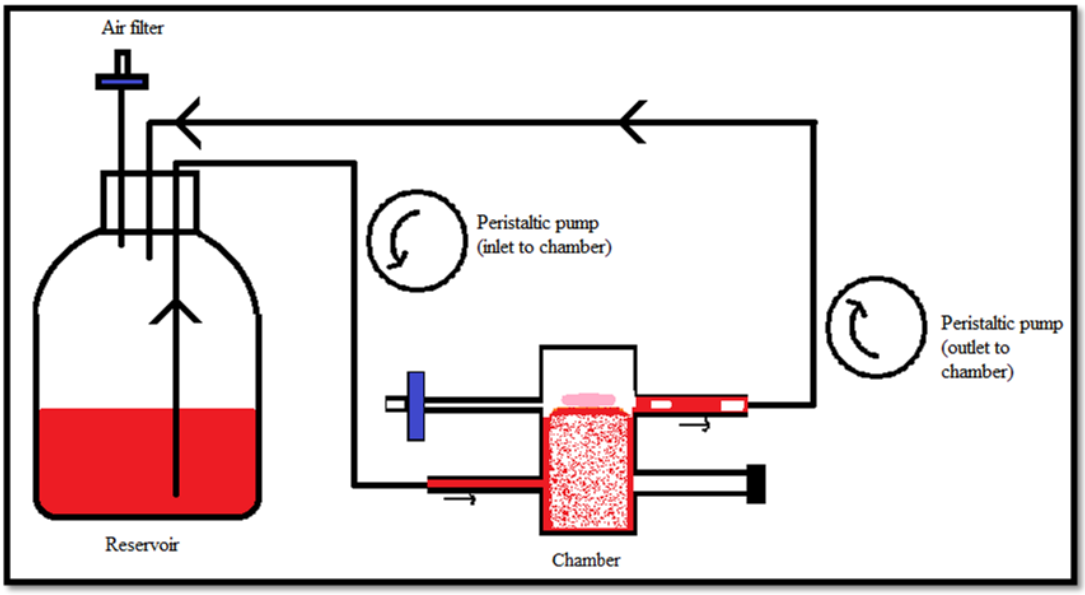

Figure 2.4: Schematic diagram of the second generation perfusion bioreactor system.

Medium is drawn out of the reservoir by the chamber inlet tube which is connected to the pump. The chamber fills up with medium until it reaches the height of the output tube when it is actively drawn out of the chamber at a faster rate than the input. To compensate for the larger volume removed, air is also drawn into the system through the sterilising filter. The medium is then returned to the reservoir and is re-circulated. The additional air drawn into the system can be vented and escape through the air filter on the reservoir bottle.

A second method to increase the output flow rate was by using a larger diameter tube on the output of the chamber. A large diameter tube had an increased cross-sectional area and hence a higher flow rate than narrow tubes. A 1.5 mm inner diameter tube was used on the chamber input, and a 3 mm inner diameter tube was used on the chamber output. A system was setup using these tubes and run to establish whether the level in the chamber would remain stable.

2.3.3 Aluminium Stand versus Empty Control

To establish the effect of placing the aluminium stand in the chamber two systems were connected on the bench as shown in figure 2.4. One system positioned an aluminium grid inside the chamber to create a stand on which to raise samples to an ALI. The second system left the chamber empty. The systems were run in parallel at a pump speed of 10 rpm to observe the response.

2.3.4 Sponge Stand

A second stand to create an ALI was created from a column of sponge cut to the size required and positioned inside the chamber. The same test to observe the effect of the stand was carried out; comparing one system with an empty chamber and another with a with a sponge stand inside the chamber using a pump speed of 20 rpm.

2.3.5 Sponge Toxicity Assessment by Resazurin Reduction

To assess whether the sponge used as an ALI stand was toxic or harmed cells resazurin sodium salt reduction was performed to assess viability following exposure. 50,000 passage 6 fibroblasts in 2 ml fibroblast medium were seeded into each well of a twelve well plate and left to attach overnight. The sponge (Boots no 7 facial exfoliating sponge, Boots, Nottingham, UK) was cut into pieces of equal mass (0.023+/- 0.001g) and sterilised by soaking in 70% industrial methylated spirit (IMS) and placing on a rocker overnight. The material was thoroughly washed with sterile PBS to remove any residues of IMS.

24 hours after seeding, transwell membranes containing the material were placed over each well so that any harmful chemicals would leach into the culture medium. On day 0 (prior to application of material), day 1 and day 7 a resazurin (Sigma Aldrich, Dorset, UK) reduction assay was performed to investigate the affect of the material on fibroblast viability.

Each well was washed 3 times with PBS and 1 ml of 1 µg/ml resazurin in PBS was added to each well. The plate was incubated for 1 hour at 37^{o}C in the dark. Following incubation 150 µl was transferred into each well of a flat bottomed 96 well plate; repeated 3 times per well. The optical absorbance of the samples was read at 570 nm and the value of the un-metabolised resazurin control was subtracted. Cells were washed thoroughly with PBS and the medium replaced. This assay is non-toxic and was repeated on the same cells at multiple time points.

Statistical Testing

To compare the viability of cells cultured in indirect contact with the sponge and the control an unpaired two tailed T-test was performed to a confidence level of 0.05.

2.3.6 Assessment of the Ability to Maintain Sterility

The second generation ALI perfusion bioreactor system was tested with the addition of culture medium under sterile conditions to assess the ability of the system to maintain a sterile environment. The system (chamber, tubes and reservoir) was connected and autoclaved to sterilise. The packaging was opened under aseptic conditions in a laminar flow hood and the components that could not be autoclaved were added (air filters and medium). The system was run for a week at a pump speed of 90 rpm (5.7 ml/min) in a bench-top ungassed 37^{o}C incubator to observe changes in the medium indicating infection.

2.4 OCT imaging of TE Skin Constructs

2.4.1 Poor Quality TE Skin Constructs

Poor quality TE skin was produced by positioning the skin construct on a porous sponge (Boots No 7 facial exfoliating sponge, Boots, Nottingham, UK) to provide the ALI following the initial two day submerged culture. Medium was filled as usual to bathe the underside of the dermis and changed every other day taking care to remove all

medium trapped inside the sponge. Constructs were cultured for 7 or 14 days. These samples were used to show the ability of OCT to identify poorly developing constructs (fig. 5.4).

2.4.2 Batch Feed versus Single Feed of TE Skin Constructs

Following submerged culture batch fed constructs were placed in a 6 well plate at an ALI on a stainless steel grid. 5 ml of medium was added and replaced 3 times a week. Single feed constructs were placed in a large Petri dish using a porous plastic grid to create a floating stand for the ALI. 30 ml of medium was added to the Petri dish at the initial time point and was not replaced during the experiment. Constructs were cultured for a period of 14 days. These samples were used to show good quality TE skin (fig. 5.2), to measure epithelial thickness (fig. 5.3 and fig. 5.5) and to create A-scans (fig. 5.6).

2.4.3 Manual Measurement of Epithelial Thickness by Line Tracing

ImageJ was used to manually measure the epithelial thickness by drawing around the structures of interest on both OCT images and histology, figure 2.5 demonstrates this concept. The area of the structure was divided by the length of the image to obtain an average thickness. In OCT images the total epidermis was defined as the region from the surface of the sample to the location that the signal increased signifying the start of the dermis (fig. 2.5a). In histology the total epidermal thickness is defined as the region from the surface of the sample to the bottom of the proliferative round nucleated cells resting on the basement membrane (fig. 2.5c).

In OCT imaging the stratum corneum was defined as the highly scattering region at the surface of the image (fig. 2.5b). In histology the stratum corneum was defined as the bright pink flaky basket weave structure on the surface of the sample (fig. 2.5d). The thickness of the living epidermis was found by subtracting the stratum corneum

thickness from the total epidermal thickness in both OCT images and histology images. The thicknesses measured from OCT images and histology images were compared on a scatter graph.

Statistical Testing

To compare epithelial thickness values between sample types and time points a one way ANOVA was performed with a post-hoc Tukey test to a confidence level of 0.05.

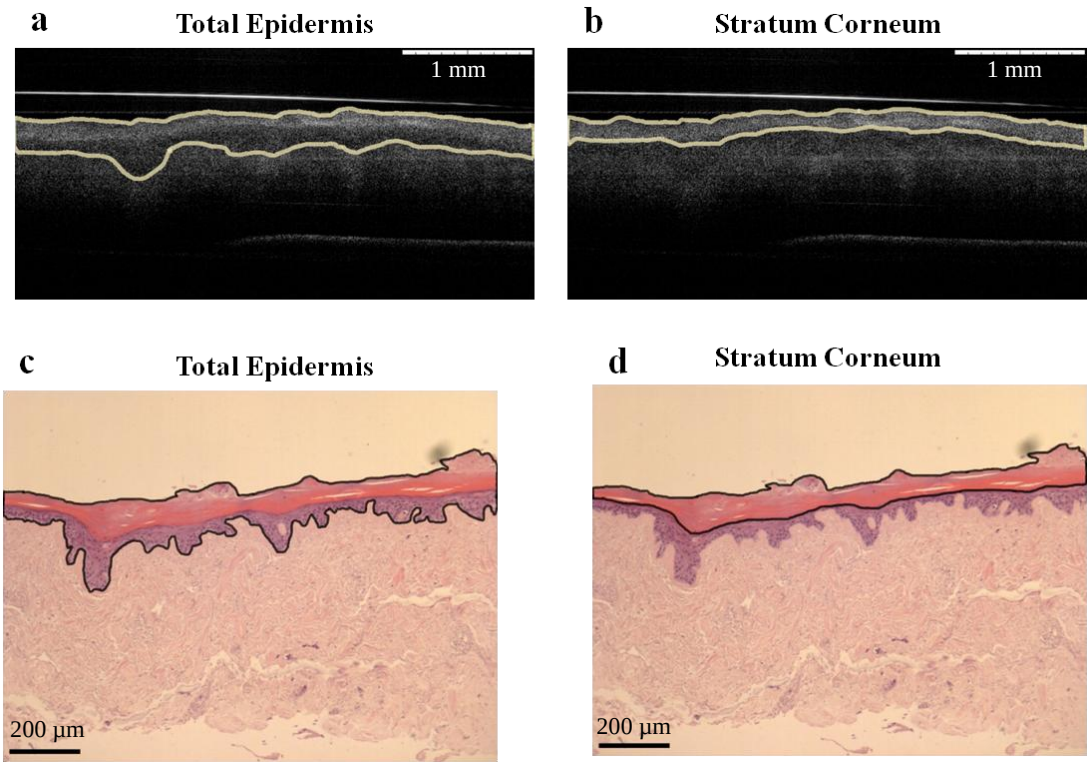

Figure 2.5: Manual measurement of epithelial thickness by line tracing method.

Examples of how epithelial thickness was measured on OCT images and histology by measuring the area of the structures.

a) Measurement of the total epithelial thickness from OCT images, b) Measurement of stratum corneum thickness from OCT images, c) Measurement of total epithelial thickness from histology, d) Measurement of stratum corneum thickness from histology.

2.4.4 Production of Averaged A-Scan

The A-scan is the OCT intensity signal with respect to depth at a single lateral position; a column of intensity values. To enable adjacent A-scans to be averaged, the surface of the image was flattened by vertically moving each column of pixels so that the surface of the sample was at the same vertical position (fig. 2.6b). A MATLAB script was created to perform this function (see appendix 1). Any number of adjacent A-scans at any lateral position could be averaged from the straightened image. The averaged A-scan was calculated by averaging the intensities across the image using a MATLAB script (see appendix 1). Figure 2.6c shows the averaged A-scan across the whole image superimposed on the straightened image.

2.5 Culturing TE Skin in First Generation Perfusion Chambers and Imaging Using OCT

Following the production of standard skin constructs as described in section 2.1.6, nine samples were split into three groups; perfused ALI culture, static ALI culture and static submerged culture.

2.5.1 Perfused ALI Sample Setup

The first generation bioreactor system was connected as shown in figure 2.3. The system was sterilised using 70% IMS and washed with sterile PBS to remove residues of IMS. The system was primed with 15 ml warmed Green's medium, and TE skin constructs were placed on the stands at an ALI within each of the three chambers. The whole system was placed inside a gassed CO_2 incubator. Medium was replaced twice a week at the same point as static controls. The investigation was run for two weeks and during this time the peristaltic pump provided a constant flow of medium at a rate of 220 μl/minute. OCT imaging was performed on day 0, 7 and 14.

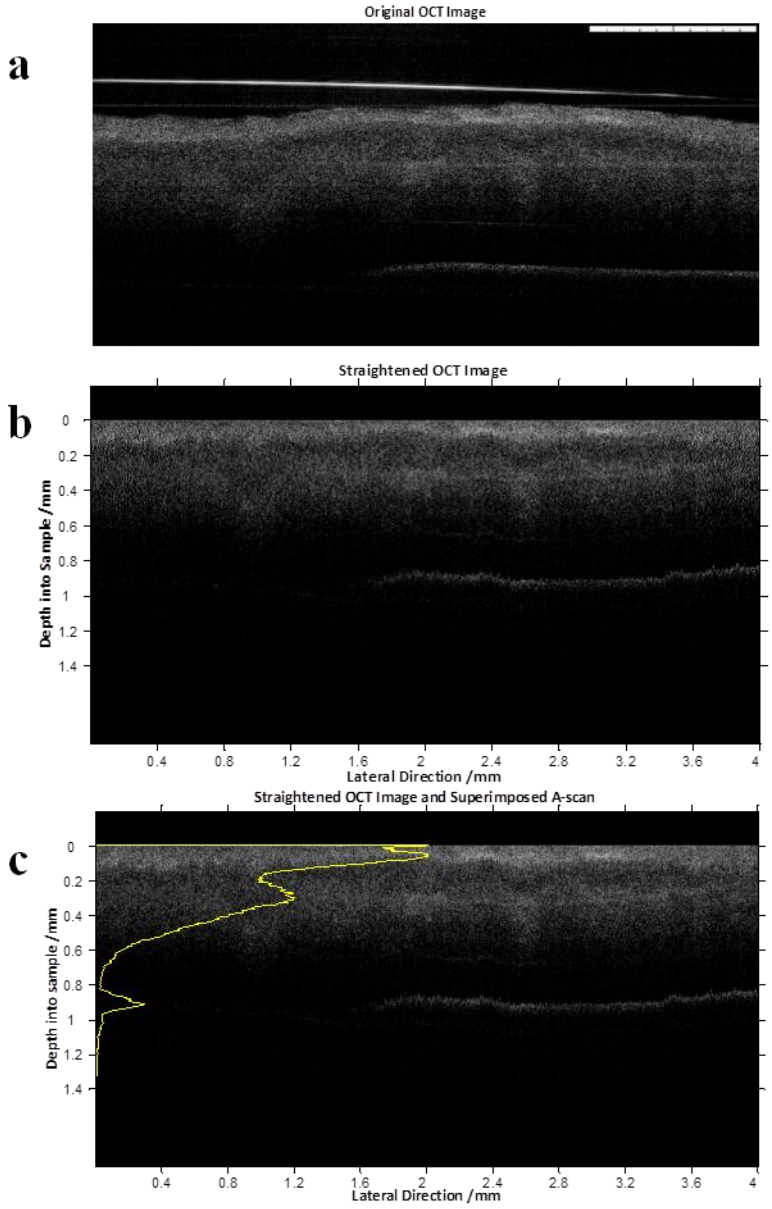

Figure 2.6: Explaining the production of the averaged A-scan

a) The original OCT image; tissue engineered skin day 14, b) OCT image following straightening with the MATLAB script; the surface is horizontal, c) The A-scan across the whole of the sample surface was calculated and superimposed on the straightened OCT image (yellow line).

2.5.2 Static ALI and Submerged Sample Culture

As a positive control TE skin constructs were cultured at a static ALI; samples were positioned on stainless steel grids for a period of two weeks and received medium changes twice a week. OCT imaging was performed in 6 well plates on day 0, 7 and 14.

As a negative control constructs were also cultured under static submerged conditions with medium changes twice a week. OCT imaging was performed in 6 well plates on day 1, 7 and 14. All sample types received the same volume of medium over the culture period.

2.5.3 OCT Imaging of Samples Cultured in First Generation Systems

The bioreactor system was removed from the incubator and each of the chambers was isolated from the system by connecting the input and output tubes together. The lid and base of each chamber were sealed with autoclave tape and OCT imaging was performed as described in section 2.1.11 in the same way as static equivalents. Following imaging bioreactor chambers containing perfused samples were re-connected to the system and returned to culture.

3. DEVELOPING THE PERFUSION CULTURE BIOREACTOR SYSTEM

3.1 Introduction

Development of 3D tissue engineered skin models is important for the investigation of skin disease pathologies, and drug or cosmetic efficacy and toxicity. These models could reduce animal testing and speed up the drug discovery process[1]. However, one significant limitation with these models is that they cannot survive for extended time periods in culture[5].

The tissue engineered (TE) skin models produced by the MacNeil research group have optimal structure between ten and fourteen days of culture at an air/liquid interface (ALI), however beyond this time point constructs begin to deteriorate[5]. Extended culture periods increase the risk of infection and the viability of the cells decreases as the culture progresses. The utility of long term experiments is limited by this short time window between the TE skin becoming fully developed and when viability declines. Therefore, long term experiments cannot be carried out to investigate long term changes, for example, when cells respond to a drug or treatment following disease initiation. Methods to improve the efficiency of culture may increase the lifespan of constructs and reduce the costs incurred.

It is thought that using culture methods that mimic the physiological conditions may help to increase the lifespan of constructs[7]. *In vivo* the organs receive a constant supply of fresh nutrients delivered by the circulation. In the skin, blood passes through vessels in the dermis and feeds the epidermis by diffusion[9]. Using the concept of blood flow, tissue engineering studies have begun to adopt the use of bioreactors to provide enhanced nutrient delivery to constructs by providing a flow of culture medium, which is analogous to a blood supply. Few studies in the literature have attempted to culture

engineered skin with both epidermal and dermal components at an ALI under flow conditions[7,49].

This research aimed to explore the use of bioreactors for the culture of a reconstructed skin model at an ALI under flow conditions. The design requirements for such a system are described in section 1.4. The reconstructed skin model under investigation was based on acellular de-epithelialized dermis (DED) which provides the cells with a ready-made environment including the extracellular matrix proteins and attachment molecules required to make up skin[5]. The cells can remodel the DED as the constituents are all naturally occurring in the skin. The construct is composed of fibroblasts which pass through the basement membrane and maintain the dermal portion, and keratinocytes that do not pass through the basement membrane and form the multilayered protective barrier known as the epidermis. The structure produced closely mimics the native structure of split thickness skin, and is thought to provide an accurate model of native skin[4]. Improving the lifespan of this construct will increase its utility for investigation as discussed previously.

Provision of a flow of medium within a bioreactor system is thought to increase the similarity of the culture environment to the physiological conditions. This in turn may increase the lifespan and accuracy of the model for investigations into disease pathologies and potential treatments. This work modifies commercially available bioreactor systems developed by Kirkstall Ltd. for the requirements of skin culture.

It was found that the Kirkstall Ltd. bioreactor chambers could be modified to provide the culture requirements of engineered skin models. Two bioreactor systems were investigated; first and second generation. An ALI was provided using a stand inserted into the chamber and a glass window in the lid of the chamber accommodated optical coherence tomography (OCT) imaging of samples *in situ*. Design iterations of the

second generation system have been considered in detail. However, it was found that the second generation bioreactor system was unable to maintain a sterile culture environment so was unsuitable for the culture of engineered skin models.

Bioreactor culture is an important step in the culture of engineered skin constructs; it is thought that a flow of medium will provide a more physiologically relevant nutrient delivery profile which could allow viability to be extended. Longer viability would have an impact on the types of experiments that could be undertaken using these skin models and also extend the transplantation window for clinical applications.

3.2 Results

3.2.1 First Generation Bioreactor System

The first generation bioreactor system was modified and tested by Kirkstall Ltd.; the setup has been shown previously in schematic diagrams (fig. 2.3) including design features and series connection of chambers. Figure 3.1 shows photographs of the setup of this system. A stand was positioned into the chamber to support the sample and provide an ALI. The stand was produced from a dental wire frame with porous sponge spanning the frame to form the platform onto which the TE construct was placed (fig. 3.1a). A glass window in the lid of the chamber enabled OCT imaging of samples within the chamber without the need to remove the sample or open the lid (fig. 3.1c). As the chamber was modified from an existing design of a submerged chamber (known as the Pisa chamber); extra ports for delivery and removal of medium were inserted into the lower half of the chamber to allow creation of an ALI. The tubes from the original design in the upper half of the chamber were unused and connected together to close the system.

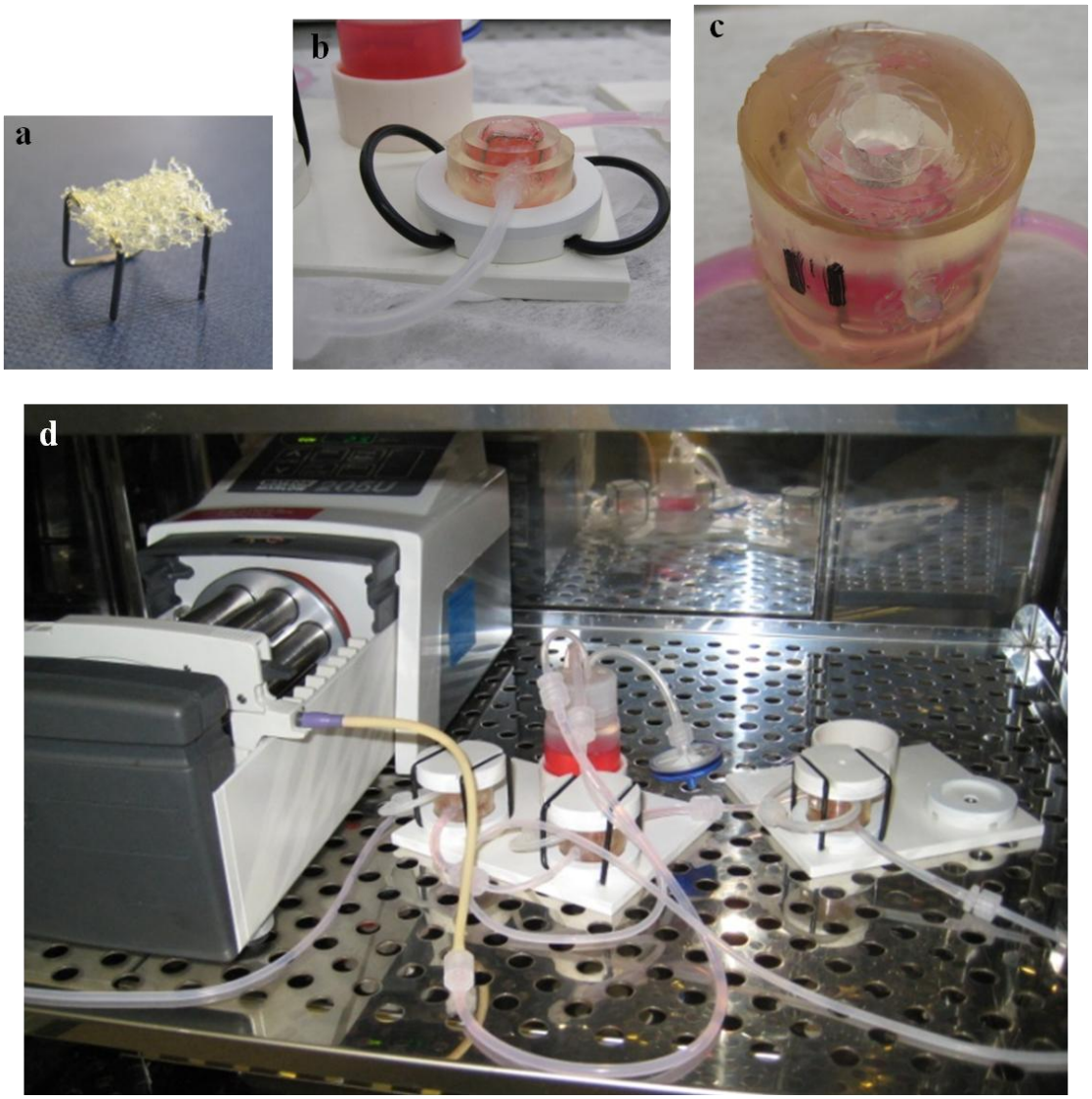

Figure 3.1: Modification and set up of the first generation "Pisa" bioreactor system.

a) The stand produced to maintain the tissue engineered skin at an air/liquid interface; a dental wire frame is spanned by a porous sponge, b) Tissue engineered skin placed on the stand within the open chamber; inlet and outlet tubes were glued into the walls of the chamber, c) Modified lid demonstrating how a window was created in the lid by cutting a round hole in the silicone and gluing a coverslip over this hole to maintain a closed environment, d) Assembled system positioned within the incubator; three chambers were connected in a series configuration. A peristaltic pump propelled the medium around the system in a continuous manner.

For simultaneous culture of multiple skin samples three chambers could be connected together in a series configuration (fig. 2.3b). The reservoir of medium would be replaced at multiple time points during culture to provide the TE skin with fresh medium, as the reservoir had a small capacity of 20 ml. The pump was positioned after the bioreactor chambers in the circuit, so that medium was drawn through the chambers as opposed to being pushed into them. The assembled system was photographed showing the complete system positioned inside the incubator (fig. 3.1d). Use of this system for tissue culture is addressed in depth in chapter 5.

This first generation system was abandoned when the manufacturer discontinued the original submerged chamber that was modified to produce the ALI chamber. The new style of submerged chamber (Quasi-Vivo 500, Kirkstall Ltd., Sheffield, UK) was easily mass produced as opposed to the Pisa chambers used in the first generation system which were individually handmade. The geometry inside each chamber remained the same, but the lid locking mechanism was changed; therefore the modified ALI chamber was required to be redesigned. The new design was known as the second generation system.

3.2.2 Second Generation System

System Modifications and Setup

The schematic diagram of the second generation ALI bioreactor system has been shown (fig. 2.4). Each system comprised of only one chamber and one reservoir. The input and the output of the chamber were both connected to the pump to actively draw medium into and out of the chamber to ensure that the level of liquid remained consistent. The output had a faster flow rate than the input and therefore drew air into the chamber through a sterilising filter to ensure contamination would not enter through this route. Exchanging the air within the system in this way was included to ensure good pH buffering of the medium when the system was placed in a CO_2 controlled atmosphere.

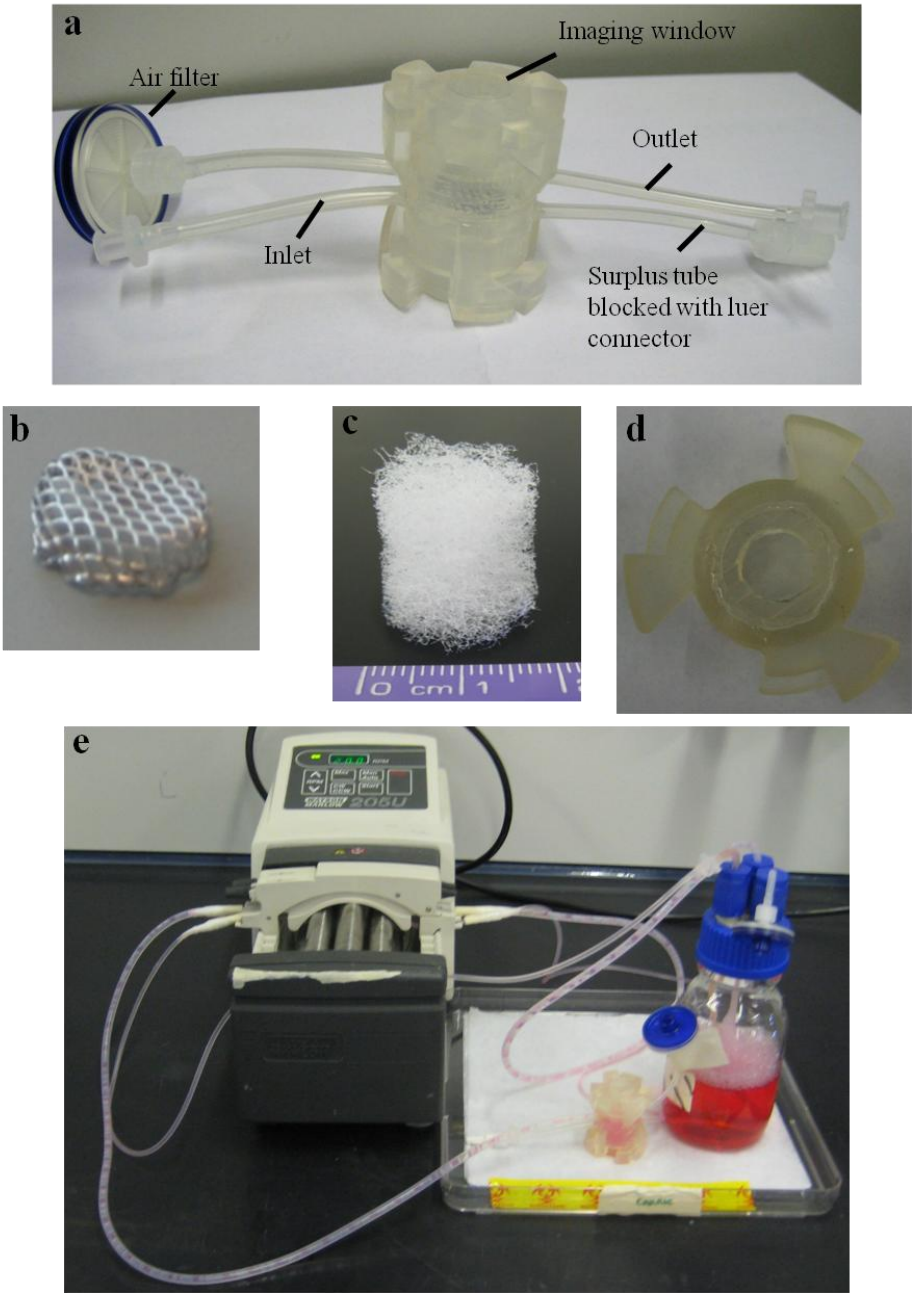

Figure 3.2: Photographs of the setup of second generation bioreactor system.

a) Assembled modified second generation chamber labelling the design features, b) Aluminium stand provided by Kirkstall Ltd. to support the sample at an air/liquid interface. This stand was inserted into the chamber and the edges were compressed against the chamber wall at the required height, c) Alternative stand made of sponge to create the air/liquid interface. This stand was inserted into the chamber as a column of the required height, and the sample was placed on top, d) Modified lid with window for OCT imaging. A hole was cut out the original lid and a glass coverslip was glued in place to provide a closed environment, e) Demonstration of the system setup and connection to the pump.

A photograph of the setup of the second generation system is shown in figure 3.2e. Modifications to the second generation chamber were undertaken by Kirkstall Ltd.; briefly, disks were removed from the roofs of two submerged chambers, these chambers were glued roof to roof to produce a cavity inside. Both the top and bottom of the chamber could be unscrewed to open the chamber; two bases became a lid and a base. A photograph of the assembled chamber is shown (fig. 3.2a). The incorporation of two submerged chambers to produce one ALI chamber resulted in four ports, or tubes into the chamber. One was unused and blocked with a luer connector, one was an air inlet port and there was also an input and output port for medium.

Two potential stands for creating an ALI are shown in figure 3.2b and c. The first stand was made from an aluminium grid which was inserted into the chamber and rested at the required height by compression against the chamber walls (fig. 3.2b). The second stand was an open porous network of fibres, designed as a facial exfoliating sponge (Boots No. 7 facial exfoliating sponge, Boots, Nottingham, UK) (fig. 3.2c). A column of this material sat inside the chamber to act as a stand on which to position the TE skin. In addition this design trapped medium within the chamber; the chamber could be removed from the system and taken for OCT imaging without the sample drying or being deprived of nutrition.

To enable OCT imaging of samples within the chamber a glass window was incorporated into the lid. A disk of material from the chamber lid was removed and replaced with a glass coverslip which was glued in place. As two submerged chambers were glued together, the chamber was very tall. The distance between the sample and the lid was more than 7.5 mm and therefore the higher resolution OCT lens (LSM02) was not suitable (as explained in the design requirements in section 1.4). The lower resolution lens (LSM03) with a long working distance of 25 mm was required for use with this chamber.

Establishing a Stable Level of Liquid in the Chamber

To ensure a stable level of liquid within the chamber to maintain the ALI the chamber output flow rate was increased in comparison to the input flow rate. Two methods of increasing the output flow rate were investigated. The first was the choice of pump adjuster position. The second was the choice of output tubing used on the pump. To allow for the difference in flow rate between the input and output the chamber drew sterile air into the system through an air filter on the air entry port. This extra air left the chamber through the output tube to make up the volume removed by the greater flow rate out of the chamber. Increasing the flow rate out of the chamber ensured that the chamber never overfilled if there were small changes in pump flow rate. The output tube was at a higher position than the input tube to prevent excess liquid being removed from the chamber which would cause the chamber to empty.

The adjuster position altered the compression of the tubes against the pump which changed the cross sectional area and thus the flow rate. Figure 3.3a shows the effect caused by changing the tube compression on fluid flow rate through a 1.5 mm inner diameter silicone tube. It was observed that by changing the compression, a change in flow rate could be produced which had a non-linear relationship. At the least compressed adjuster position the flow rate was increased by approximately 18% from the middle adjuster position. At one adjuster position down, the flow rate was approximately 7% greater. When the compression was increased above the middle position no change in flow rate was observed.

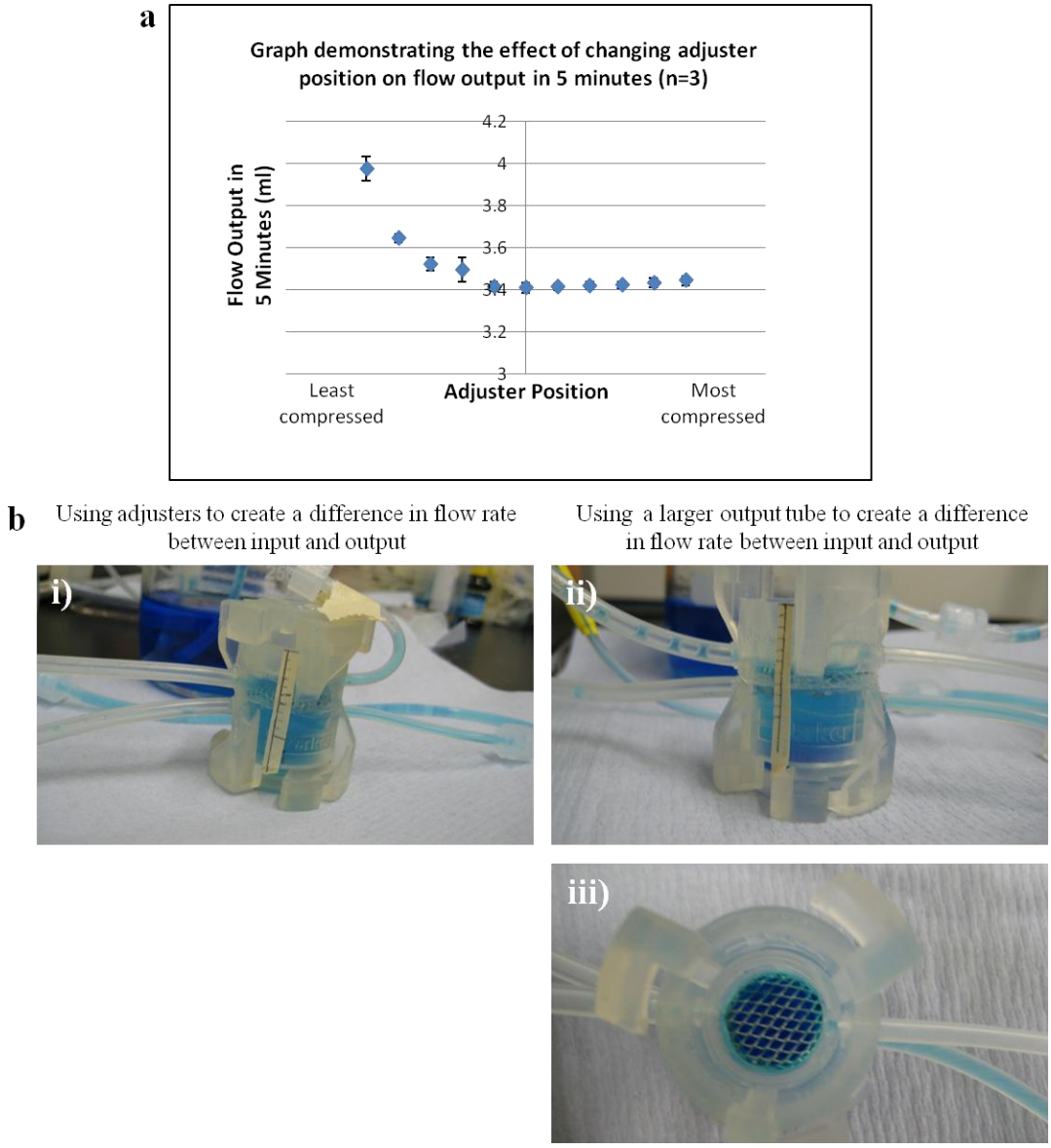

Figure 3.3: Methods to ensure output flow rate exceeds input flow rate.

a) Graph of the flow rate obtained at each adjuster position (n=3); flow rate depended on the compression of the tube against the pump, bi) Demonstration that the difference in flow rate created by setting opposite adjuster positions on input and output tubes did not cause a sufficient difference between flow rates and the chamber began to overflow, bii) Demonstration that use of a larger output tube on the pump sufficiently increased the output flow rate to prevent the chamber overfilling. A large volume of air was drawn into the chamber to compensate for this increased flow rate, biii) Aerial view of the chamber shows that the level of liquid inside the chamber was correct under these conditions.

When both input and output pump tubes were the same size (1.5 mm inner diameter), and the difference in flow rate was increased using the output adjuster at the least compressed position and the input adjuster at the most compressed position the system was not able to maintain output flow and the chamber began to overflow (fig. 3.3bi). With time the overflowing liquid began to travel along the air port. The air filter was removed as the fluid approached it to prevent damage. As seen in figure 3.3bi there is blue liquid in the input tube, but it is not drawn out through the output tube. Therefore the adjuster position did not create a large enough difference in flow rate to reliably maintain the required difference in flow rate.

The outcome of using a larger diameter output tube on the output pump channel is shown in figure 3.3bii and iii. These photographs demonstrate the effect of using a 3 mm inner diameter tube on the output and a 1.5 mm inner diameter tube on the input to create a difference in flow rate. This difference in flow rate was able to remove sufficient liquid to prevent the chamber overfilling. A large quantity of air was subsequently drawn through the system as shown as air bubbles in the output tube to the left of the photograph (fig. 3.3bii). Figure 3.3biii shows an aerial view of the chamber indicating that the level of liquid reached the stand and was therefore the correct height to form an ALI. Using a large diameter output tube allowed the level of the liquid in the chamber to be maintained at the correct height.

Determining the Optimal Stand to Provide the Air/Liquid Interface

It was observed that when the aluminium stand (photograph shown in figure 3.2b) was inserted into the chamber the level of liquid in the chamber would drop after the system was run continuously for a few days. However, the time at which this occurred was not constant. Figure 3.4 shows photographs demonstrating the decrease in the level of the liquid when the aluminium stand was used. On day 0 the system was setup and the level of liquid marked on the side of the chamber with black pen (fig. 3.4ai and ii). By day 8

the level of liquid had decreased and it was observed that the liquid no longer reached the bottom of the stand (fig. 3.4aiii and iv). Figure 3.4b shows a control using a chamber without a stand; it was observed that the level of liquid did not change after 8 days (fig. 3.4bii). The presence of the aluminium stand caused the level of liquid to fall within the chamber when the system was continuously run for extended time periods, when the stand was not present the level of liquid did not change. Use of the aluminium stand was not an appropriate method of creating an ALI.

Subsequently use of a stand made of a porous sponge (Boots No. 7 facial exfoliating sponge, Boots, Nottingham, UK) was investigated (fig. 3.2c). This sponge trapped liquid within it and when saturated provided a moist surface to feed the TE skin. The system was setup (fig 3.5a) using the sponge as a stand and the level was observed over a period of 13 days continuous flow (fig. 3.5c). A circle of filter paper was positioned onto the stand so that the extent of the moistness was easily visible. It was found that the filter paper remained well wetted throughout the experimental time course, indicating that the sponge stand may be suitable for creating an ALI as it was able to maintain a stable, suitable level of liquid within the chamber.

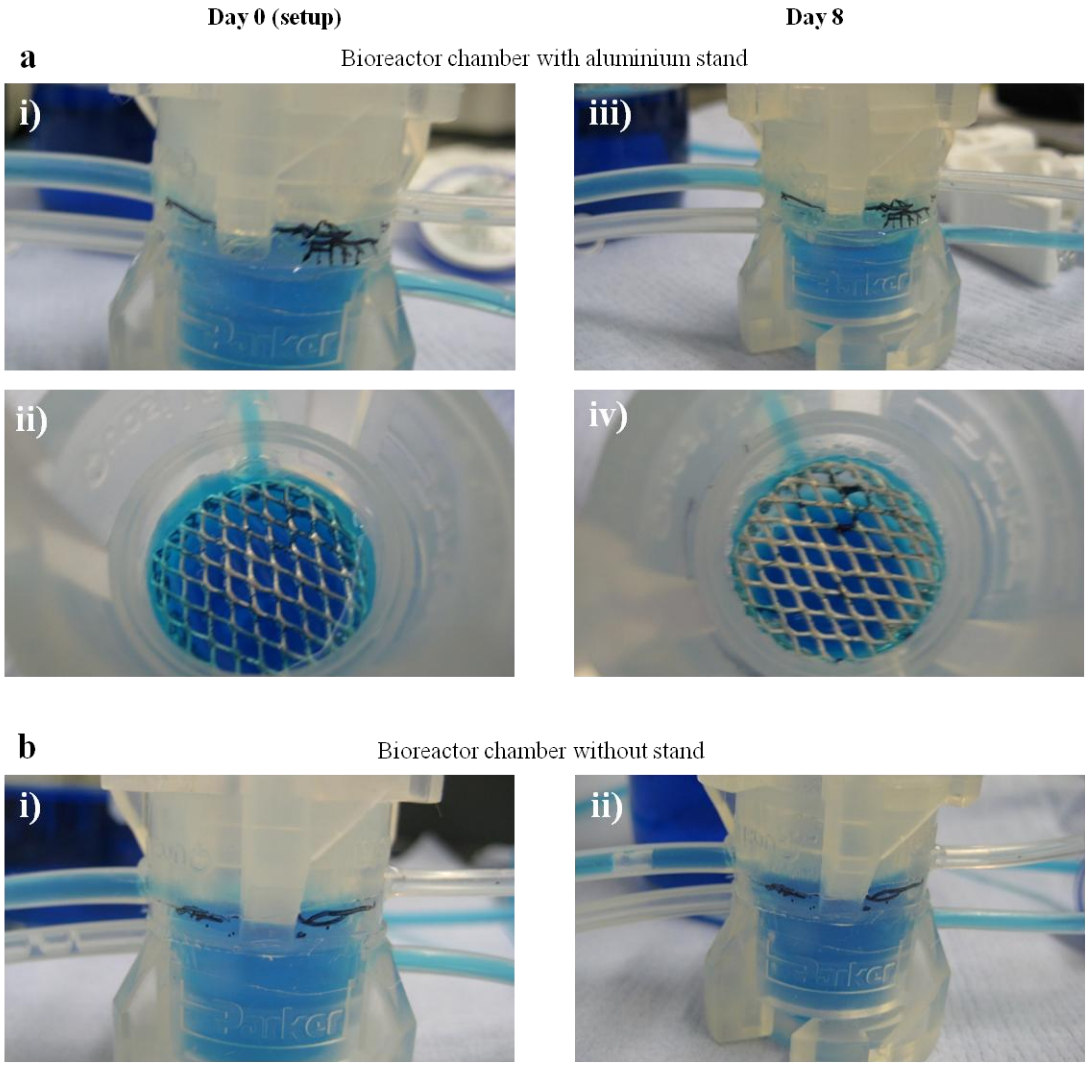

Figure 3.4: Photographs illustrating the effect of the aluminium grid on the level of liquid inside the chamber.

When the systems were setup on day 0 the level of liquid in the chamber was marked on the side with black pen as a reference. ai) Bioreactor with aluminium stand inserted on day 0, aii) Corresponding aerial view of this chamber, aiii) The chamber with the aluminium stand on day 8 following circulation of liquid (water and blue food colouring). The level of liquid decreased, aiv) The aerial view on day 8 shows that the level of liquid in the chamber does not reach the aluminium stand and is too low to provide an air/liquid interface, bi) Control bioreactor chamber without a stand as setup on day 0, bii) The level of liquid inside the control chamber did not change after 8 days.

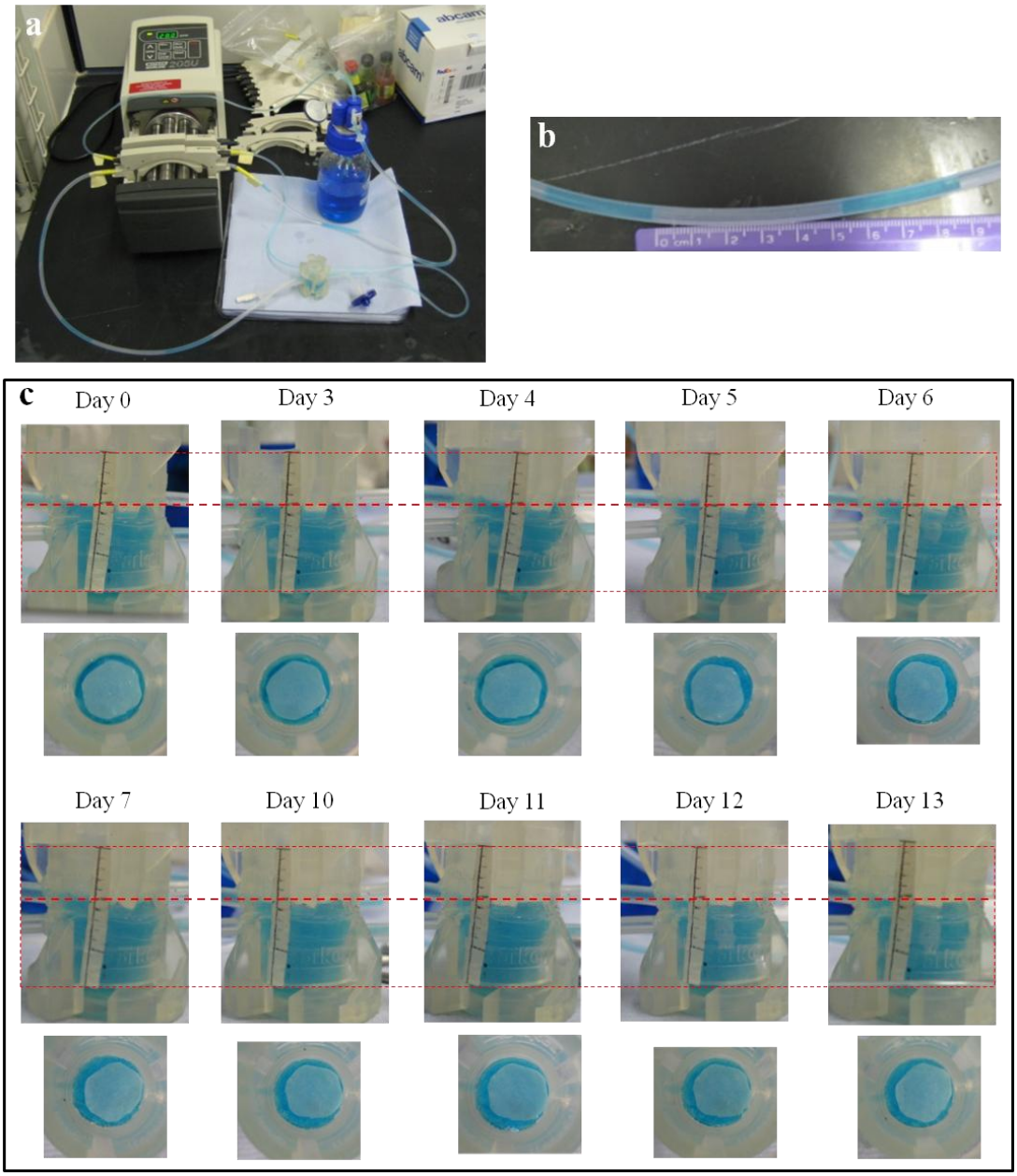

Figure 3.5: Determining the suitability of using porous sponge as a stand to maintain air/liquid interface.

a) Photograph of the setup, b) Photograph of the output flow profile; demonstrating the air drawn into the system, c) Photographs demonstrating that the level of liquid inside the chamber was fairly stable over a period of 13 days of continuous circulation. Upper images show the level within the chamber against a scale, lower images show an aerial view inside the chamber; the filter paper placed on the sponge stand remained very moist over the time of the study.

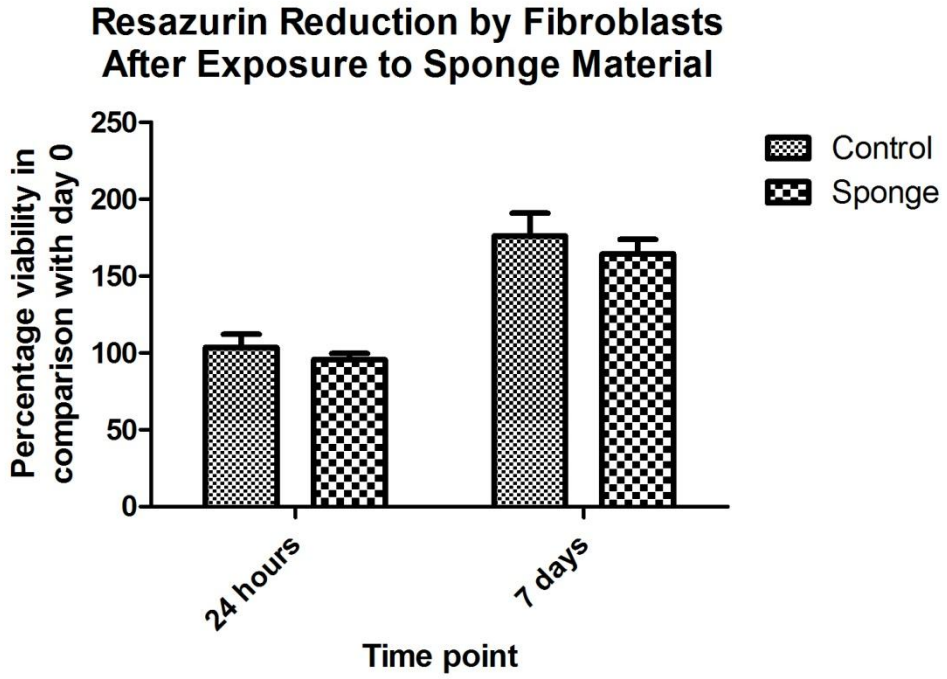

Unpaired t test	
P value	0.8623
P value summary	ns
Are means signif. different? (P < 0.05)	No
One- or two-tailed P value?	Two-tailed
t, df	t=0.1967 df=2

Figure 3.6: Graph showing viability of fibroblasts following indirect exposure to the sponge investigated as a stand to maintain an air/liquid interface.

Resazurin reduction was performed following 24 hours and 7 days exposure to the sponge used as an air/liquid interface stand in the second generation bioreactor chambers. Values were normalised to initial values of reduction to take account of differences in seeding density between samples. Resazurin reduction is proportional to viability. Viability increased similarly for the control and those exposed to the sponge over time. There was no significant difference observed between the control (fibroblasts seeded on tissue culture plastic) and the fibroblasts indirectly exposed to the sponge.

It was then important to investigate the suitability of the sponge material for cell culture; it must not cause toxicity to the cells used in the TE skin constructs. Resazurin sodium salt reduction was performed on fibroblasts that had been in indirect contact with the sponge material to establish viability following exposure (fig 3.6). Fibroblasts were seeded in a 12 well plate and sponge was placed in transwell membranes so it was in contact with the medium but not directly touching the cells. After both 24 hours and 7 days exposure to the sponge material the fibroblasts were tested for resazurin reduction. It was found that there was no significant difference in viability between the control without exposure to the sponge and the samples exposed to sponge at either time point. The presence of sponge had no effect on viability of fibroblasts therefore it was concluded that this material would be safe for use in cell culture.

Ability of the System to Maintain Sterility

Having established that the system had a stable level and could provide a suitable ALI to samples, the ability to maintain sterility was established (fig. 3.7). For simplification of the system the sponge stand was not inserted into the chamber. The majority of the system was connected together and autoclaved to make sterile setup more straightforward. The remaining components were assembled in the laminar flow hood; air filters, chamber lid and addition of medium to reservoir. The system was positioned inside an un-gassed bench-top 37^{o}C incubator and connected to the pump. The system was run continuously and the medium was observed daily in comparison to an equivalent sealed bottle of sterile medium. As the incubator was not gassed the medium within the bioreactor system became more pink than the medium in the sealed bottle due to suboptimal pH buffering.

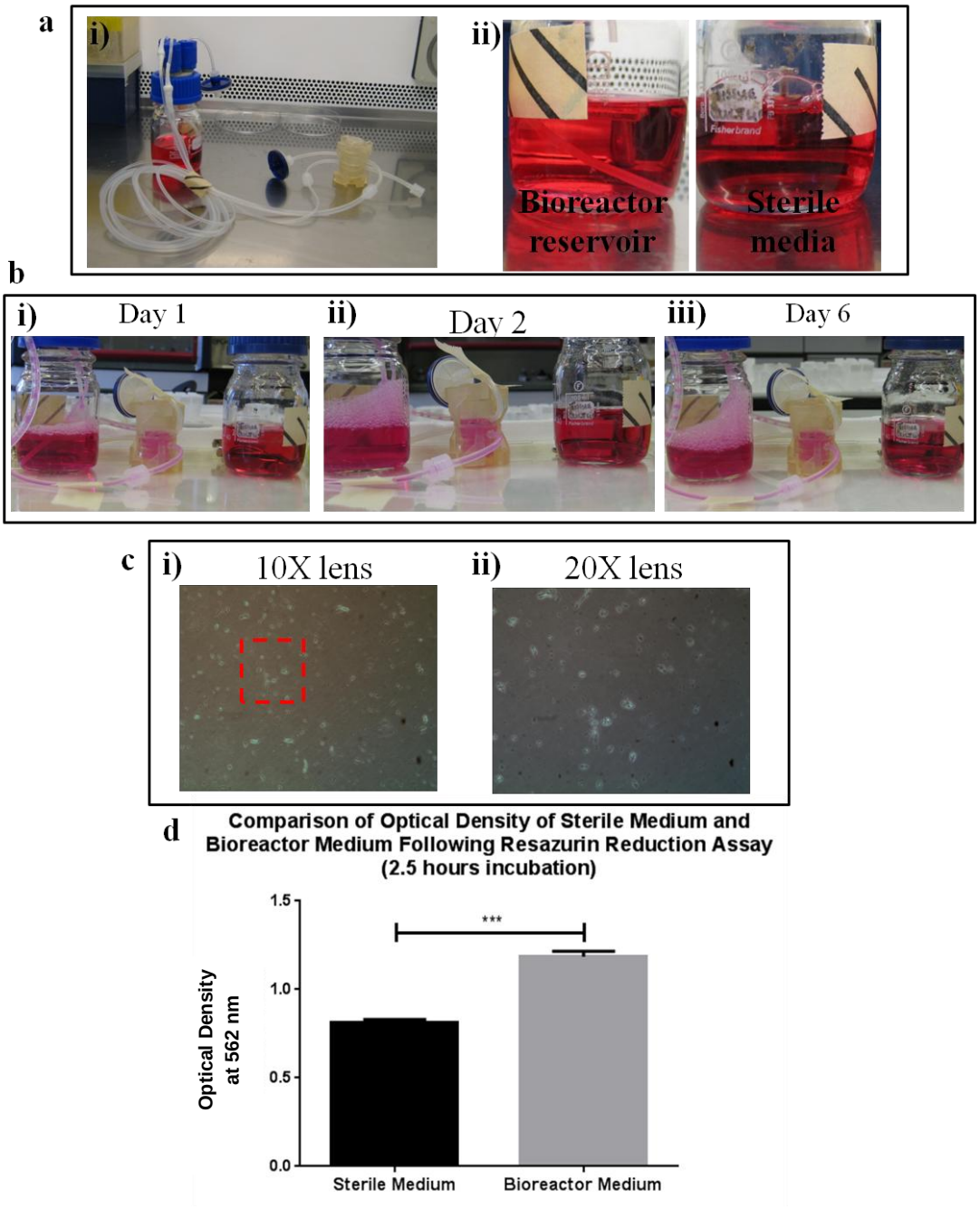

Figure 3.7: Assessing the ability of the bioreactor system to maintain sterility.

ai) The setup of the system under sterile conditions, aii) Initial observation of culture medium comparing bioreactor reservoir with a sealed bottle of medium, b) Demonstrating the medium becoming more cloudy over time in comparison to the bottle of sterile medium, c) Light microscope images confirming infection after 7 days, d) Graph of resazurin reduction of the bioreactor medium compared to sterile medium at the day 7 time point. Increased optical density (at 562 nm) of the bioreactor medium compared to sterile medium confirms that the bioreactor medium contained living organisms.

By day 2 the medium had started to become cloudy in comparison to the sterile medium (fig. 3.7bii), which is an indicator of infection. After 7 days a sample of the medium was taken and observed under the light microscope (fig 3.7ci and ii), infection was clearly present and noted by small rounded entities and clumps in the medium. Resazurin reduction was also performed on the medium from the bioreactor system and the sterile bottle (fig. 3.7d). It was found that medium from the bioreactor system had a significantly greater reduction of the resazurin, indicating it contained living organisms.

3.3 Discussion

The work presented has been undertaken in collaboration with Kirkstall Ltd. to develop a specialised bioreactor chamber and system for the culture of TE skin at an ALI. The development of new ALI chambers used standard submerged culture chambers which were modified for the specific requirements of TE skin and to allow *in situ* OCT imaging. Two bioreactor systems have been described and details of the optimisation process of the second generation system have been explained in detail.

Initially first generation ALI chambers were developed by modification of the "Pisa" submerged culture chambers provided by Kirkstall Ltd. These were modified by addition of input and output tubes into the lower part of the chamber so that it was possible to half fill the chamber with culture medium, enabling creation of an ALI. The system was closed to atmospheric pressure so that it was possible to run the system using a single pump channel which actively drew liquid through the system. This also enabled multiple chambers connected together with ease. The ability to connect multiple chambers together in one system is advantageous to allow multiple repeats to be set up in the same experiment. This setup also reduces the amount of tubing required to reach between the reservoir and pump and makes set up simpler. However, it should be noted that degradation of the medium along the chain of bioreactor chambers may

have a negative effect on the final sample in the chain due to lack of nutrients and excess waste[7].

The setup of the system meant that gas exchange into the medium was not actively promoted which may have implications for the pH buffering of the medium[87]. Although there was an air filtering port on the reservoir to allow sterile air to enter the system, this would only occur by passive diffusion along a long narrow tube and so the rate of exchange would be low. Furthermore, the reservoir used in this system had a capacity of approximately 20 ml, which is very small and would require the medium to be changed regularly when multiple samples were set up in series. This would prevent the investigation of the effect of batch feeding versus single feeding of constructs, and increase the labour involved in culture using this system.

When the production process implemented by Kirkstall Ltd. altered the design of the original submerged chamber, the design of the ALI chamber also required redesign. Therefore the design of the first generation system was not optimised and developed with the identification of these considerations. However, an *in vitro* skin culture study was undertaken with this system which will be discussed in chapter 5. This work highlighted some of the considerations for future designs including; ease of setup, size of reservoir bottle, ability to perform OCT imaging *in situ* and the number of chambers required in each system. Work then progressed to testing the use of the second generation of ALI chambers which were produced from Kirkstall Ltd.'s Quasi-Vivo 500 submerged chambers.

The modified second generation chambers were provided by Kirkstall Ltd. Vigorous testing was required to determine whether this design was fit for purpose. This system had quite a different design in comparison to the first generation system. Table 3.1 compares features of the two systems.

1st Generation system	**2nd Generation system**
One pump channel (located on the chambers' output)	Two pump channels (active pumping on both input and output)
Multiple chambers connected in series	Single chamber connected to single reservoir
20 ml reservoir bottle	100 ml reservoir bottle, but any size between 100 ml and 1 l could be used
Passive gas exchange	Active movement of filtered air into the system
Allows *in situ* OCT imaging with LSM03 lens	
Provides air/liquid interface using a stand positioned inside the chamber	

Table 3.1: Comparing features of the first and second generation bioreactor systems.

The first generation system had a very small reservoir bottle which meant that the medium had to be changed during culture. When investigating the second generation system a larger 100 ml reservoir bottle was used to address this problem. However, any size of glass bottle could be used provided that the thread matched that of the specialised port lid implemented. A large medium bottle is required to allow the implementation of a single feed regime, which was not possible using the first generation system. The volume of medium required for the whole culture period would determine the choice of reservoir size. A single feed reduces the labour required in maintaining a bioreactor system which is advantageous in terms of cost and risk of contamination.

Some studies in the literature have suggested that a single pass of medium is desirable to completely remove waste products from the system[7,43,45]. In this case a large volume of medium may be required, especially if culture period is long, and could be provided

using a large reservoir vessel. Although, other studies have implemented a continuous re-circulating regime which ensures proteins and signals secreted by the cells are not removed from the system, and also allows faster flow rates to be used[44,48,49]. Opinion is divided over the implementation of single pass or re-circulation of medium and experimental investigation of this consideration would be of value to determine the optimal flow regime.

The design of the second generation system included a window for OCT imaging in the lid of the chamber. This window was formed from a glass coverslip glued in place. When closing the chamber it was important to be very gentle as the glass window was very fragile and brittle, making it easy to break. Future designs could use a plastic window which would be less brittle and provide a more robust window. Provided that the thickness and refractive index were not significantly different to glass there would be no problems using a different material. Breaks or cracks in the window would be a problem as it would provide a route for contamination of the sample, especially with the negative pressure drawing air into the chamber.

In addition the height of the chamber was considerable (approximately 40 mm) as it was created from two submerged chambers, so had a double height. The position of the output tube determined the height at which the ALI occurred and therefore where the stand and the sample were positioned. Therefore, the sample was quite low in the chamber, approximately 19 mm from the top of the lid. This distance determined the lens that could be used for OCT imaging; the OCT beam must have a focal position longer than this distance to allow the lens to get close enough to the sample. To accommodate this distance the lens with the long working distance of 25 mm (LSM03) would be required when using the second generation system. Ideally, the design would have been developed so that the LSM02 lens with a 7 mm working distance and a

lateral resolution of 13 μm could be used which would enable higher resolution images to be obtained.

The ability to perform OCT imaging on samples *in situ* within the bioreactor chambers is important; OCT imaging can enable investigators to assess development with time and to give an indication of the quality of the construct non-destructively during culture[52,88]. The potential of this technology in relation to skin tissue engineering will be further considered in the chapter 4.

It is essential that an ALI is provided to the TE skin constructs; this is the stimulus for the epidermis to terminally differentiate and produce an impermeable protective barrier[23]. Terminal differentiation of the uppermost keratinocytes into corneocytes to form the stratum corneum reproduces the *in vivo* condition of the skin to produce a physiologically more relevant model. In standard static culture methods the ALI is usually achieved by positioning samples on a perforated stainless steel grid[5]. Medium is filled to just below the surface of the skin construct to provide nutrition by diffusion through the dermis. In the case of perfusion culture it was not possible to use the same stainless steel grids to provide the ALI as they required a different size and shape of stand to fit within the bioreactor chambers.

Initially an aluminium mesh was used to create a stand which was positioned at the required height within the chamber by compression against the walls. This was difficult to position while maintaining good aseptic techniques; future designs would benefit from a built-in stand within the chamber. In addition it was noticed that when using this stand the level of liquid inside the chamber was not maintained over an extended time period. The time after which this failure occurred was not consistent. In the example shown in figure 3.4 failure occurred after 8 days; the level inside the chamber dropped

and an ALI was no longer provided. If this occurred during an experiment investigating the culture of a TE skin construct, the sample would not receive adequate nutrition.

It is not entirely clear why this stand caused this inconsistent failure of the system. It was observed that when failure occurred, the liquid continued to be drawn out of the chamber, but air was not also taken up. Therefore the increased output flow rate removed too much liquid from the chamber. The liquid appeared to stick to the walls of the chamber and the stand and immediately left the chamber before it was filled. This may have been due to water tension effects of the liquid. Therefore, alternative methods to provide an ALI were investigated to solve this problem.

A column of sponge was investigated as an alternative stand to provide an ALI. The sponge material was highly wettable and when saturated had a very moist surface. It did not appear so absorbent that the skin would not receive adequate nutrition due to medium being trapped inside the sponge. The appearance was of a network of fibres with a very open porous structure. Initial inspection indicated that it was a suitable material. It was also shown that the level of liquid inside the chamber could be maintained within reasonable variation (fig. 3.5); the disk of filter paper positioned on top of the sponge stand remained well wetted during the investigation. Therefore, it was shown that a stable level of liquid could be maintained inside the chamber when using a stand made from this sponge. In addition the sponge was found to be non-toxic to fibroblasts and safe to use in cell culture (fig. 3.6).

The design of the system used active pumping on both the input and output to the chamber, in addition, the output had a higher flow rate than the input. These measures ensured that the level of liquid in the chamber was consistent and maintained. The increased output flow rate enabled components of the system to be positioned at different heights if required, allowing the pump to be positioned outside of the

incubator. The output could maintain the correct liquid level by ensuring sufficient liquid was removed or increasing uptake of air if the liquid level was too low during times when the volume of liquid in the chamber was temporarily altered due to height changes or inconsistencies in pump speed. The use of two pump channels per system meant that a large amount of tubing was required, making the system difficult to set up and handle.

The active pumping of the input and output meant that the system could be open to the atmosphere and allow air entry for pH buffering, unlike the first generation system which became pressurised in response to the pump drawing liquid through the chambers. The ALI was maintained at a very stable level using active pumping of both the input and output for a single chamber. However, the addition of multiple chambers into the system in either a series or parallel configuration was not feasible as this required pressurisation of the system to maintain matched, stable levels between chambers. Therefore, the connection of a single chamber per system was concluded to be the most suitable configuration. This made the setup of multiple repeats in an experiment very costly in materials, time and labour as multiple systems needed to be handled.

As already discussed, the chamber output ran at a faster flow rate than the input. This meant that the output of the chamber removed a greater volume than was entering the chamber; a negative pressure inside the chamber drew in air. An air filtering port was provided to remove contaminants from the air that entered the system. Drawing gassed air into the system from the 5% CO_2 atmosphere of the incubator would allow gas exchange with the medium, ensuring good pH buffering essential for growth of cells[87].

The lowest resistance path for air to enter was through the air filter which sterilised air as it entered. However, it is possible that a small amount of unsterilized air could enter

through higher resistance routes. These routes would not filter the air as it entered; examples are through the seal of the lid and the join between the two submerged chambers that make up the ALI chamber. It is possible that contaminated air entered the system through these routes and caused the infections experienced in figure 3.7.

Upon discovery of the inability of the second generation chambers to maintain sterility it was determined that use of these bioreactor systems was unsuitable for use in tissue culture applications. Future work would need to redesign the chambers and system for culture of TE skin at an ALI and provide more emphasis on establishing the maintenance of sterility at an earlier stage of the development process. This work has drawn attention to some of the issues faced with developing a bioreactor system for culture of engineered skin models. The literature available detailing the design and use of perfusion bioreactors for culture of skin models at an ALI is very limited[7,49] and work was not expanded in later studies, which may be explained by the challenges experienced in the development of such systems.

3.4 Summary

The aims of this work were to develop a bioreactor system to culture TE skin at an ALI which would permit *in situ* OCT imaging. The setup of first and second generation bioreactor systems has been described. The development and optimisation of the second generation system was explained in detail. The development process has highlighted important design features for perfusion systems for the culture of TE skin at an ALI.

Important design requirements were considered to be; provision of a stable ALI, ability to perform OCT imaging on samples within the chamber, ease of setup and maintenance of sterility. It was found that although the system optimisation enabled the reliable maintenance of a stable level and ALI in the second generation system, sterility could not be maintained and the system suffered infections within a few days.

In addition, although OCT imaging could be performed with the long working distance lens, the design of the chamber would not permit imaging using the high resolution lens which had a shorter working distance. Future designs of ALI chamber would address this problem by shortening the distance from the ALI to the lid of the chamber to allow higher resolution images to be obtained. It was also found that in practice the setup of this system was difficult and time consuming, especially as repeats were cultured in separate systems. Therefore, the development of the second generation perfusion system was not successful as it did not fulfil the requirements and could not be implemented to perform culture of TE skin at an ALI. Further work would need to re-design the system with reference to the problems encountered in this work.

4. OPTICAL COHERENCE TOMOGRAPHY IMAGING OF TISSUE ENGINEERED SKIN CONSTRUCTS

4.1 Introduction

Optical coherence tomography (OCT) is an optical imaging technique that can be used to obtain cross sectional images of the structures within a sample. Near infra-red light is directed into the sample and back-scattered when it encounters a refractive index mismatch which occurs due to changes in physical structure. In this way two dimensional maps of internal structures are produced. OCT has been applied with great success to *in vivo* imaging, especially in the eye[57]. Investigation of OCT for diagnostics in dermatology have also made progress since 1997 when it was first described[53,72].

Unlike ultrasound imaging, OCT does not require contact between the detector and the sample as a piezo-electric transducer is not implemented for signal detection. Furthermore, the samples do not require specialist preparation. Contrast is achieved by the structures within the sample, rather than addition of exogenous contrast agents[53]. The property of optical sectioning allows cross sectional images through the sample thickness to be obtained without destruction of the sample[50]. This contrasts with conventional histology which requires destructive physical sections to be taken to observe the internal structure of a three dimensional sample. The ability to observe cross sectional images of three dimensional samples non-invasively is complemented by the capacity to view the sample in real time and obtain images immediately[52]. Moreover, fast image acquisition rates allow volume stacks to be produced, giving three-dimensional information about the sample[68].

The properties that have been described indicate the suitability of OCT imaging in the field of tissue engineering. Samples may be viewed while they are sealed inside culture vessels due to the qualities of non-contact, non-invasive imaging without processing or

addition of contrast agents. The lack of processing accelerates the time required to obtain images, allowing real time assessment of construct development. The maintenance of the sterile environment by keeping samples within culture vessels is essential for tissue culture and allows samples to be returned to culture following imaging. Observation of samples at multiple time points permits time course experiments to be undertaken with few samples and repeated analysis of the same sample[80,82]. It is also safe and would not damage the sample, unlike the powerful lasers used in some imaging techniques such as multiphoton microscopy.

OCT has previously been implemented for the observation of tissue engineered constructs, this was first accomplished in 2003 to observe the recovery of burned samples with time[78,89]. These time-course experiments observed the changes in laser burned engineered skin constructs containing fibroblasts and keratinocytes based on collagen I gels over the culture period of 7 and 10 days. A similar time-course study in 2006 using collagen I gels seeded with fibroblasts and keratinocytes assessed the ability of OCT to distinguish the structures in developing TE skin constructs[80]. Further information on the sample was obtained from observation of the A-scan (the depth wise intensity signal) averaged over ten adjacent lateral positions. Location of a characteristic valley in the A-scans was said to correspond to the location of the basement membrane of the sample and could be used to measure epithelial thickness.

Use of OCT for the investigation of TE skin constructs based on de-epithelialized dermis (DED) has also been performed. This was initially to follow the development of a new epidermis on the construct[8], followed by investigation of wound healing after a scalpel wound and melanoma invasion[81]. These samples were imaged within their normal culture vessels and subsequently returned to culture allowing multiple imaging time points. OCT imaging of the TE skin constructs revealed a distinction between the dermis and epidermis, so it was possible to monitor epithelial development over time[8].

It was shown that the upper region of the epidermis was a bright signal, the lower epidermis was darkly signal and the dermis beneath was characterised by an increase in the signal.

Melanoma invasion was characterised by a change in the structure of the epidermal surface which became rough and irregular[81]. Additionally, skin wounding with a scalpel was followed over time and observation of wound closure was possible by the decrease in the diameter of the gap between the wound edges. The addition of a fibrin clot was shown to accelerate healing and closure of the wound[81]. OCT has been used in a qualitative manner by this research group to visually show the state of the skin constructs under various experimental conditions. However, deeper analysis into quantitatively measuring epithelial thickness or analysing the shape of the averaged A-scan signal was not performed.

Quantitative analysis of parameters such as the epithelial thickness from OCT images of TE skin constructs is important to establish quality control measures. Use of OCT as a non-invasive, non-destructive technique for quality assessment has the potential to reduce the costs associated with the production of these constructs by reducing waste of materials and the necessity to perform histology. Effective quality assessment requires the establishment of specific standards and characteristics of the sample which can be repeatedly and reliably used to give information about the internal structure. This work begins to address this problem by considering methods to measure the epithelial thickness which is likely to be an important parameter in the establishment of the quality of TE skin constructs.

The results presented in this chapter explain the observation of OCT images of TE skin constructs. The development of TE skin constructs were followed at weekly time intervals and comparison between OCT images and histology revealed the structures

which could be observed using OCT. Examples of good quality and poor quality TE skin constructs are presented. Additionally, measurement of epithelial thickness from histology and OCT images has been compared. OCT imaging of TE skin constructs shows promise to observe and indicate the quality and state of the internal structure of samples provided that robust characterisation of the expected and undesirable features are performed.

4.2 Results

The OCT systems implemented in this work have been described in section 2.1.9. Standard TE skin constructs were produced seeding fibroblasts and keratinocytes onto DED. Details of the methods implemented are described in depth in section 2.4.

4.2.1 Interpreting OCT images

OCT imaging can be used to visualise the internal structure of TE skin. To demonstrate and explain the interpretation of OCT images, an OCT image and histology image of the same TE skin construct were presented (fig. 4.1). These images were resized to the same scale to demonstrate the difference in field of view. Both the OCT image and the histology are cross sections of the sample, however the OCT image is an optical cross section whereas the histology is a physical section cut invasively from the sample using a microtome.

The stratum corneum is the first layer encountered at the surface of the sample; it is formed from multiple layers of terminally differentiated keratinocytes known as corneocytes. The stratum corneum is characterised by a highly back-scattering and bright intensity region on the OCT image. In the H&E stained histology the stratum corneum is characterised by a bright pink eosin stained anuclear basket weave structure at the surface of the sample.

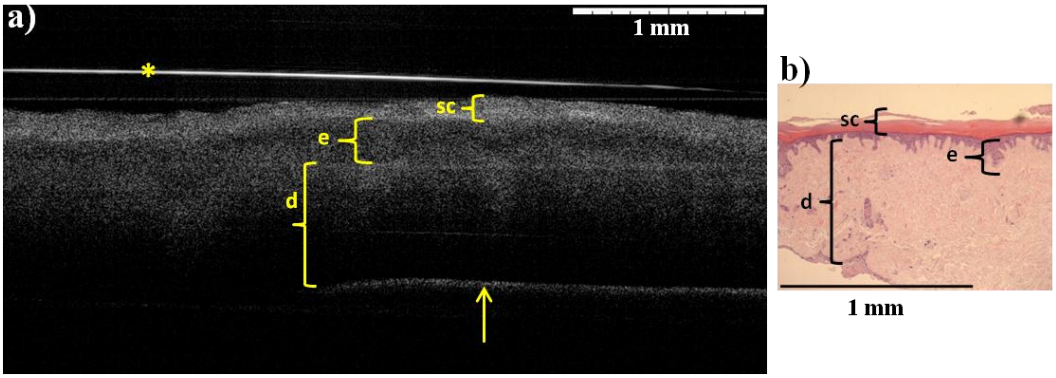

Figure 4.1: OCT image interpretation.

The images show the structure of standard tissue engineered skin cultured at an air/liquid interface for 14 days. Images are resized to the same scale. a) Shows an OCT image using the EX1301 system. b) Shows a haematoxylin and eosin stained histology section. Scale bars represent 1 mm. sc= stratum corneum, e=epidermis, d=dermis, star=lid of Petri dish, arrow=stainless steel grid.

The living epidermis is the region containing proliferative cells which provide the stock of undifferentiated cells that move to the surface and differentiate to form the stratum corneum. The living epidermis is characterised by the dark band below the stratum corneum on the OCT image. These proliferative cells are less scattering and consequently provide a lower intensity signal. The living epidermis is characterised by the dark purple staining on the histology. The nuclei in these cells take up the purple haematoxylin dye.

The dermis is a collagenous extracellular matrix. The dermis has a higher OCT signal intensity than the living epidermis so the image brightness increases below the living epidermis. In the histology the dermis is observed as the pink region below the living epidermis. The dermis contains copious extracellular matrix which is stained by the pink eosin dye.

In addition the OCT image shows artefacts that are present on some of the images shown in this work. The asterisk indicates the lid of the Petri dish which the sample was

sealed inside to prevent contamination. The lid of the Petri dish is the first structure that the incident OCT beam encounters and some of the beam is reflected at this point to produce a signal. The arrow indicates the stainless steel grid used in ALI culture to elevate the sample above the base of the culture dish. It has been shown that OCT imaging can be used to visualise the structure of TE skin during culture. Comparison with histology shows that the three major layers; stratum corneum, living epidermis and dermis can be distinguished from OCT images.

4.2.2 Time Course Development of TE Skin Constructs

After determining the ability of OCT images to distinguish between the layers of TE skin, OCT was used to follow the development of the TE skin over time (fig. 4.2). Standard TE skin constructs were cultured at an ALI for a period of 14 days with OCT imaging on day 0, 7 and 14. The non-invasive nature of OCT allows the investigator to observe the development of the same construct at multiple time points. Image c) was taken using the polarisation sensitive OCT system on day 0, whereas images a), d) and e) of DED and TE skin on day 7 and 14 respectively were taken on the EX1301 OCT microscope system (Michelson Diagnostics, Kent, UK).

The OCT image of the DED (fig. 4.2a) shows a ridged surface, indicating that the rete ridges of the native architecture are still present. The corresponding histology also displays an undulating surface (fig. 4.2b). Observation of the TE skin on day 0 of culture at an ALI (two days after seeding) shows that the surface of the construct has become smooth, indicating that the ridges have become filled with cells (fig. 4.2c). Sporadic bright regions on the surface may indicate clumps of cells.

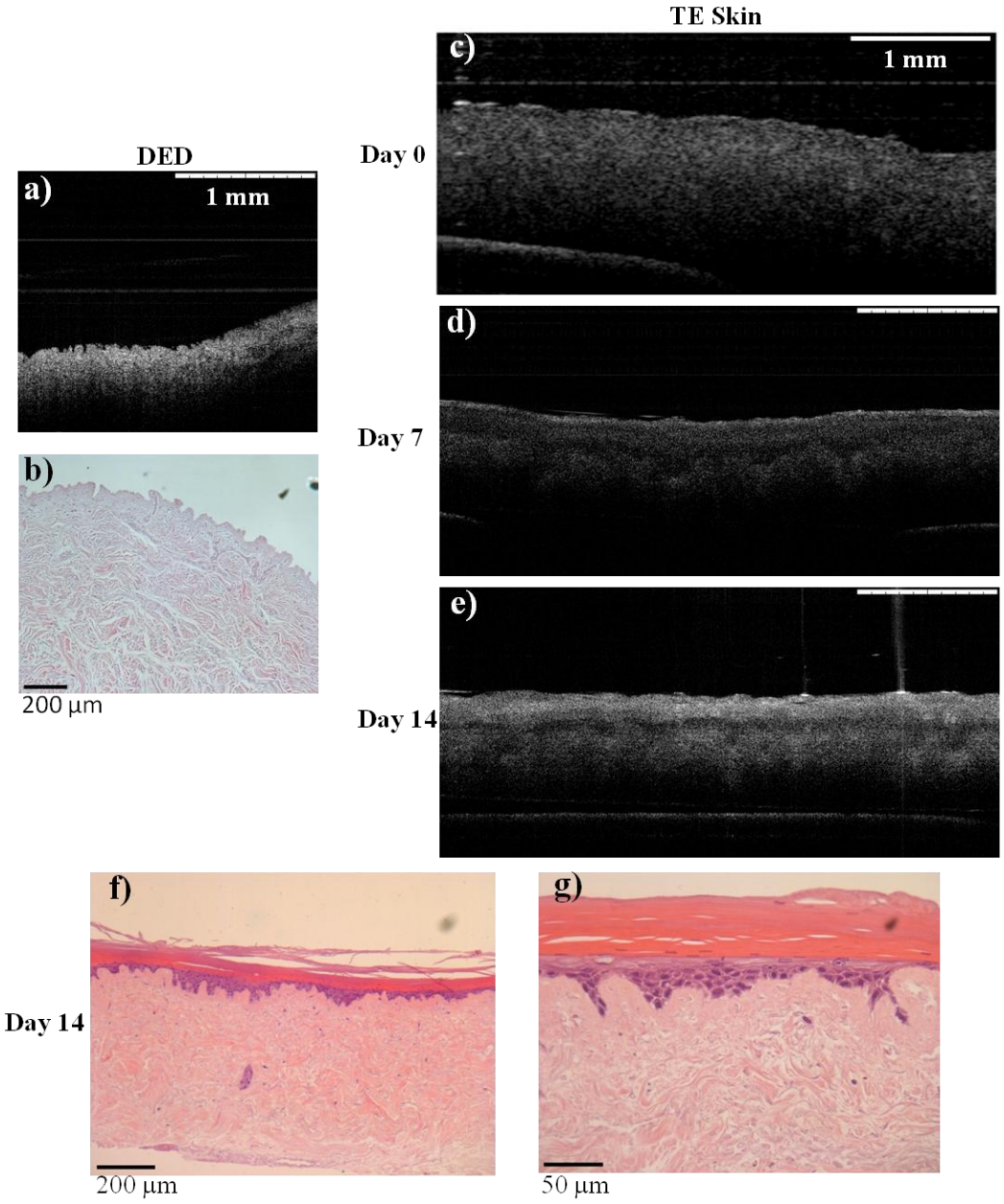

Figure 4.2: OCT images and histology of good quality TE skin.

OCT images showing time course of experiment, and corresponding H&E stained histology at end time point. a) OCT image of DED prior to addition of cells, b) H&E stained histology of the DED, c) Day 0 OCT image (taken on PS OCT system), d) Day 7 OCT image, e) Day 14 OCT image (images d and e taken on EX1301 system), d) H&E stained histology of this sample at day 14 (scale bar represents 200 µm), e) Higher magnification image of H&E stained histology at day 14 (scale bar represents 50 µm).

By day 7 the upper region of the construct is a thick dark layer characteristic of undifferentiated cells in the living epidermis (fig. 4.2d). The lower region of this layer has an undulating boundary which may correspond to the larger rete ridges. The surface has a thin bright layer indicative of differentiated keratinocytes in the stratum corneum. The dermis has a brighter signal than this upper region.

Observation of the OCT image corresponding to the sample on day 14 shows that the uppermost layer is a bright, highly back-scattering layer (fig. 4.2e). Inclusion of an air pocket towards the right of the image indicates this is the basket weave structure of the stratum corneum. The stratum corneum has thickened and become a more consistent brightness in comparison to day 7. There is still a prominent dark region with an undulating boundary corresponding to the living epidermis beneath the stratum corneum. Beneath the living epidermis the brightness increases again to signify the dermis.

The corresponding histology of this TE skin sample at the final day 14 time point confirms the structure of the samples (fig. 4.2f and g). The structure of the samples observed under OCT imaging during culture indicated that the structure was developing with time. The histology shows that the quality was good. The dermis contains a few fibroblasts embedded within the extracellular matrix. The living epidermis contains multiple layers of well attached, rounded proliferative keratinocytes, which gradually flatten and differentiate to lose their nuclei and become the corneocytes that make up the stratum corneum. The stratum corneum displays the characteristic basket weave structure and is well attached to the living epidermis. Nearer the surface it becomes more flaky and gaps form between layers. OCT images can give similar qualitative information on the development of TE skin constructs in comparison to standard histology however, the resolution is lower.

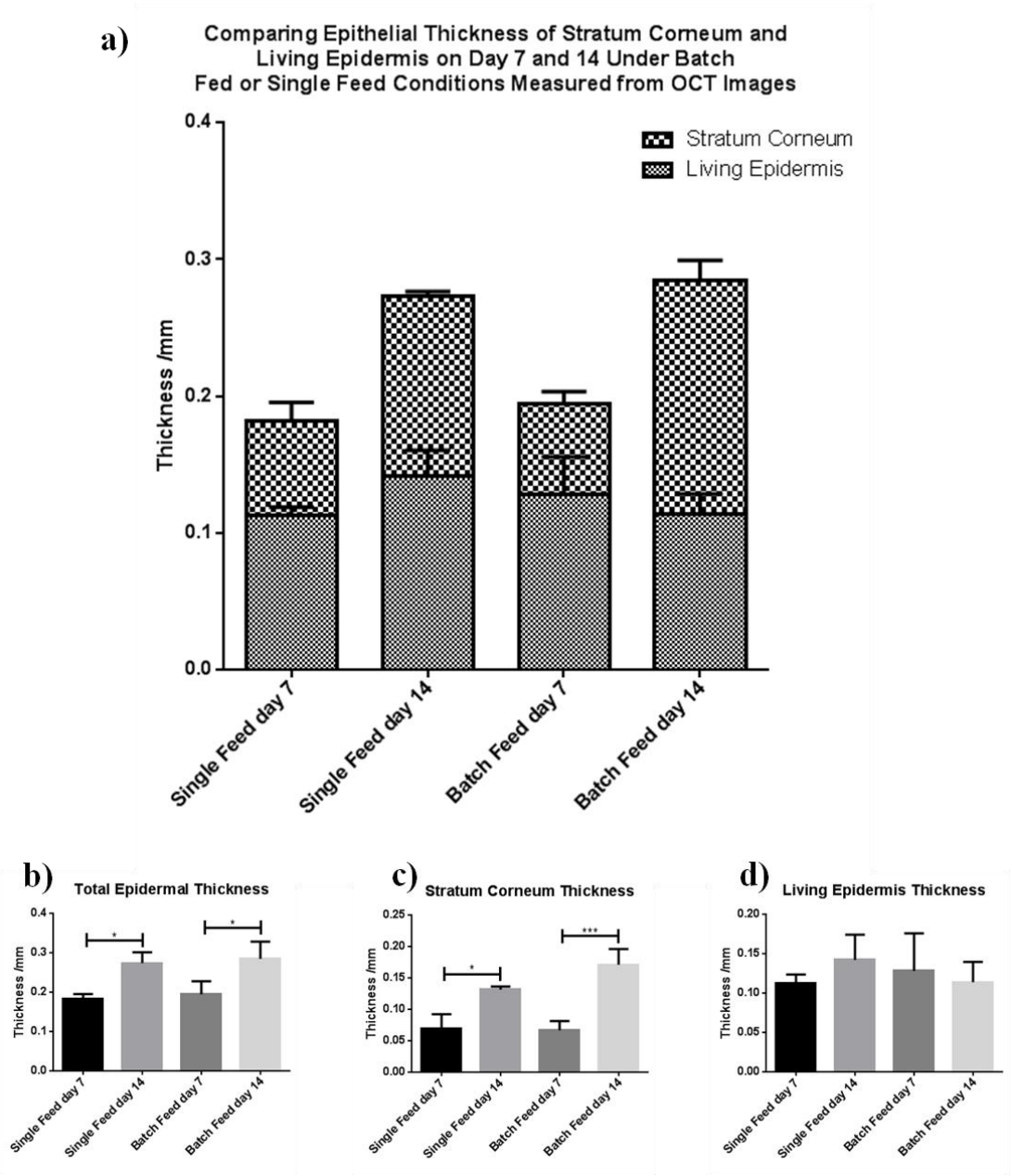

Figure 4.3: Graph to compare epithelial thickness measured from OCT images on day 7 and 14; investigating the difference between feeding regime.

a) Epithelial thickness of batch fed versus single fed TE skin constructs were compared on day 7 and 14 in terms of proportions of living epidermis and differentiated stratum corneum. Measurements were made by the line tracing method. Error bars represent the standard error. b), c) and d) showing statistical significance of each condition by the Tukey multiple comparisons ANOVA test. The total epidermal thickness and stratum corneum thickness was significantly different on day 7 and day 14. The living epidermal thickness was not significantly different. (n=3)

Epithelial thickness from OCT images on day 7 and 14 was measured using the line tracing method and displayed graphically (fig. 4.3) for the samples in the previous figure. Samples were cultured under static ALI conditions using a single feed or batch feed regime. There was no significant difference observed between the total epithelial thicknesses of the two feeding regimes on day 7 or on day 14 (fig. 4.3b). For both feeding regimes there was a significant difference between the total epidermal thickness on day 7 and day 14. There was also a significant difference between the stratum corneum thickness on day 7 and day 14 for both feeding regimes (fig. 4.3c). However, the thickness of the living epidermis was not significantly different between time point or feeding regime (fig. 4.3d).

4.2.3 Poor Quality TE Skin

OCT has been used to monitor the development of good quality TE skin (fig. 4.2) however; it is also a useful technique to alert the researcher to problems that may arise in the constructs during culture. It is important to understand how poor quality TE skin affects the OCT images obtained; images of TE skin constructs from the EX1301 OCT microscope system (Michelson Diagnostics, Kent, UK) are presented (fig. 4.4). Poor quality TE skin constructs were stimulated by poor delivery of nutrients to samples which were placed on sponge stands, rather than porous stainless steel grids to maintain the ALI.

On day 0 at ALI the surface was smooth and exhibited occasional bright regions, thought to correspond to clusters of cells (fig. 4.4a and d). On day 7 a thin, flat band of dark proliferative cells is observed with a few thin, brighter regions corresponding to the stratum corneum (fig. 4.4b and e). The corresponding histology for day 7 (fig 4.4c) shows a strange morphology of cells and poor organisation of the structure with a very flaky stratum corneum.

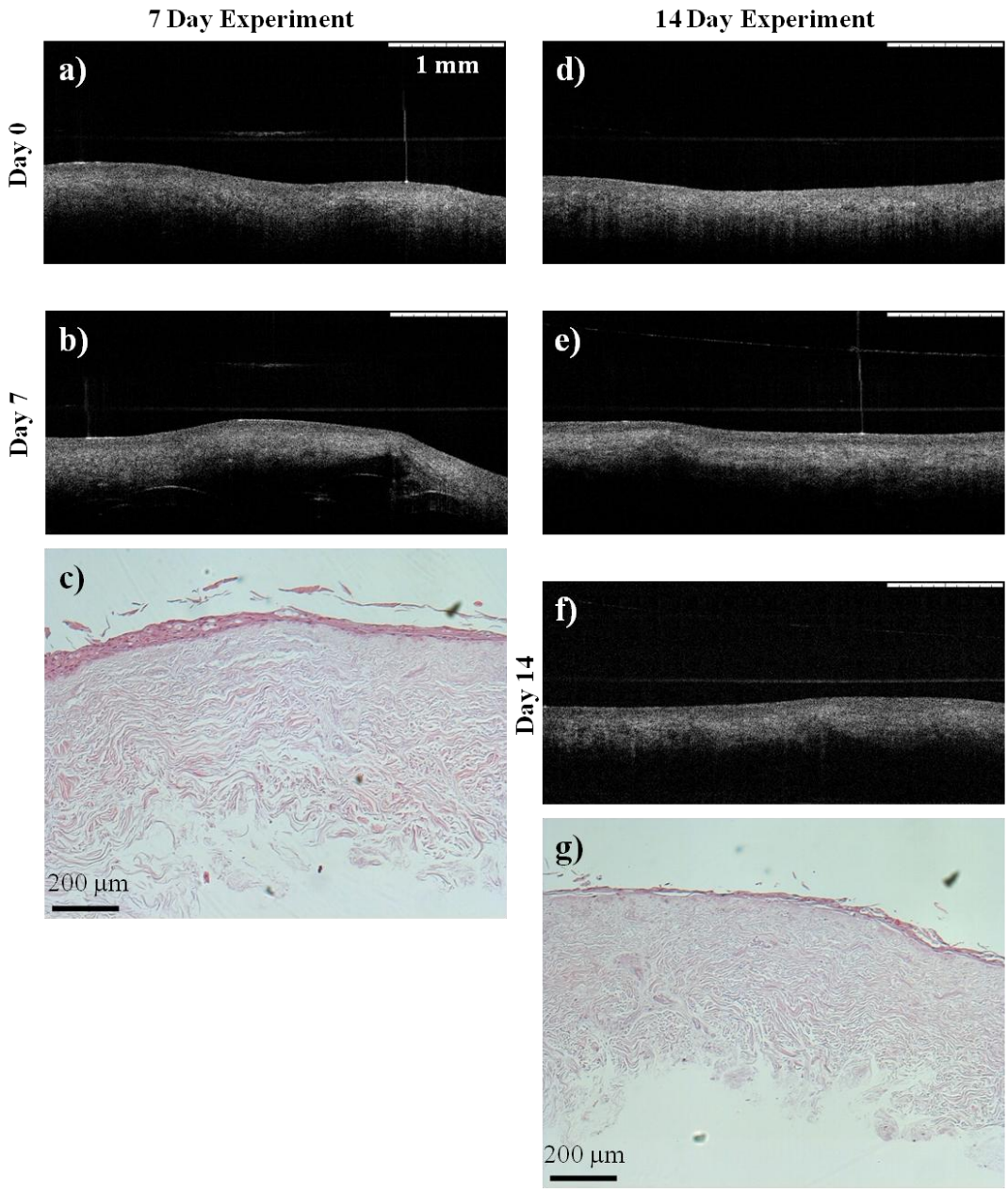

Figure 4.4: Demonstrating the ability of OCT to detect poorly developing constructs.

TE skin constructs were cultured on sponges to limit nutrient delivery and imaged using the EX1301 OCT system. OCT images were compared with H&E histology on day 7 and 14. a) and d) day 0 OCT images, b) and e) day 7 OCT images, f) day 14 OCT image (OCT scale bars represent 1 mm), c) day 7 histology, g) day 14 histology (histology scale bars represent 200 µm).

On day 14 the OCT images displayed less contrast between the dark living epidermis and the brighter dermis in comparison to day 7 (fig. 4.4f). In addition there is very little sign of the bright surface region corresponding to the stratum corneum, exhibited as a bright region at the surface. Comparison of OCT images indicates that between day 7 and 14 the structure has deteriorated exhibited by the decrease in contrast. The corresponding histology for day 14 confirms the deterioration of the sample indicated by a very thin layer of cornified cells which was poorly attached to the surface (fig. 4.4g). There were no longer any nucleated proliferative keratinocytes remaining.

4.2.4 Analysis of Epithelial Thickness Measurements from OCT and Histology

In order to investigate the ability of OCT images to measure the epithelial thickness, measurements from OCT and histology images were compared (fig. 4.5). Measurements were taken manually using a line tracing method to draw around the area of interest and dividing the area by the length of the image to obtain an average thickness value. Measurements of epithelial thickness from 6 good quality TE skin samples were analysed as scatter plots of histology versus OCT measurements. The error bars indicate the standard error; horizontally for the histology and vertically for the OCT images. The line of best fit was constrained to pass through the origin as it was anticipated that differences in measurement would be consistent for structures of different sizes. The gradient of the line of best fit indicated the general difference in measurement between OCT images and histology images.

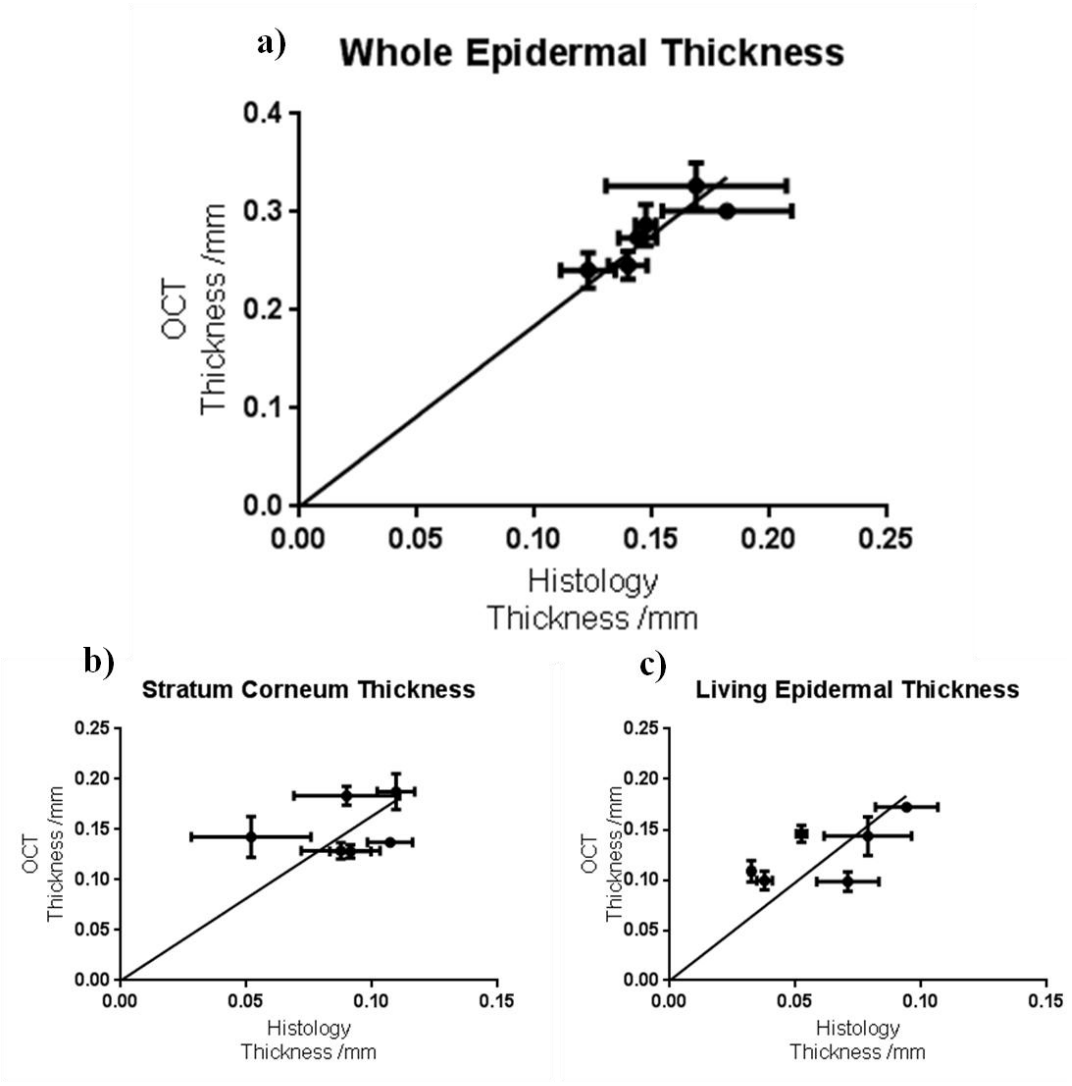

d)

	Gradient	R^2
Whole Epidermal Thickness	1.85	0.62
Stratum Corneum Thickness	1.63	-0.87
Living Epidermal Thickness	1.95	-0.40

Figure 4.5: Graphs comparing epithelial thickness measurements from histology and OCT images.

Each data point is calculated from the average measurements of 3 histology images and 3 or 4 OCT images of a single sample of TE skin. Error bars show the standard error of the measurements; histology horizontally, OCT vertically. The line of best fit has been set to pass through the origin. a) The thickness of the whole epithelium measured from histology versus OCT images, b) The thickness of the stratum corneum measured from histology versus OCT images, c) The thickness of the living region of the epidermis measured from histology versus OCT images, d) Table comparing features of graphs; gradients and the coefficient of determination (r^2 value) which gives information on how well the data fits the line of best fit.

The correlation between measurements of the full epithelial thickness; including the stratum corneum and living epidermis is shown in figure 4.5a. The coefficient of determination (r^2 value) was 0.62 which showed there was a relationship between measurements from OCT images and histology images. The measurements from histology images were consistently lower than predicted by OCT images, leading to a line of best fit with a gradient of 1.85. This indicated that histology measurements were generally 1.85 times smaller than equivalent measurements from OCT images.

The corresponding data to compare the measurement of the thickness of the stratum corneum from these samples is shown in figure 4.5b. The data points on this graph are more dispersed than in graph a) which is reflected in the coefficient of determination which was -0.87, indicating a poor fit. The gradient is slightly smaller (1.63) suggesting that the histology measurements are generally more similar to the OCT than in whole epithelial or living epidermal measurements.

The thickness of the living region of the epidermis from histology and OCT is shown in figure 4.5c. Similarly the fit was poor with a coefficient of determination of -0.40. This measurement had the largest gradient at 1.95; this shows the largest difference between OCT and histology measurements.

4.2.5 Production of Averaged A-Scans

A number of studies have used an averaged A-scan to determine information such as the epithelial thickness of the sample[53,59,80]. Therefore this concept was investigated to determine the utility of performing A-scan analysis to obtain objective information about TE skin samples. In order to plot the averaged A-scan, the sample surface was initially flattened to produce an image with a horizontal surface. It was then possible to take an average of the adjacent A-scan signals; this was done around the central position of the image.

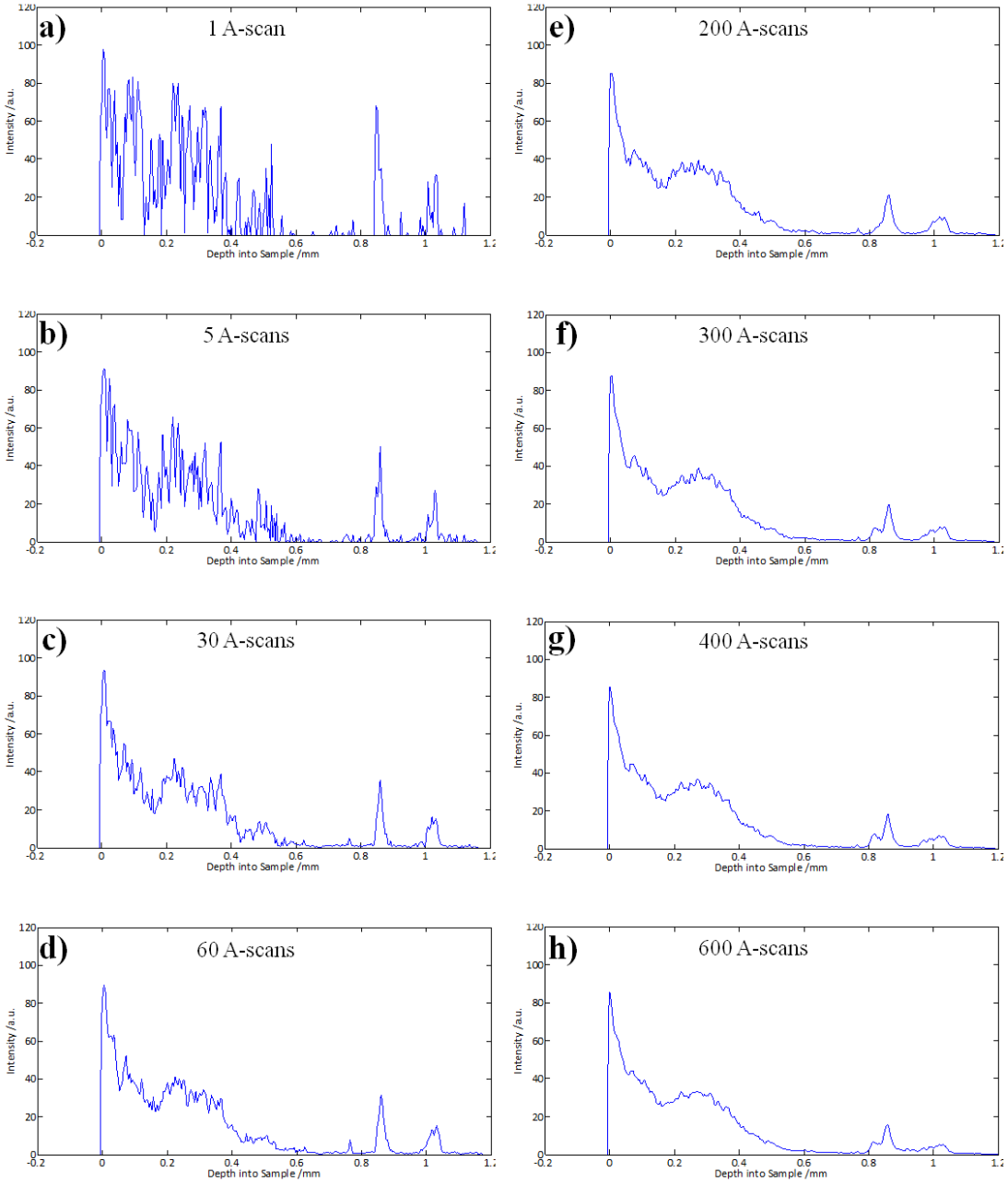

Figure 4.6: A-scan study on 7 day TE skin construct.

Investigating the effect of increasing the number of A-scans used in the averaged A-scan plot. The number of A-scans averaged is indicated on each graph. Averaged A-scans using 1 signal to 600 signals are shown. The y-axis indicates intensity and the x-axis indicates depth into sample. As the number of A-scans increases the noise is reduced.

In order to determine the optimal number of A-scans to average, a range of numbers of A-scans were analysed (fig. 4.6). A single A-scan produced a very noisy shape (fig. 4.6a). As the number of A-scans in the average increased the noise decreased, when 200 A-scans were averaged (fig. 4.6e) the signal was smoothed but did not loose detail. When the number of A-scans in the average was above 300, the signal became over-smooth and information was lost as the peaks and valleys (which are thought to indicate changes in epithelial structure) became less defined. However, it was found that the optimal number of A-scans to use in the average varied between images and samples.

4.3 Discussion

This study has investigated the application of OCT as a method to follow the development of TE skin constructs at multiple time points throughout culture. It has been shown that the epidermal structures within TE skin could be identified on OCT images. The stratum corneum was found to be a highly back-scattering region at the surface of the construct. It was most easily identified on day 14 when it became thicker and inclusions of air were observed between flakes in the basket weave morphology. The living region of the epidermis, which likely consists of the stratum basale and stratum spinosum, was identified as a dark low intensity signal, which in good quality TE skin showed an undulating boundary with the dermis. The dermis was located beneath the dark signal of the living epidermis and found to have a comparatively bright signal.

These observations conflict with those from *in vivo* studies of palmoplantar skin which observed a very dark stratum corneum, a bright living epidermis and a slightly darker dermis[53]. Elsewhere the stratum corneum was reported to be too small to be resolved and the living epidermis was a dark layer at the surface following the initial entrance spike. Beneath this the dermis had a brighter signal[51]. It is possible that the environment experienced by the *in vivo* skin causes differences in refractive indices of the structures

observed. For example the hydration, blood supply and melanin content of the skin could cause these effects on the OCT signals. In addition, the attenuation of the signal in images of palmoplantar skin may have caused the dermis to appear dark in comparison to the other structures.

Comparison of the observations made in the current study with those from previous work using the same *in vitro* TE skin model in this research group also shows differences. Previously the whole epidermis was identified as the bright signal at the surface of the image[8,81]. The signal dipped and increased to indicate the dermis which had a bright signal; the dermal epidermal junction was identified as the under-surface of the surface bright layer. It is possible that the dip in the signal between the bright upper signal and the dermis could correspond to the living epidermis and may have been initially misinterpreted. In this case the initial bright layer would correspond to the stratum corneum, not the whole epidermis, and the comparison between the current work and the previously described work would agree.

In the OCT images of TE skin the living epidermis comprises many nucleated proliferative cells and exhibits a low intensity signal. The dermis is largely acellular and is packed with collagenous extracellular matrix. The signal from the dermis is more intense than the living epidermis, and less intense than the stratum corneum. The difference in brightness between the living epidermis and the dermis may be explained by consideration of the refractive indices of their components; type I collagen has a refractive index of 1.43[90] and cell nuclei have a refractive index of 1.36[91]. The difference in refractive index causes the back-scattered OCT signal; the greater the difference in refractive index the greater the back-scattering. The abundant cell nuclei in the living epidermis have a small refractive index which may explain the low OCT signal. Similarly, the more intense OCT signal produced by the dermis could be due to

the high collagen content. Collagen bundles have been shown to cause the dermis to become highly reflective[53].

Having established the characteristic signals of OCT images of TE skin based on DED, a time-course was presented (fig. 4.2). OCT was able to follow the development of constructs qualitatively over time. The low intensity region of the living epidermis was shown to increase in thickness between day 0 and day 7. On day 7 there was also a medium bright region within the dark region which could be due to keratinocytes beginning to differentiate and gradually changing in optical properties (fig. 4.2d). On day 14 the OCT image mirrors the corresponding histology, demonstrating three clearly visible structures of the stratum corneum, living epidermis and dermis (fig. 4.2e).

In contrast to the good quality TE skin constructs shown in figure 4.2, the structure of poor quality TE skin was also observed (fig. 4.4). Poor quality TE skin had a flat dermal epidermal junction. The layer of proliferative cells was thin and between day 7 and day 14 the structure deteriorated rather than improved, indicated by a decrease in image contrast. Corresponding histology confirmed the initial observations from the OCT images. The advantage of performing OCT imaging was that the internal structure could be observed immediately, before constructs were removed from culture and before lengthy preparation for histology was performed. In addition, OCT was able to inform the researcher that the TE skin constructs were not progressing and that the expected structure was not developing, giving an early indication of quality.

In order to implement OCT imaging for quality control of TE skin, criteria would need to be established as indicators of quality. The measurement of epithelial thickness has been considered to be an important parameter for quality determination as it is easily observed on OCT images and indicates the stage of development of the sample. The epithelial thickness was measured on day 7 and 14 for TE skin samples cultured under

batch or single feed conditions (fig. 4.3). This analysis was able to show a significant difference in total epithelial thickness and stratum corneum thickness between day 7 and 14. It was shown that during this time the living epidermal thickness did not change. In addition, the feeding regime was shown not to effect epithelial thickness measurements. Therefore, analysis of epithelial thickness from OCT images has been shown to provide interesting information about the sample in a non-destructive way during culture.

Subsequently epithelial thickness from OCT images was compared with corresponding measurements from histology to determine the correlation between measurements from these imaging techniques (fig. 4.5). The closest correlation was found between the measurements of the whole epithelial thickness. Correlation between measurements of the stratum corneum thickness and living epidermal thickness were poor.

The poor correlation observed between the thickness of the stratum corneum from OCT and histology images (fig. 4.5b) may have been due to errors in measurements. In the histology images the stratum corneum often became flaky and strands would lift up away from the rest of the epidermis which caused measurements to overestimate thickness. The extent to which this occurred was highly variable between samples and even image locations. It was also possible for the strands that broke away from the bulk of the stratum corneum to fall off completely which would cause measurements to be underestimated. Thus there was huge potential for variation in measurements of stratum corneum thickness between histology images and OCT images, leading to poor correlation.

The correlation between OCT images and histology images was also poor for measurement of the living epidermal thickness; this may have been influenced by the small sample size of just six constructs. A larger study may aid verification of these

results. In addition for each sample multiple OCT and histology images were analysed and averaged to determine epithelial thickness. However, the same location was not found in corresponding OCT and histology images so the variations in construct thickness across the surface may have caused differences in measurements. In order to resolve this issue, future studies should develop a reliable method to indicate imaging location for OCT and histology. This may enable a closer correlation between measurements from OCT and histology images in future work.

OCT images consistently measured thicker structures than the corresponding histology; this observation may be explained by the shrinkage of samples during the processing techniques implemented during histology. The sample shrinkage and distortion has been previously reported for formalin fixed, paraffin embedded samples during histology[83–85]. Shrinkage occurs during the formalin fixation, dehydration and clearing, embedding and sectioning steps of the histology process[85]. Therefore, the smaller thickness values observed from histology images were expected. It has been suggested that using cryostat histology would prevent sample distortion and allow closer comparisons to be made between measurements using these imaging techniques[76]. The advantage with using OCT imaging is that it shows the samples in their original form, before any distortions created by the histology, so may be considered the more accurate epithelial measurements.

In addition to these reasons for the differences in measurements from OCT images and histology images, errors may be introduced by the subjectivity associated with the manual measurement technique. This is a greater problem for the OCT image assessment as the changes in brightness can sometimes appear very slight and gradual. Therefore, it would be advantageous to remove the human observer from this task. Many studies have suggested using the averaged A-scan to determine measurements of

structures shown in OCT images[69,74,80]. The A-scan is the OCT signal with respect to the depth into the sample; it is a column of intensity values through the sample.

A range of averaged A-scans for one image of a TE skin construct cultured for 7 days at ALI has been shown (fig. 4.6). When a single A-scan was plotted the signal was very noisy and erratic. The signal was too poorly defined to give information about the sample. The signal became less noisy as the number of A-scans in the average was increased. The average of 200 A-scans showed the clearest definition of the curve, without the potential loss of information experienced when a greater number of A-scans were averaged. The downward slope of the signal when 400 A-scans were averaged showed that the signal has been over-smoothed; characteristic peaks and troughs were no longer visible, indicating a loss of important information about the sample.

It was found that the optimal number of A-scans in the average was not universal for all samples and images. Further work is required to determine the optimal number of A-scans to average before work can continue to assess measurements of epithelial thickness from samples. Although at this stage it is not possible to determine the utility of A-scan analysis, its successful implementation would avoid the subjective nature of manual measurement of epithelial thickness.

OCT imaging has previously been implemented to observe the development[8] and response to stimuli[81] of TE skin constructs based on DED in a qualitative manner. However, the quantitative measurements required to establish quality control criteria have not previously been investigated for this TE skin model.

4.4 Summary

This work aimed to investigate the use of OCT imaging for the observation of TE skin during culture and to design methods to analyse the resulting images in terms of quality control. OCT imaging is non-invasive and permits imaging at multiple time-points

during culture which allows assessment of construct development without damaging the sample. Therefore, OCT is ideally suited to perform quality assessment of tissue engineered constructs prior to further use.

This study has described the characteristics of the structure of TE skin constructs based on DED, which displays a different OCT signal pattern in comparison to *in vivo* palmoplantar skin, but a similar pattern to normal skin. OCT images have been used to perform a time-course experiment observing the developing structure in visual images and in terms of epithelial thickness measurements. Measurement of epithelial thickness on day 7 and 14 confirmed that the construct was developing well. The epithelial thickness was also compared to corresponding histology. Large differences in measurements were discovered; explanations may include distortion of samples during histology and errors in user measurement. Following from similar research, initial results are shown for the generation of the averaged A-scan which could be used in further work to find information such as the epithelial thickness from samples.

The work presented has successfully demonstrated the ability of OCT to perform observation of the developing structure of TE skin constructs within culture without contamination or destruction. This method has permitted the discrimination of structurally good quality and poor quality TE skin. In addition initial results have been presented for the analysis of the structure of TE skin constructs as a starting point to establish quality control parameters by measurement of epithelial thickness. However, extensive further work is required to implement this in a robust, reliable manner.

5. OCT IMAGING OF TE SKIN CONSTRUCTS CULTURED UNDER PERFUSION CONDITIONS

5.1 Introduction

Tissue engineered (TE) skin is a valuable resource[1] with applications from clinical wound repair [25] to toxicity testing of substances[92]. Although these models provide a good approximation of native skin by displaying a similar structure[5], there are limitations. Constructs have a short lifespan and viability is not maintained for prolonged culture periods. Beyond two weeks in culture constructs deteriorate[5] which has implications for when transplantation onto a patient must occur and the timescale of *in vitro* investigations that can be carried out. Furthermore, non-destructive observation of constructs is not well established. Therefore, assessment of developmental stage or quality is not possible without performing destructive histology.

It has been hypothesised that perfusion culture techniques improve nutrient delivery to TE constructs, ensuring constant medium composition and a steeper diffusion gradient as the medium in contact with the construct is continuously refreshed[6]. Using a single feed of medium during the culture period avoids the sudden spikes in medium composition experienced when the medium is changed during batch fed protocols, which has been said to have an impact on cell survival *in vitro*[7]. The study by Kalyanaraman *et al.* (2008) showed that re-circulating perfusion culture of TE skin constructs was able to maintain viability over a three week culture period and improve viability in comparison to static controls[49].

A further limitation with TE skin constructs is that assessment of the internal structure is routinely undertaken by histology. Preparation of samples for histology is a time consuming process which is destructive in nature[82]. Optical coherence tomography (OCT) imaging has been proposed as a suitable tool for non-invasive, non-contact *in*

situ imaging of TE skin constructs during culture[8]. The ability of OCT imaging to observe the internal structure of 3D samples in real time without disturbing culture has huge potential in tissue engineering.

The work presented in this chapter aims to address the limitations of lifespan and non-destructive assessment of the internal structure of samples using a combination of perfusion culture techniques and OCT imaging. Using perfusion culture techniques to culture TE skin at an air/liquid interface (ALI), good quality TE skin was produced which appeared morphologically very similar to equivalent static ALI controls. In addition OCT imaging was used to non-invasively observe the development of the TE skin over the time course of the experiment. Changes in the structure of samples were observed, and it was possible to differentiate between samples cultured under submerged and ALI conditions. It is hypothesised that combining these two techniques will aid the advancement of skin culture both as a research tool and for therapeutics.

5.2 Results

TE skin constructs were cultured under perfusion conditions within first generation ALI bioreactor chambers for a period of two weeks at a continuous flow rate of 220 µl/minute. The system was connected and setup as previously shown in figures 2.3 and 3.1. Skin constructs were cultured under static submerged conditions as a negative control (fig. 5.1a) to produce poor structural organisation. Conventional static ALI conditions acted as the positive control (fig. 5.1c). These conditions were compared with constructs cultured under perfused ALI conditions (fig. 5.1b) to assess the potential of perfusion culture to produce good quality TE skin constructs. OCT imaging was performed every 7 days from when samples were raised to an ALI to record the construct development with time (fig. 5.1i to iii) using the in-house swept source system[8] (fig. 2.1). On day 15 conventional histology was performed (fig. 5.1iv to v).

5.2.1 Setup of the Perfusion System

The perfusion system was more complicated to set up than standard static culture methods. The perfusion system was re-usable so was first connected together and sterilised by circulation of 70% IMS and rinsed with sterile PBS which was a time consuming process. The system was primed with 15 ml Green's medium and the samples were inserted. The reservoir had a maximum capacity of 20 ml and three chambers containing TE skin were connected together. Therefore, the medium was changed twice weekly at the same time points as the static controls as the reservoir was not large enough to contain the total volume of medium required for the whole experiment. All samples received the same volume of medium over the experiment, however, the perfused samples shared the medium and static samples were isolated. Both static and perfused samples were subject to spikes in medium composition associated with batch feeding techniques. To transport the samples for OCT imaging, each of the chambers was disconnected from the circuit inside a laminar flow hood. Chamber input and output tubes were connected together to isolate each chamber and maintain a closed environment.

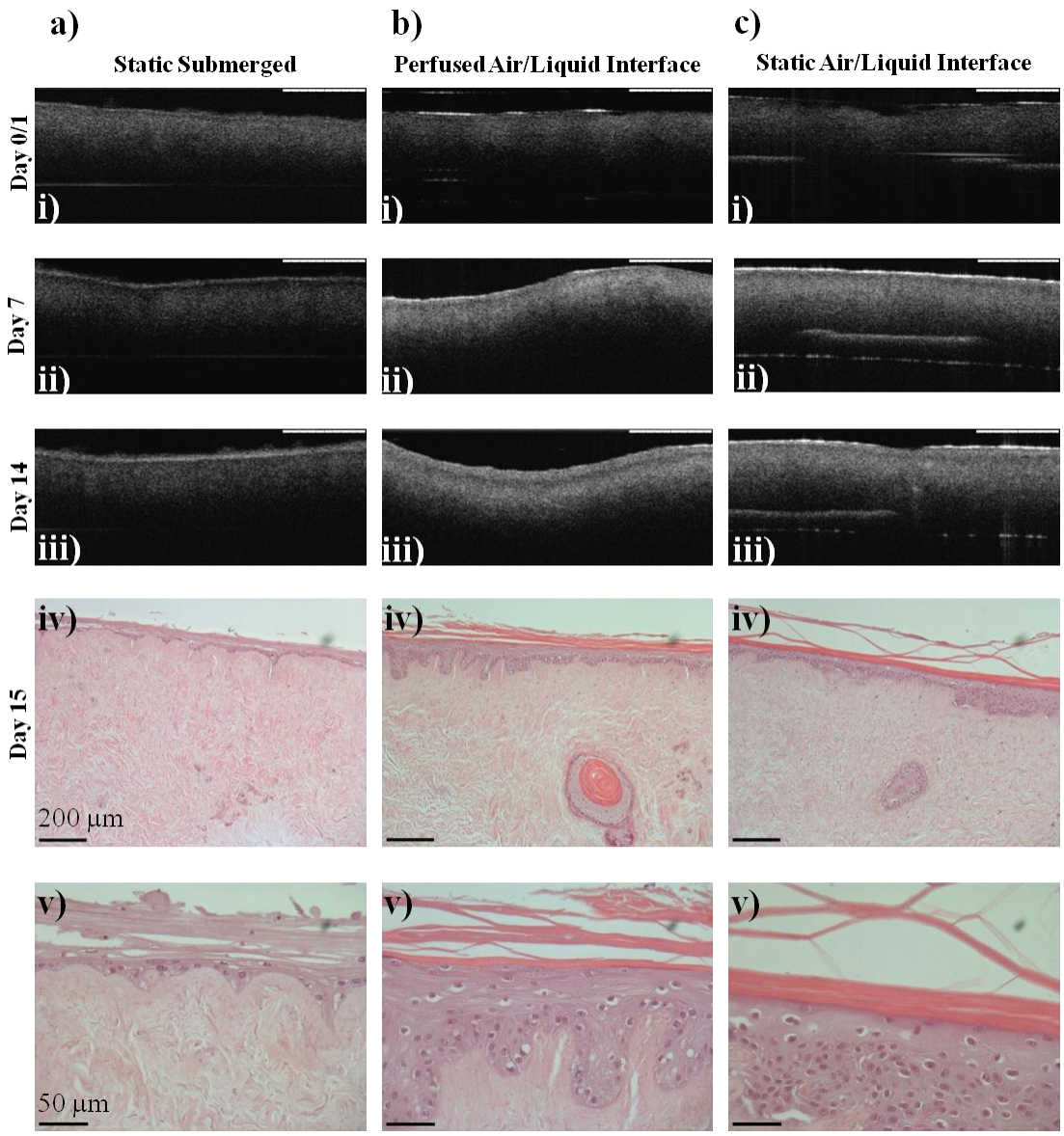

Figure 5.1: Time course OCT images and corresponding histology

Static submerged (a) and static air/liquid interface (c) samples were compared with perfused air/liquid interface (b) samples cultured for a period of two weeks after raising to the air/liquid interface (n=3). i) OCT images on day 0 (static ALI (c) and perfused ALI (b)) or day 1 (static submerged (a)). ii) OCT images on day 7. iii) OCT images on day 14. Scale bars represent 1 mm. iv) H&E histology on day 15 (scale bar represents 200 µm). v) H&E histology at higher magnification on day 15 (scale bar represents 50 µm). All images shown were representative of the samples.

5.2.2 Implementation of OCT for Observation of Construct Development

OCT images of the construct development on day 0 (ALI samples) or day 1 (submerged samples), day 7 and day 14 have been presented for each of the culture conditions. At the first time point the constructs imaged at the ALI (fig. 5.1bi and ci) show very strong, horizontal reflections on the surface. This is likely to be due to a thin film of liquid on the surface of the sample remaining from when the samples were lifted from a submerged condition to an ALI shortly before the imaging was undertaken. The static submerged sample does not exhibit this signal as the construct was imaged while it was submerged in medium which more closely matched the refractive indices. Aside from this difference all the samples looked fairly similar, with a homogeneous internal structure.

On day 7 (fig. 5.1ii) the static submerged sample (fig. 5.1aii) displayed a generally darker signal in comparison to the samples cultured at an ALI. At this time point each of the samples had a bright, high intensity surface signal. It is possible that this layer is the initial formation of the stratum corneum. Beneath this bright surface layer, a thin dark band can be distinguished indicating the living region of the epidermis; this is most evident in the image of the static ALI samples (fig. 5.1cii). Finally the signal increases to signify the dermis.

On day 14 (fig. 5.1iii) the static submerged sample (fig. 5.1aiii) displays a thickened bright surface layer in comparison to the image taken on day 7. The static ALI sample (fig. 5.1ciii) shows a small change since day 7. There is still a relatively thin bright surface layer; however, the dark layer beneath this has not noticeably increased in thickness. In contrast, the perfused ALI sample (fig. 5.1biii) displays a slightly less intense surface signal in comparison to the corresponding image from day 7 and the static ALI sample on day 14. However, a thicker, bright surface signal is observed and appears much like the stratum corneum as identified in chapter 4. Beneath this there is a

dark band, which corresponds to the proliferative cells of the living part of the epidermis. Then the signal increases once more to signify the dermis.

5.2.3 Observation of Histology

On day 15 the samples were sacrificed and routine histology with H&E staining was performed (fig. 5.1iv and v). The histology showed that the static submerged samples (fig. 5.1aiv and av) displayed a very different structure in comparison to samples cultured at the ALI. The layer of keratinocytes forming the epidermis was thinner. The most basal keratinocytes contained nuclei, however, this layer was at most only one or two cells thick, and in some places was missing entirely. The attachment of the nucleated cells was sporadic across the surface of the sample. The majority of the keratinocytes appeared to have differentiated to form a stratum corneum like structure that was a few layers thick. This structure was unable to take up eosin dye to the same extent as samples cultured at the ALI and consequently appeared as a pale pink structure. In addition, this stratum corneum contained a few nuclei, indicating that differentiation occurred very rapidly.

In contrast the samples cultured under static ALI conditions (fig. 5.1civ and cv) displayed a multilayered proliferative living epidermis that was more than 5 layers of rounded proliferative cells thick and well attached to the dermis. The keratinocytes gradually differentiated and became flattened forming the stratum corneum. The stratum corneum was bright pink and had a flaky basket weave structure. The samples cultured under perfused ALI conditions (fig. 5.1biv and bv) displayed the same structure described for the samples cultured at a static ALI.

a)

Dermis				Epidermis					
Number of fibroblasts		**Depth of penetration into matrix**		**Dermal Epidermal Attachment**		**Organisation of dividing cells**		**Stratum corneum**	
None seen	0	No penetration	0	No attachment	0	No epithelium	0	No stratum corneum	0
Few/ Occasional	1	Less than 1/3 thickness	1	Poor attachment	1	Monolayer	1	Thin stratum corneum	1
Abundant	2	Between 1/3 and 2/3 thickness	2	Mostly Attached	2	Sporadic layering	2	Poorly attached/ nucleated	1
		More than 2/3 thickness	3	Fully attached- no gaps in dermal epidermal junction	3	More than 2 layers of dividing cells throughout	3	Multilayered stratum corneum	2

b)

	Dermis		Epidermis			Total Score	Average
Sample	**Number of fibroblasts**	**Depth of penetration into matrix**	**Dermal Epidermal Attachment**	**Organisation of dividing cells**	**Stratum corneum**		
Static Submerged 1	1	1	2	1	1	6	7
Static Submerged 2	1	1	3	1	1	7	
Static Submerged 3	1	2	3	1	1	8	
Perfused ALI 4	1	1	3	3	2	10	10
Perfused ALI 5	1	1	3	3	2	10	
Perfused ALI 6	1	1	3	3	2	10	
Static ALI 7	1	2	3	3	2	11	11
Static ALI 8	1	3	3	2	2	11	
Static ALI 9	1	3	3	3	1	11	

Figure 5.2: Scoring of the TE skin constructs.

The skin constructs were assigned numerical values according to the quality of specific features of their structure as defined by a). The whole length of the construct was observed for each sample. Scores for each sample are given in b). Scores of multiple samples of the same culture condition were averaged to find an overview of the quality.

5.2.4 Quantitative Comparison of Sample Structure Using Construct Scoring

A scoring system was implemented to fairly compare samples against the same criteria. Each feature of the sample was given a numerical score depending on the quality of the structure. The judging criteria are shown in figure 5.2a and the scores awarded for each sample in figure 5.2b. Images of the entire length of the sample were used for this observation. Healthy native skin would receive a maximum score of 13/13 as it would display all the expected structural features. Overall the static submerged samples had a worse structure than the samples cultured at an ALI, scoring an average of 7/13. These samples also had the most variable structure according to the scoring. The static ALI samples achieved the highest score with an average of 11/13, while the perfused ALI samples came close behind with 10/13.

5.3 Discussion

This chapter has considered the culture of TE skin under perfusion conditions in combination with *in situ* OCT imaging. OCT imaging was able to show changes in structure at different time points and between samples (fig. 5.1). At the first time point samples raised to an ALI exhibited a highly reflective signal at the surface which was attributed to liquid on the surface of the samples which had recently been raised to the ALI. The submerged samples did not exhibit this signal; the samples were imaged while submerged and refractive index matching between the medium and sample occurred to reduce these Fresnel reflections at the surface[62]. The samples cultured at a perfused ALI showed development over the course of the experiment and by day 14 the structure observed was similar to images shown in chapter 4. The stratum corneum had a bright signal, the living epidermis a dark signal and the dermis a bright signal.

The sample cultured at a static ALI shown in figure 5.1ciii did not exhibit such a clear OCT image on day 14 in comparison to the perfused sample. The living epidermis and

stratum corneum were thinner and displayed less contrast. However, observation of the corresponding histology showed that the static and perfused samples have a very similar structure and would not predict this difference between OCT images. The poor OCT image of the static ALI sample may be explained by the location on the sample that the image was taken which may have had a worse structure than the majority of the sample. Otherwise this difference could be explained by inadequate location of the correct focal distance.

The OCT images shown in figure 5.1 generally showed less detail than the OCT images shown in chapter 4; the images were taken using the in-house OCT system previously described[8] which used the LSM03 lens with a lateral resolution of 25 µm as opposed to the commercial EX1301 system (Michelson Diagnostics, Kent, UK) which had a lateral resolution of 7.5 µm as used in chapter 4. The in-house system was implemented because the commercial system had not been acquired at this stage. Therefore, this explains the differences between OCT images shown in chapter 4 and those presented in figure 5.1.

The static submerged samples observed on day 15 histology showed that the surface was coated with the basket weave structure of stratum corneum. The keratinocytes appeared to have rapidly differentiated and sometimes still contained nuclei in the stratum corneum. The layer of nucleated proliferative keratinocytes was at most one cell thick but fairly well attached. The corresponding OCT imaging showed a very bright surface layer on this sample which related to the stratum corneum. This layer was thin and below this the dark signal corresponding to proliferative keratinocytes in the living epidermis was not observed, probably because it was too thin. The signal decreased in response to the dermis which is uncharacteristic of TE skin which normally shows a bright dermis in comparison to the other structures. It may be that the

stratum corneum was uncharacteristically bright, which made the dermis appear dark in comparison.

The samples cultured at a perfused ALI displayed good structure according to the histology with a multilayered proliferative epidermis which gradually differentiated to form the stratum corneum. The corresponding OCT images displayed this layered structure; clearly showing a bright surface of stratum corneum, a dark living epidermis and a bright dermis. The static ALI samples showed a good structure by histology, however, this was not reflected so clearly in the OCT images which lacked contrast between the layers.

Observation of the histology of TE skin cultured under perfused ALI conditions for 15 days showed that the structure was significantly better than that observed for samples cultured under static submerged conditions. Static submerged samples had an abnormal morphology with a small layer of proliferative keratinocytes coated with a larger layer of prematurely differentiated keratinocytes forming stratum corneum. This structure indicates a cellular stress response. In contrast the perfused ALI samples showed a multilayered stratum spinosum containing nucleated cells which gradually differentiated to form a multilayered stratum corneum. This structure indicates good quality TE skin, as displayed by the positive control; TE skin cultured at a static ALI.

The scoring confirmed that the static submerged samples displayed the worst structure with an exceptionally flaky stratum corneum and prematurely differentiating keratinocytes. Both ALI conditions had an improved score, although the static ALI samples gained one point on the perfused ALI samples. Three samples for each condition were compared, but inclusion of more repeats would confirm if there was any difference between perfused and static ALI samples.

There have only been two other studies investigating the perfusion culture of TE skin at an ALI[7,49]. However, there are a number of other studies that have examined the use of bioreactors in the culture of skin materials which have been discussed in detail in chapter 1. The data presented here has shown that perfusion culture was able to produce good quality TE skin (with a similar morphological quality to skin cultured under standard culture techniques) which is in agreement with the other work in this field[7,49].

The morphology of TE skin cultured under standard static ALI conditions is accepted as a good approximation of *in vivo* skin[5]. Therefore the main goal of the implementation of perfusion culture techniques is to improve the lifespan of TE skin constructs. It would also be interesting to establish whether skin cultured in this way could respond in a physiologically relevant way to stimuli such as angiogenesis and wound healing.

It has previously been shown that perfusion culture was able to maintain the viable lifespan of TE skin constructs for a longer culture period than static controls[49]. Although the current study did not assess the viability of constructs, this would be a very important parameter to assess in future when considering whether TE skin constructs could survive for longer culture periods. Maintained or increased viability over an extended culture period several weeks long would confirm whether perfusion techniques could provide a benefit over static culture techniques.

Although this study did not assess viability, proliferation, barrier formation or wound healing *in vivo*, it was able to observe the development of constructs *in situ* and completely non-destructively using OCT imaging, which the other studies did not demonstrate. This is an incredibly useful feature to assess the structural development and progression of stimuli without damaging the construct. Future studies using higher resolution OCT systems have the potential to provide a real insight into the structural characteristics of a sample.

5.4 Summary

This work has aimed to culture TE skin within perfusion bioreactors and to use *in situ* imaging by OCT at multiple time points during culture to observe the developing structure. The combination of these technologies was hypothesised to help address the problems of limited lifespan of TE skin constructs and the inability to non-destructively observe development while constructs were in culture.

The results presented have shown that OCT imaging has been able to demonstrate changes in TE skin structure between samples and time points. It was demonstrated that *in situ* imaging was possible in both first generation bioreactor chambers and 6 well plates and that OCT image quality was not compromised. Corresponding histology indicated that samples cultured in perfusion culture bioreactors were able to produce a very similar structure to samples cultured at a static ALI. Scoring of TE skin constructs confirmed that on a whole samples cultured under both a static and perfused ALI produced a similar structure, indicating that perfusion culture was successful. However, the viability of constructs was not assessed so further work is required to assess the ability of perfusion culture techniques to improve viability and lifespan. In order to improve viability over time, nutrient delivery parameters such as; feeding regime, re-circulation or single pass of medium and flow rate may need to be optimised.

6. SUMMARY AND CONCLUSIONS

6.1 Summary

This study has aimed to develop improvements in the culture and imaging of tissue engineered (TE) skin constructs with applications both *in vivo* and *in vitro*. The improvements to the culture methodology aimed to use perfusion culture techniques to extend the lifespan of TE skin constructs. In addition, the implementation of optical coherence tomography (OCT) imaging was considered important to permit non-invasive, non-destructive observation of the development of these constructs, which has previously required destructive histology to be performed following culture. This work has attempted to characterise the structures of the TE skin model as observed in OCT images to allow quality assessment to be performed during culture.

Chapter 3 has described the setup of first and second generation air/liquid interface (ALI) perfusion bioreactor systems. The ALI chambers implemented were modified from existing submerged culture products (provided by Kirkstall Ltd.). The first generation system was discontinued when design of the initial chamber was changed, instigating the development of the second generation system. Design iterations of this second generation system were described, giving an insight into issues and problems faced during the development of these systems. Ultimately the aims of this chapter were not fully fulfilled as the system developed was unable to culture TE skin due to problems maintaining sterility. Furthermore, the system was difficult to set up and OCT imaging was only possible using the lower resolution lens which had a long working distance, as the distance between the ALI and the chamber lid was large.

Parallel work was described in chapter 4 assessing the potential of OCT imaging for the observation of TE skin constructs during culture. OCT imaging has been shown to provide a method to non-invasively observe the developing structure of TE skin samples during culture. The OCT images presented have allowed the qualitative

assessment of the structural development over time by trained observers. It was also considered important to set criteria for objective assessment of quality.

The epithelial thickness was suggested as a suitable parameter to examine for quality assessment. Epithelial thickness measurement using a manual line tracing method was presented to compare construct development over time. OCT imaging has proven a promising technique to use in tissue engineering, allowing observation of internal structures without destruction of the sample. However, further work is required to definitively describe the quality of constructs from the observation of OCT images. Measurement of epithelial thickness is considered to be a feasible parameter for the assessment of skin quality.

Finally the concepts of perfusion culture and OCT imaging of TE skin were combined in the results presented in chapter 5. TE skin constructs were cultured within first generation ALI chambers and imaged over time using OCT. The OCT images showed the developing structure of the constructs, however, the images were less well defined than the images taken with the higher resolution commercial OCT system used in chapter 4. The quality of the TE skin constructs cultured under perfusion conditions was comparable to equivalent constructs cultured under static ALI conditions in terms of morphology observed by histology images.

The viability of static and perfused constructs was not compared so differences in viability could not be determined. Assessment of viability would be an important indicator of health of constructs in future studies. Culture of TE skin under perfusion conditions was successful suggesting future work would be valuable in this field. OCT imaging was promising, and with implementation of the higher resolution commercial EX1301 OCT system in future studies would be advantageous if the perfusion system could be designed to support the short working distance of the lens.

6.2 Future Work

A new perfusion bioreactor system should be developed to address the issues considered in this report. It is important that the bioreactor system is as simple to set up as possible and provides significant advantages over static culture techniques for it to be accepted. It is hypothesised that one of the advantages could be the extension of the viable lifetime of the construct. Therefore, this is an important parameter to assess over an extended culture period of TE skin cultured under perfusion conditions.

The ability to perform OCT imaging during culture should be considered in the design of the new perfusion chamber due to the advantages of OCT over conventional histology. The future application of OCT imaging of TE skin constructs during culture should further address the establishment of quality control measures to obtain the maximum potential of this technology. Further assessment of the averaged A-scan may unlock objective information about the sample, including the epithelial thickness.

6.3 Conclusions

This work has highlighted some of the challenges associated with the design and development of a perfusion system for the culture of TE skin at an ALI. The issues and solutions presented will aid researchers in the future to design these systems. The most important parameters to ensure are the ability of the system to maintain sterility and to provide a reliable and stable ALI. A desirable feature of a perfusion culture system for TE skin constructs is the ability to perform OCT imaging *in situ*.

OCT imaging has been shown to be a useful real time imaging technique to observe the structure of TE skin constructs over time in a non-destructive manner, allowing samples to be returned to culture following imaging. Observation of OCT images has been able to distinguish between healthy and poor quality TE skin constructs. The work presented here suggests that the measurement of epithelial thickness may prove a useful

determinant of TE skin quality. The application of OCT imaging for observation of samples within perfusion culture chambers is not challenging provided that the sample can be positioned close to the lens and that a transparent window can be supplied above the sample.

The combination of perfusion culture and OCT imaging has shown potential. OCT imaging was able to show development of the construct inside the perfusion chamber without damaging the construct. However, implementation of the higher resolution commercial EX1301 OCT system would be important to obtain the most useful images. Perfusion culture successfully produced structurally good quality TE skin; however viability over an extended time-course was not examined and should be the basis for future work.

7. REFERENCES

1. MacNeil, S. Progress and opportunities for tissue-engineered skin. *Nature* **445**, 874–80 (2007).

2. Shevchenko, R. V, James, S. L. & James, S. E. A review of tissue-engineered skin bioconstructs available for skin reconstruction. *Journal of the Royal Society Interface* **7**, 229–58 (2010).

3. Supp, D. M. & Boyce, S. T. Engineered skin substitutes: practices and potentials. *Clinics in dermatology* **23**, 403–12 (2005).

4. Ralston, D. R. *et al.* Keratinocytes contract human dermal extracellular matrix and reduce soluble fibronectin production by fibroblasts in a skin composite model. *British journal of plastic surgery* **50**, 408–15 (1997).

5. Ralston, D. R. *et al.* The requirement for basement membrane antigens in the production of human epidermal/dermal composites in vitro. *The British journal of dermatology* **140**, 605–15 (1999).

6. Yang, Y. I., Seol, D. L., Kim, H. I., Cho, M. H. & Lee, S. J. Continuous perfusion culture for generation of functional tissue-engineered soft tissues. *Current Applied Physics* **7**, e80–e84 (2007).

7. Sun, T., Norton, D., Haycock, J. W., Ryan, A. J. & MacNeil, S. Development of a closed bioreactor system for culture of tissue-engineered skin at an air-liquid interface. *Tissue engineering* **11**, 1824–31 (2005).

8. Smith, L. E., Bonesi, M., Smallwood, R., Matcher, S. J. & MacNeil, S. Using swept-source optical coherence tomography to monitor the formation of neo-epidermis in tissue-engineered skin. *Journal of tissue engineering and regenerative medicine* **4**, 652–8 (2010).

9. Marieb, E. N. *Essentials of Human Anatomy and Physiology*. 107–128 (Pearson Education: 2006).

10. Harding, C. R. The stratum corneum: structure and function in health and disease. *Dermatologic Therapy* **17**, 6–15 (2004).

11. American Society of Plastic Surgeons Evidence-based Clinical Practice Guideline: Chronic Wounds of the Lower Extremity. at <http://www.plasticsurgery.org/Documents/medical-professionals/health-policy/evidence-practice/Evidence-based-Clinical-Practice-Guideline-Chronic-Wounds-of-the-Lower-Extremity.pdf>

12. NHS Leg ulcer, venous. at <http://www.nhs.uk/Conditions/Leg-ulcer-venous/Pages/Introduction.aspx>

13. Rainey, J. *Wound Care: A Handbook for Community Nurses*. (Whurr: 2002).

14. Morgan, J., Sheridan, R., Tompkins, R., Yarmush, M. & Burke, J. Burn Dressings and Skin Substitutes. *Biomaterials Science: An Introduction to Materials in Medicine* 602–613 (2004).

15. Burke, J. F., Bondoc, C. C. & Quinby, W. C. Primary burn excision and immediate grafting: a method shortening illness. *The Journal of trauma* **14**, 389–95 (1974).

16. National Centre for the Replacement Refinement and Reduction of Animals in Research NC3Rs. at <http://www.nc3rs.org.uk/landing.asp?id=2>

17. Rheinwald, J. G. & Green, H. Serial cultivation of strains of human epidermal keratinocytes: the formation of keratinizing colonies from single cells. *Cell* **6**, 331–43 (1975).

18. Rheinwald, J. G. & Green, H. Formation of a keratinizing epithelium in culture by a cloned cell line derived from a teratoma. *Cell* **6**, 317–30 (1975).

19. Rheinwald, J. G. & Green, H. Epidermal growth factor and the multiplication of cultured human epidermal keratinocytes. *Nature* **265**, 421–424 (1977).

20. O'Connor, N., Mulliken, J., Banks-Schlegel, S., Kehinde, O. & Green, H. Grafting of Burns with Cultured Epithelium Prepared from Autologous Epidermal Cells. *The Lancet* **317**, 75–78 (1981).

21. Hernon, C. a *et al.* Clinical experience using cultured epithelial autografts leads to an alternative methodology for transferring skin cells from the laboratory to the patient. *Regenerative medicine* **1**, 809–21 (2006).

22. Chakrabarty, K. H. *et al.* Development of autologous human dermal-epidermal composites based on sterilized human allodermis for clinical use. *The British journal of dermatology* **141**, 811–23 (1999).

23. Mak, V. H. W. *et al.* Barrier Function of Human Keratinocyte Cultures Grown at the Air-Liquid Interface. *Journal of Investigative Dermatology* **96**, 323–327 (1991).

24. Harrison, C. A. *et al.* Transglutaminase inhibitors induce hyperproliferation and parakeratosis in tissue-engineered skin. *The British journal of dermatology* **156**, 247–57 (2007).

25. Sahota, P. S. *et al.* Development of a reconstructed human skin model for angiogenesis. *Wound Repair and Regeneration* **11**, 275–284 (2003).

26. Sahota, P. S., Burn, J. L., Brown, N. J. & MacNeil, S. Approaches to improve angiogenesis in tissue-engineered skin. *Wound repair and regeneration* **12**, 635–42 (2004).

27. Krajewska, E., Lewis, C., Staton, C., MacGowan, A. & Macneil, S. New insights into induction of early-stage neovascularization in an improved tissue-engineered model of psoriasis. *Journal of tissue engineering and regenerative medicine* **5**, 363–74 (2011).

28. Wendt, D., Riboldi, S., Cioffi, M. & Martin, I. Potential and bottlenecks of bioreactors in 3D cell culture and tissue manufacturing. *Advanced materials* **21**, 3352–67 (2009).

29. Bancroft, G. N. *et al.* Fluid flow increases mineralized matrix deposition in 3D perfusion culture of marrow stromal osteoblasts in a dose-dependent manner. *Proceedings of the National Academy of Sciences of the United States of America* **99**, 12600–5 (2002).

30. Sikavitsas, V. I., Bancroft, G. N., Holtorf, H. L., Jansen, J. A. & Mikos, A. G. Mineralized matrix deposition by marrow stromal osteoblasts in 3D perfusion culture increases with increasing fluid shear forces. *Proceedings of the National Academy of Sciences of the United States of America* **100**, 14683–8 (2003).

31. Hoerstrup, S. P., Sodian, R., Sperling, J. S., Vacanti, J. P. & Mayer, J. E. New pulsatile bioreactor for in vitro formation of tissue engineered heart valves. *Tissue engineering* **6**, 75–9 (2000).

32. Martin, I., Wendt, D. & Heberer, M. The role of bioreactors in tissue engineering. *Trends in Biotechnology* **22**, 80–86 (2004).

33. Prenosil, J. E. & Villeneuve, P. E. Automated production of cultured epidermal autografts and sub-confluent epidermal autografts in a computer controlled bioreactor. *Biotechnology and bioengineering* **59**, 679–83 (1998).

34. Kino-Oka, M. & Prenosil, J. E. Growth of Human Keratinocytes on Hydrophilic Film Support and Application to Bioreactor Culture. *Journal of Chemical Engineering of Japan* **31**, 856–859 (1998).

35. Prenosil, J. E. & Kino-oka, M. Computer Controlled Bioreactor for Large-scale Production of Cultured Skin Grafts. *Annals of the New York Academy of Sciences* **875**, 386–397 (1999).

36. Kino-Oka, M. & Prenosil, J. E. Development of an on-line monitoring system of human keratinocyte growth by image analysis and its application to bioreactor culture. *Biotechnology and bioengineering* **67**, 234–9 (2000).

37. Kalyanaraman, B. & Boyce, S. Assessment of an automated bioreactor to propagate and harvest keratinocytes for fabrication of engineered skin substitutes. *Tissue engineering* **13**, 983–93 (2007).

38. Kalyanaraman, B. & Boyce, S. T. Wound healing on athymic mice with engineered skin substitutes fabricated with keratinocytes harvested from an automated bioreactor. *The Journal of surgical research* **152**, 296–302 (2009).

39. Lim, S.-H., Son, Y., Kim, C.-H., Shin, H. & Kim, J. Il The effect of a long-term cyclic strain on human dermal fibroblasts cultured in a bioreactor on chitosan-based scaffolds for the development of tissue engineered artificial dermis. *Macromolecular Research* **15**, 370–378 (2007).

40. Ladd, M. R., Lee, S. J., Atala, A. & Yoo, J. J. Bioreactor maintained living skin matrix. *Tissue engineering. Part A* **15**, 861–8 (2009).

41. Palmiero, C., Imparato, G., Urciuolo, F. & Netti, P. Engineered dermal equivalent tissue in vitro by assembly of microtissue precursors. *Acta biomaterialia* **6**, 2548–53 (2010).

42. Lei, X. *et al.* NASA-approved rotary bioreactor enhances proliferation of human epidermal stem cells and supports formation of 3D epidermis-like structure. *PloS one* **6**, e26603 (2011).

43. Halberstadt, C. R. *et al.* The in vitro growth of a three-dimensional human dermal replacement using a single-pass perfusion system. *Biotechnology and bioengineering* **43**, 740–6 (1994).

44. Navarro, F. A., Mizuno, S., Huertas, J. C., Glowacki, J. & Orgill, D. P. Perfusion of medium improves growth of human oral neomucosal tissue constructs. *Wound Repair and Regeneration* **9**, 507–512 (2001).

45. Kremer, M., Lang, E. & Berger, A. Organotypical engineering of differentiated composite-skin equivalents of human keratinocytes in a collagen-GAG matrix (INTEGRA Artificial Skin) in a perfusion culture system. *Langenbeck's archives of surgery* **386**, 357–63 (2001).

46. Mizuno, S., Watanabe, S. & Takagi, T. Hydrostatic fluid pressure promotes cellularity and proliferation of human dermal fibroblasts in a three-dimensional collagen gel/sponge. *Biochemical Engineering Journal* **20**, 203–208 (2004).

47. Seol, D. L. *et al.* Enhanced Biological and Mechanical Properties of Artificial Dermis Prepared Using a Perfusion Culture System. *Key Engineering Materials* **288-289**, 23–26 (2005).

48. Figallo, E., Flaibani, M., Zavan, B., Abatangelo, G. & Elvassore, N. Micropatterned biopolymer 3D scaffold for static and dynamic culture of human fibroblasts. *Biotechnology progress* **23**, 210–6 (2007).

49. Kalyanaraman, B., Supp, D. M. & Boyce, S. T. Medium flow rate regulates viability and barrier function of engineered skin substitutes in perfusion culture. *Tissue engineering. Part A* **14**, 583–93 (2008).

50. Huang, D. *et al.* Optical Coherence Tomography. *Science* **254**, 1178–1181 (1991).

51. Gambichler, T. *et al.* Applications of optical coherence tomography in dermatology. *Journal of dermatological science* **40**, 85–94 (2005).

52. Mason, C., Markusen, J. F., Town, M. A., Dunnill, P. & Wang, R. K. The potential of optical coherence tomography in the engineering of living tissue. *Physics in Medicine and Biology* **49**, 1097–1115 (2004).

53. Gambichler, T., Jaedicke, V. & Terras, S. Optical coherence tomography in dermatology: technical and clinical aspects. *Archives of dermatological research* **303**, 457–73 (2011).

54. Swanson, E. A. *et al.* In vivo retinal imaging by optical coherence tomography. *Optics letters* **18**, 1864–6 (1993).

55. Izatt, J. A. *et al.* Micrometer-scale resolution imaging of the anterior eye in vivo with optical coherence tomography. *Archives of ophthalmology* **112**, 1584–9 (1994).

56. Fercher, A. F., Hitzenberger, C. K., Drexler, W., Kamp, G. & Sattmann, H. In Vivo Optical Coherenece Tomography. *American Jounal of Ophthalmology* **116**, 113–114 (1993).

57. Sakata, L. M., Deleon-Ortega, J., Sakata, V. & Girkin, C. A. Optical coherence tomography of the retina and optic nerve - a review. *Clinical & experimental ophthalmology* **37**, 90–9 (2009).

58. Wessels, R. *et al.* Optical biopsy of epithelial cancers by optical coherence tomography (OCT). *Lasers in medical science* (2013).doi:10.1007/s10103-013-1291-8

59. Welzel, J. Optical coherence tomography in dermatology: a review. *Skin research and technology* **7**, 1–9 (2001).

60. Wojtkowski, M. High-speed optical coherence tomography: basics and applications. *Applied optics* **49**, D30–61 (2010).

61. Jang, I.-K. *et al.* Visualization of coronary atherosclerotic plaques in patients using optical coherence tomography: comparison with intravascular ultrasound. *Journal of the American College of Cardiology* **39**, 604–609 (2002).

62. Pedrotti, F., Pedrotti, L. S. & Pedrotti, L. M. *Introduction to Optics*. (Pearson Education: 2008).

63. Michelson, A. A. & Morley, E. W. On the Relative Motion of the Earth and the Luminiferous Ether. *American Journal of Science* **34**, 333–345 (1887).

64. Fujimoto, J. G. Optical coherence tomography. *Comptes Rendus de l'Académie des Sciences - Series IV - Physics* **2**, 1099–1111 (2001).

65. Tomlins, P. H. & Wang, R. K. Theory, developments and applications of optical coherence tomography. *Journal of Physics D: Applied Physics* **38**, 2519–2535 (2005).

66. Tearney, G. J. *et al.* Determination of the refractive index of highly scattering human tissue by optical coherence tomography. *Optics Letters* **20**, 2258 (1995).

67. Schmitt, J. M., Knüttel, A., Yadlowsky, M. & Eckhaus, M. A. Optical-coherence tomography of a dense tissue: statistics of attenuation and backscattering. *Physics in medicine and biology* **39**, 1705–20 (1994).

68. Zysk, A. M., Nguyen, F. T., Oldenburg, A. L., Marks, D. L. & Boppart, S. A. Optical Coherence Tomography: A review of clinical development from bench to bedside. *Journal of Biomedical Optics* **12**, 051403 (2007).

69. Welzel, J., Reinhardt, C., Lankenau, E., Winter, C. & Wolff, H. H. Cutaneous Biology Changes in function and morphology of normal human skin : evaluation using optical coherence tomography. **150**, 220–225 (2004).

70. Anderson, R. R. & Parrish, J. A. The optics of human skin. *The Journal of investigative dermatology* **77**, 13–9 (1981).

71. Carroll, L. & Humphreys, T. R. LASER-tissue interactions. *Clinics in dermatology* **24**, 2–7 (2006).

72. Welzel, J., Lankenau, E., Birngruber, R. & Engelhardt, R. Optical coherence tomography of the human skin. *Journal of the American Academy of Dermatology* **37**, 958–63 (1997).

73. Welzel, J., Bruhns, M. & Wolff, H. H. Optical coherence tomography in contact dermatitis and psoriasis. *Archives of dermatological research* **295**, 50–5 (2003).

74. Gambichler, T., Matip, R., Moussa, G., Altmeyer, P. & Hoffmann, K. In vivo data of epidermal thickness evaluated by optical coherence tomography: effects of age, gender, skin type, and anatomic site. *Journal of dermatological science* **44**, 145–52 (2006).

75. Lademann, J. *et al.* Application of Optical Coherent Tomography for Skin Diagnostics. *Laser Physics* **15**, 288–294 (2005).

76. Gambichler, T. *et al.* Validation of optical coherence tomography in vivo using cryostat histology. *Physics in medicine and biology* **52**, N75–85 (2007).

77. Gambichler, T. *et al.* Epidermal thickness assessed by optical coherence tomography and routine histology: preliminary results of method comparison. *Journal of the European Academy of Dermatology and Venereology* **20**, 791–5 (2006).

78. Yeh, A. T. *et al.* Imaging wound healing using optical coherence tomography and multiphoton microscopy in an in vitro skin-equivalent tissue model. *Journal of biomedical optics* **9**, 248–53 (2004).

79. Yang, Y. *et al.* Investigation of optical coherence tomography as an imaging modality in tissue engineering. *Physics in medicine and biology* **51**, 1649–59 (2006).

80. Spöler, F. *et al.* High-resolution optical coherence tomography as a non-destructive monitoring tool for the engineering of skin equivalents. *Skin research and technology* **12**, 261–7 (2006).

81. Smith, L. E. *et al.* Using swept source optical coherence tomography to monitor wound healing in tissue engineered skin. *Progress in Biomedical Optics and Imaging - Proceedings of SPIE* **7566**, 75660I–75660I (2010).

82. Smith, L. E., Smallwood, R. & Macneil, S. A comparison of imaging methodologies for 3D tissue engineering. *Microscopy research and technique* **73**, 1123–33 (2010).

83. Kuranov, R., Sapozhnikova, V., Prough, D., Cicenaite, I. & Esenaliev, R. Correlation between optical coherence tomography images and histology of pigskin. *Applied Optics* **46**, 1782–1786 (2007).

84. Bechara, F. G. *et al.* Histomorphologic correlation with routine histology and optical coherence tomography. *Skin research and technology* **10**, 169–73 (2004).

85. Boonstra, H., Oosterhuis, J. W., Oosterhuis, A. M. & Fleuren, G. J. Cervical tissue shrinkage by formaldehyde fixation, paraffin wax embedding, section cutting and mounting. *Virchows Archiv. A, Pathological anatomy and histopathology* **402**, 195–201 (1983).

86. Lu, Z., Kasaragod, D. K. & Matcher, S. J. Optic axis determination by fibre-based polarization-sensitive swept-source optical coherence tomography. *Physics in medicine and biology* **56**, 1105–22 (2011).

87. Potter, S. M. & DeMarse, T. B. A new approach to neural cell culture for long-term studies. *Journal of Neuroscience Methods* **110**, 17–24 (2001).

88. Bagnaninchi, P. O. *et al.* Chitosan microchannel scaffolds for tendon tissue engineering characterized using optical coherence tomography. *Tissue engineering* **13**, 323–31 (2007).

89. Kelly, K. M., Liaw, L.-H. L. & Nelson, J. S. Optical coherence tomography for in vitro monitoring of wound healing after laser irradiation. *IEEE Journal of Selected Topics in Quantum Electronics* **9**, 222–226 (2003).

90. Wang, X., Milner, T. E., Chang, M. C. & Nelson, S. J. Group refractive index measurement of dry and hydrated type I collagen films using optical low-coherence reflectometry. *Journal of Biomedical Optics* **1**, 212–216 (1996).

91. Dunn, A. & Richards-Kortum, R. Three-dimensional computation of light scattering from cells. *IEEE Journal of Selected Topics in Quantum Electronics* **2**, 898–905 (1996).

92. Ponec, M. Skin constructs for replacement of skin tissues for in vitro testing. *Advanced Drug Delivery Reviews* **54**, S19–S30 (2002).

8. APPENDICES

Appendix 1

MATLAB script to open the OCT image and straighten the surface. Calculations for the averaged A-scan are included in addition to scripts to plot graphs from this data.

```
% Shannon and Caroline script to straighten OCT images from png
files
clc
clear all
close all

% Variables
threshold = 90; %to remove speckle noise: set this depending on
%image; remove very bright artefacts
%before using this command
offset = 50; %Depth at which surface of sample is in straightened
image
reallatdim = 4; % Real lateral dimension of image is 4mm
endY=400;


cd (uigetdir) % Opens dialogue box to choose directory and changes
%directory to this new directory

a=uigetfile; % Open image file in MATLAB
b=imread(a);
% Opens dialogue box to choose image, opens the image in MATLAB to
enable
% you to plot as picture

%
**********************************************************************
% Calculate variables needed by the rest of the script
%**********************************************************************

B = rgb2gray(b); % Convert RGB image to grayscale image
size_B=size(B);

row=size_B(1);
col=size_B(2);

Xstart = 0;
Xstop  = col;
Ystart = 0;
Ystop = (row + offset); % Y direction is longer in the straightened
image
y=Ystart:(Ystop-1);

scale = reallatdim/col; % Scale axes by this value to get dimension
in mm
% not pixels

% Find the dimensions of the image in pixels
```

```
realaxdim=(reallatdim/col)*row; % Real axial dimension in mm
realaxdimSI = (reallatdim/col)*Ystop; % Real axial dimension in mm
for
% straightened images (to take account of addition of black pixels)

straightrowno = row+offset;


%*********************************************************************
% Using information obtained in previous section to plot graphs
%*********************************************************************


%Plot the RGB scale image
figure (1)
imshow(b)
xlabel('Lateral Direction /mm','fontsize',12,'fontweight','b');
ylabel('Axial Direction Through Sample
/mm','fontsize',12,'fontweight','b');
title ('OCT Image (RGB scale)','fontsize',12,'fontweight','b')
axis on
set(gca,'XTick', 0: col/10:col)
set(gca,'XTickLabel',  0: reallatdim/10: reallatdim)
set(gca,'YTick', 0:offset:endY)
set(gca,'YTickLabel', 0: (offset*scale):(endY*scale))


% Plot grayscale image
figure (2)
imshow(B)
xlabel('Lateral Direction /mm','fontsize',12,'fontweight','b');
ylabel('Axial Direction Through Sample
/mm','fontsize',12,'fontweight','b');
title ('OCT Image (grayscale)','fontsize',12,'fontweight','b')
axis on
set(gca,'XTick', 0: col/10:col)
set(gca,'XTickLabel',  0: reallatdim/10: reallatdim)
set(gca,'YTick', 0:offset:endY)
set(gca,'YTickLabel', 0: (offset*scale):(endY*scale))

% Straighten the image

flag = zeros(1,col);

B = double(B);
C = zeros(straightrowno,col);

% Loop through the image
for c = 1:col
    r_new = 0;
    for r = 1:row
        if B(r,c)>threshold && flag(1,c)==0 && B(r,c)~=250
            flag(1,c) = 1;
        end
        if (flag(1,c)==1)
            C(r_new+offset,c) = B(r,c);
            r_new = r_new+1;
        end
    end
```

```
end

C = uint8(C);
% C is the matrix of the straightened image

% Plot the straightened image
figure (3)
imshow(C);
xlabel('Lateral Direction /mm','fontsize',12,'fontweight','b');
ylabel('Depth into Sample /mm','fontsize',12,'fontweight','b');
title ('Straightened OCT Image','fontsize',12,'fontweight','b')
axis on
set(gca,'XTick', 0: col/10:col)
set(gca,'XTickLabel', 0: reallatdim/10: reallatdim)
set(gca,'YTick', 0:endY/8:endY)
set(gca,'YTickLabel', (-1*offset*scale): (offset*scale):endY*scale)
% set(gca,'YTick', 0:Ystop/11:Ystop)
% set(gca,'YTickLabel', (-1*offset*scale):
realaxdimSI/11:realaxdimSI)


% Find the average across columns with respect to depth
CT = C';
sumCT = sum(CT);
avgCT = sumCT/col;


% To plot A-scan
figure (4)
plot (avgCT, y)
set(gca,'YTick', 0:endY/8:endY)
set(gca,'YTickLabel', (-1*offset*scale): (offset*scale):endY*scale)
xlabel('Average Intensity of A-Scan /arbitrary
units','fontsize',12,'fontweight','b');
ylabel('Depth into sample /mm','fontsize',12,'fontweight','b');
title ('Average A-scan','fontsize',12,'fontweight','b')
% Only use next command if you want the graph on rotated 90 degrees
% to complement the OCT image

set(gca,'YDir','Reverse') % To put graph on its side

% To plot A-scan superimposed on straightened OCT image
figure (5)
imshow(C)
hold on
plot (avgCT, y, 'y', 'LineWidth', 2.5)
% This plot does not need forcing on its side, MATLAB recognises the
% dimensions and fits it to the image
axis on
set(gca,'XTick', 0: col/10:col)
set(gca,'XTickLabel', 0: reallatdim/10: reallatdim)
set(gca,'YTick', 0:endY/8:endY)
set(gca,'YTickLabel', (-1*offset*scale): (offset*scale):endY*scale)
% set(gca,'YTick', 0:Ystop/11:Ystop)
% set(gca,'YTickLabel', (-1*offset*scale):
realaxdimSI/11:realaxdimSI)
xlabel('Lateral Direction /mm','fontsize',12,'fontweight','b');
ylabel('Depth into sample /mm','fontsize',12,'fontweight','b');
title ('Straightened OCT Image and Superimposed A-
scan','fontsize',12,'fontweight','b')
```